

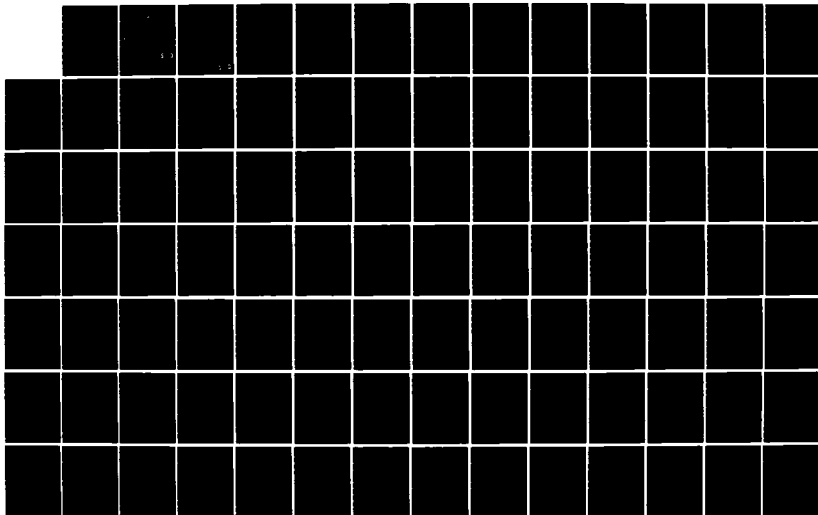
AD-A153 848

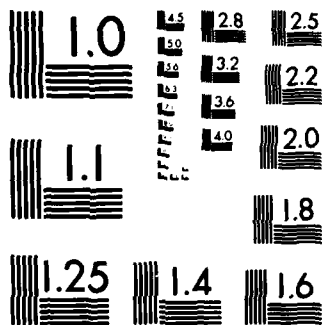
SOLUTION TO EIGENVALUE PROBLEMS OF ANTISYMMETRIC
CROSS-PLY AND ANTISYMMET. (U) AIR FORCE INST OF TECH
WRIGHT-PATTERSON AFB OH SCHOOL OF ENGI. Z A CHAUDHRY
DEC 84 AFIT/GAE/AA/84D-5 F/G 13/4

1/2

UNCLASSIFIED

NL

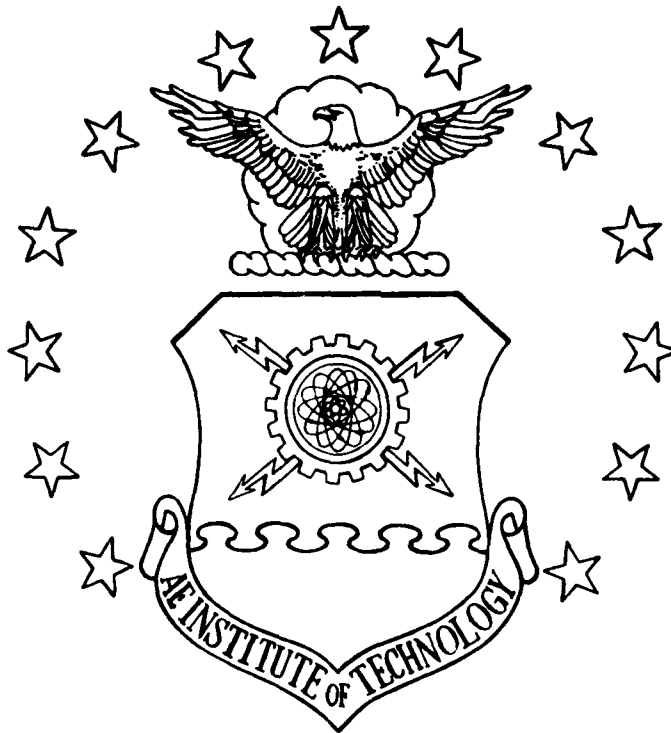




MICROCOPY RESOLUTION TEST CHART
NATIONAL BUREAU OF STANDARDS-1963-A

AD-A153 040

10



SOLUTION TO EIGENVALUE PROBLEMS OF
 ANTISYMMETRIC CROSS-PLY AND
 ANTISYMMETRIC ANGLE-PLY LAMINATED PLATES
 USING AFFINE TRANSFORMATIONS

THESIS

Zaffir A. Chaudhry
 Flight Lieutenant, PAF
 AFIT/GAE/AA/84D-5

DISTRIBUTION STATEMENT A
 Approved for public release
 Distribution Unlimited

DTIC ELECTE
 APR 30 1985
 S B

DEPARTMENT OF THE AIR FORCE
 AIR UNIVERSITY

AIR FORCE INSTITUTE OF TECHNOLOGY

Wright-Patterson Air Force Base, Ohio

85 4 05 029

DTIC FILE COPY

AFIT/GAE/AA/84D-5

SOLUTION TO EIGENVALUE PROBLEMS OF
ANTISYMMETRIC CROSS-PLY AND
ANTISYMMETRIC ANGLE-PLY LAMINATED PLATES
USING AFFINE TRANSFORMATIONS

THESIS

Zaffir A. Chaudhry
Flight Lieutenant, PAF
AFIT/GAE/AA/84D-5

Approved for public release; distribution unlimited.

DTIC
ELECTE
S APR 30 1985 D
B

AFIT/GAE/AA/84D-5

SOLUTION TO EIGENVALUE PROBLEMS OF ANTISYMMETRIC CROSS-PLY
AND ANTISYMMETRIC ANGLE-PLY LAMINATED PLATES
USING AFFINE TRANSFORMATIONS

THESIS

Presented to the Faculty of the School of Engineering
of the Air Force Institute of Technology
Air University

In Partial Fulfillment of the
Requirements for the Degree of
Master of Science in Aeronautical Engineering

Zaffir A. Chaudhry, B. S.
Flight Lieutenant, PAF

December 1984

Approved for public release; distribution unlimited.

Preface

The purpose of this thesis was to find a solution of the eigenvalue problems for antisymmetric cross-ply and anti-symmetric angle ply laminated plates using Affine Transformations. The present methods of solutions for these problems provide a very sketchy overview of how the solutions depend on individual constants. The primary difficulty is too many variables in any particular problem. Affine transformations give solutions in terms of significantly fewer combinations of constants.

The eigenvalue problem of specially orthotropic rectangular plates has already been solved using the affine transformation [1]. The same approach was followed except in this case the solution is much more complicated because of the anti-symmetry.

For both antisymmetric angle-ply and antisymmetric cross-ply a solution for uni-axial buckling and vibration has been developed and the solution is dependent on only two strong material constants. With the reduction in the number of material constants it is now possible to predict solution trends for this class of problems.

Since the two problems are independent, the thesis is divided in two parts. Each part has its own theory and results.

In doing this thesis, I have had a great deal of help from my thesis advisor, Dr. E. J. Brunelle. I am deeply indebted to him for his continuing patience and assistance. I also wish to thank Janet Pastor for typing my thesis. Finally, I wish to thank my wife for her understanding and patience on those nights when I was working in the computer room.

Zaffir A. Chaudhry



| | |
|-------------------------------------|--------------------------|
| Accession No. | |
| <input checked="" type="checkbox"/> | <input type="checkbox"/> |
| PER CALL JE | |
| Author Code | |
| Date and/or | |
| Dist | Special |
| A-1 | |

Table of Contents

| | |
|---|--------|
| Preface | (ii) |
| List of Symbols | (vi) |
| List of Figures (Part I) | (viii) |
| List of Figures (Part II) | (viii) |
| List of Tables | (xi) |
| Abstract | (xii) |
| I. Introduction | 1 |
| Part I Antisymmetric Cross-Ply | |
| II. Theory | 5 |
| Buckling | 5 |
| F2 in Terms of D* and ϵ | 7 |
| DB as a Function of N and F | 8 |
| Minimum Buckling Load | 8 |
| Lower Bound for Buckling Load | 9 |
| Value of D* Calculated by Micromechanics Theory | 10 |
| Relationship Between D* Specially Orthotropic and D* Antisymmetric Cross-Ply | 11 |
| D* Antisymmetric Cross-Ply | 11 |
| Approximation of F2 | 11 |
| Vibration | 13 |
| Lower Bound for Vibration Frequency | 15 |
| Approximation of $F2/T^2$ | 16 |
| III. Results and Discussion | 17 |
| Effect of Variation of D* | 17 |
| Effect of Variation of F | 18 |
| Lower Bound for Buckling | 19 |
| Lower Bound for Vibration | 19 |
| Approximation of Buckling Load | 20 |
| Effect of ϵ on k_o | 21 |

Part II
Antisymmetric Angle-Ply

| | |
|--|----|
| IV. Theory | 37 |
| Buckling | 37 |
| Minimum Buckling Load | 44 |
| Relationship Between Real and Affine Aspect Ratio. | 44 |
| V. Results and Discussion | 45 |
| Effect of Aspect Ratio | 45 |
| Effect of D^*_0 | 48 |
| Effect of ϵ^0 | 49 |
| Effect of K^0 | 50 |
| VI. Conclusions | 86 |
| Bibliography | 88 |
| Vita | 89 |

List of Symbols

| | | |
|--|---|---|
| a/b | = | plate aspect ratio |
| a_o/b_o | = | plate affine aspect ratio |
| $A_{11}, A_{12}, A_{22}, A_{66}$ | = | plate constants |
| $B_{11}, B_{22}, B_{16}, B_{26}$ | = | plate constants |
| $D_{11}, D_{12}, D_{22}, D_{26}$ | = | plate constants |
| D^* | = | generalized rigidity ratio |
| D_o^* | = | generalized rigidity ratio at zero lamination angle |
| ϵ | = | generalized poissons ratio |
| ϵ_o | = | generalized poissons ratio at zero lamination angle |
| k_o | = | plate buckling coefficient |
| $(k_o)_{SOT}$ | = | plate buckling coefficient for specially orthotropic laminate |
| m | = | number of half waves in x direction |
| n | = | number of half waves in y direction |
| \bar{N}_x | = | uniaxial compressive resultant force |
| x, y | = | real space plate dimensions |
| x_o, y_o | = | affine space plate dimensions |
| $Q_{11}, Q_{12}, Q_{22}, Q_{16}, Q_{26}, Q_{66}$ | = | reduced stiffnesses of a laminated plate |
| \bar{Q}_{ij} | = | transformed reduced stiffnesses |
| ω_{mn} | = | physical frequency |
| Ω_{mn} | = | frequency coefficient |
| $(\Omega_{mn})_{SOT}$ | = | frequency coefficient for specially orthotropic laminate |

| | |
|----------------|---|
| T | = similarity parameter |
| F | = ratio of principal lamina stiffnesses = E_2/E_1 |
| K | = square root of ratio of principal lamina stiffnesses = $\sqrt{E_1/E_2}$ |
| u,v,w, | = variations of displacements in the x, y, z directions respectively |
| E_1 | = Youngs modules in the 1 - direction of lamina |
| E_2 | = Youngs modules in the 2 - direction of lamina |
| G_{12} | = Shearing modulus in the 1-2 plane of lamina |
| ν_{12} | = Poissons ratio for contraction (expansion) in the 2-direction due to tension (compression) in the 1-direction |
| θ | = off-axis fiber angle |
| E_f, E_m | = longitudinal modulus of fiber and matrix respectively |
| G_f, G_m | = Shear modulus of fiber and matrix, respectively |
| V_f, V_m | = volume (fraction) of fiber and matrix, respectively |
| ν_f, ν_m | = Poisson's ratio of fiber and matrix, respectively |
| N | = Number of layers in a laminated plate |
| ρ | = density of laminated plate |
| t | = thickness of laminated plate |
| M | = cross-ply ratio |

List of Figures

| Figure | Page |
|--|------|
| Part I | |
| 1. DB vs. Ratio of Principal Lamina Stiffnesses | 23 |
| 2. D^* vs. Volume of Fiber | 24 |
| 3. Specially Orthotropic Buckling Coefficient vs. | 25 |
| 4. Constant G vs. Similarity Parameter | 26 |
| 5. $(k_o)_{min}$ vs. Aspect Ratio DB = 0.1 | 27 |
| 6. $(k_o)_{min}$ vs. Aspect Ratio DB = 0.4 | 28 |
| 7. Frequency Coefficient vs. T DB = 0.1 | 29 |
| 8. Frequency Coefficient vs. T DB = 0.4 | 30 |
| 9. $(k_o)_{min}$ vs. Ratio of Principal Lamina Stiffnesses | 31 |
| 10. Lower Bound for Buckling Load | 32 |
| 11. Lower Bound for Frequency | 33 |
| 12. $(k_o)_{min}$ vs. Aspect Ratio | 34 |
| 13. F2 vs. Similarity Parameter | 35 |
| Part II | |
| 1. Real Aspect Ratio vs. Affine Aspect Ratio | 52 |
| 2. $(k_o)_{min} - 2D_o^*$ vs. Real Aspect Ratio | 53 |
| 3. $(k_o)_{min}$ vs. θ Graphite Epoxy and Glass Epoxy Aspect Ratio = 1 | 54 |
| 4. $(k_o)_{min}$ vs. θ Graphite Epoxy and Glass Epoxy Aspect Ratio = 1.5 | 55 |
| 5. $(k_o)_{min}$ vs. θ Graphite Epoxy and Glass Epoxy Aspect Ratio = 2 | 56 |

| | | | |
|-----|----------------|--|----|
| 6. | $(k_o)_{\min}$ | vs. θ Graphite Epoxy 2 Layers | 57 |
| 7. | $(k_o)_{\min}$ | vs. θ Graphite Epoxy 4 Layers | 58 |
| 8. | $(k_o)_{\min}$ | vs. θ Boron Epoxy 2 Layers | 59 |
| 9. | $(k_o)_{\min}$ | vs. θ Boron Epoxy 4 Layers | 60 |
| 10. | $(k_o)_{\min}$ | vs. θ Graphite Epoxy 4 Layers | 61 |
| 11. | $(k_o)_{\min}$ | vs. θ Boron Epoxy 4 Layers | 62 |
| 12. | $(k_o)_{\min}$ | vs. θ Effect of D_o^* Aspect Ratio = 1.2 Layers . . | 63 |
| 13. | $(k_o)_{\min}$ | vs. θ Effect of D_o^* Aspect Ratio = 1.5, 2 Layers . | 64 |
| 14. | $(k_o)_{\min}$ | vs. θ Effect of D_o^* Aspect Ratio = 2, 2 Layers . . | 65 |
| 15. | $(k_o)_{\min}$ | vs. θ Effect of D_o^* Aspect Ratio = 1, 4 Layers . . | 66 |
| 16. | $(k_g)_{\min}$ | vs. θ Effect of D_o^* Aspect Ratio = 1.5, 4 Layers . | 67 |
| 17. | $(k_o)_{\min}$ | vs. θ Effect of D_o^* Aspect Ratio = 2, 4 Layers . . | 68 |
| 18. | $(k_o)_{\min}$ | vs. θ Comparison of Graphite Epoxy AS/3508 and Graphite Epoxy T300/5208 Aspect Ratio = 1,2 Layers . . | 69 |
| 19. | $(k_o)_{\min}$ | vs. θ Comparison of Graphite Epoxy AS/3508 and Graphite Epoxy T300/5208 Aspect Ratio = 2, 2 Layers . . | 70 |
| 20. | $(k_o)_{\min}$ | vs. θ Comparison of Graphite Epoxy AS/3508 and Graphite Epoxy T300/5208 Aspect Ratio = 1, 4 Layers . . | 71 |
| 21. | $(k_o)_{\min}$ | vs. θ Comparison of Graphite Epoxy AS/3508 and Graphite Epoxy T300/5208 Aspect Ratio = 2, 4 Layers . . | 72 |
| 22. | $(k_o)_{\min}$ | vs. Real Aspect Ratio Lamination Angle = 60 Deg. | 73 |
| 23. | $(k_o)_{\min}$ | vs. Real Aspect Ratio Lamination Angle = 45 Deg. | 74 |
| 24. | $(k_o)_{\min}$ | vs. θ Effect of ϵ | 75 |
| 25. | $(k_o)_{\min}$ | vs. θ Effect of K Aspect Ratio = 1, 2 Layers . . | 76 |
| 26. | $(k_o)_{\min}$ | vs. θ Effect of K Aspect Ratio = 2, 2 Layers . . | 77 |
| 27. | $(k_o)_{\min}$ | vs. θ Effect of K Aspect Ratio = 1, Infinite Number of Layers | 78 |

| | | |
|-----|--|----|
| 28. | $(k_o)_{\min}$ vs. θ Effect of K Aspect Ratio = 2, Infinite Number of Layers | 79 |
| 29. | $(k_o)_{\min}$ vs. Real Aspect Ratio Lamination Angle = 60 Deg. . | 80 |
| 30. | $(k_o)_{\min}$ vs. Real Aspect Ratio Lamination Angle = 45 Deg. . | 81 |
| 31. | $(k_o)_{\min}$ vs. θ Graphite Epoxy AS/3501 and Boron Epoxy Aspect Ratio = 1, 2 Layers | 82 |
| 32. | $(k_o)_{\min}$ vs. θ Graphite Epoxy AS/3501 and Boron Epoxy Aspect Ratio = 2, 2 Layers | 83 |
| 33. | $(k_o)_{\min}$ vs. θ Graphite Epoxy AS/3501 and Boron Epoxy Aspect Ratio = 1, 4 Layers | 84 |
| 34. | $(k_o)_{\min}$ vs. θ Graphite Epoxy AS/3501 and Boron Epoxy Aspect Ratio = 2, 4 Layers | 85 |

$$F2 = \frac{T^6 + T^2 + \frac{D^*}{2} [(T^4+1)^2 - (T^4-1)^2 \epsilon]}{T^2 \left\{ T^2 + \frac{D^*}{2} [(1-\epsilon)(1+T^4) - 2\epsilon D^* T^2] \right\}}$$

The function F2 for a given D^* and ϵ is plotted along with the buckling coefficient for specialty orthotropic lamina in Fig. 3. It is immediately noticed that the shape of F2 and the buckling coefficient is almost exactly the same. This is not entirely surprising because

$$F2)_{\epsilon=0} = T^2 + \frac{1}{T^2}$$

which is

$$k_{oSOT})_{D^*=0}$$

This suggested that F2 could possibly be expressed as some fraction of the specially orthotropic buckling coefficient or as a constant being subtracted off from the specially orthotropic buckling coefficient for a given value of T . The later approach was chosen because of its simplicity. F2 was expressed as:

$$F2 = k_{o \text{ specially orthotropic}} - (G) \quad (20)$$

where G is a constant. Hence

$$G = k_{o \text{ SOT}} - F2 \quad (21)$$

The constant G plotted vs. T for a given D^* is shown in Figure 4 and it is noticed that G is strongly dependent on the value of ϵ . The higher the value of ϵ the lesser is the value of G . Also it is

$$\begin{aligned}
D^* &= \frac{2(\nu_f V_f + \nu_m V_m)}{\left(V_m V_f \left(\frac{E_f}{E_m} + 1/E_f \right) + V_f^2 + V_m^2 + 1 \right)} + \\
&\left[\frac{2 \left(V_m \frac{E_f}{E_m} + V_f \right)}{\left(\frac{E_t}{E_m} \cdot V_m (1 + \nu_m) + V_f (1 + \nu_f) \right) \left(V_m^2 + V_f^2 + V_f V_m \left(\frac{E_f}{E_m} + 1/E_f \right) \right)} \right] \\
&\left[1 - \frac{(\nu_f V_f + \nu_m V_m)^2}{V_m^2 + V_f^2 + V_f V_m \left(\frac{E_f}{E_m} + 1/E_f \right)} \right] \quad (18)
\end{aligned}$$

This relationship is plotted in Fig. 2., and it is noticed that the range of D^* is indeed bounded by zero and unity.

Relationship Between D^* Specially Orthotropic and D^* Antisymmetric Corss-Ply:

The generalized rigidity ratio D^* for antisymmetric cross-ply differs from D^* for specially orthotropic laminates. The difference arises from the fact that in an antisymmetric cross-ply $D_{11} = D_{22}$, whereas in specially orthotropic laminates $D_{11} \neq D_{22}$.

The two D^* 's are however related to each other through the ratio of principal lamina stiffnesses F .

$$D^*_{\text{antisymmetric cross-ply}} = \frac{2\sqrt{F}}{(1+F)} \quad D^*_{\text{specially orthotropic}} \quad (19)$$

Approximation of F2

F2 expressed as a function of D^* , ϵ , T is

which is one fourth of the lower bound for the single layered specially orthotropic lamina. It is also noticed that the lower bound is material independent.

Value of D^* Calculated by Micromechanics Theory

$$D^* = \frac{D_{12} + 2D_{66}}{(D_{11}D_{22})^{\frac{1}{2}}}$$

Again using the stiffnesses displayed by Tsai [5] for anti-symmetric cross-ply laminates with an even number of alternating 0 - 90 layers.

$$D^* = \frac{2(Q_{12} + 2Q_{66})}{(1+F)Q_{11}}$$

Substituting for Q_{11} , Q_{12} , and Q_{66}

$$D^* = \frac{2 \left[E_2 \nu_{12} + 2G_{12} (1 - \nu_{12}^2) \frac{E_2}{E_1} \right]}{(E_1 + E_2)} \quad (17)$$

By using the simplest micromechanical relations [7]:

$$E_1 = E_f V_f + E_m V_m$$

$$E_2 = \frac{E_f E_m}{V_f E_f + V_m E_m}$$

$$G_{12} = \frac{G_m G_f}{V_m G_f + V_f G_m}$$

$$\nu_{12} = \nu_f V_f + \nu_m (1 - V_f)$$

D^* may be expressed as a function of V_f , E_f/E_m and ν_f and ν_m .

If k_o is plotted vs. T it is noticed that $k_o \min$ occurs at $T = 1$.
 Therefore, for a given aspect ratio a/b the value of m which makes T
 closer to 1 will give the minimum buckling load.

Lower Bound for Buckling Load

The function $F2$ expressed as a function of D^* and ϵ is as
 follows:

$$F2 = \frac{T^6 + T^2 + \frac{D^*}{2} [(T^4+1)^2 - (T^4-1)^2\epsilon]}{T^2 \left\{ T^2 + \frac{D^*}{2} [(1-\epsilon)(1+T^4) - 2\epsilon D^* T^2] \right\}}$$

$D^* = 0$ gives the lower bound value for $F2$ which is:

$$F2)_{D^*=0} = T^2 + \frac{1}{T^2}$$

and hence from Eqn. (10)

$$k_o = T^2 + \frac{1}{T^2} - \left(T^2 + \frac{1}{T^2} \right) DB$$

DB will have a maximum value for minimum number of layers which
 is 2 and

$$\left(\frac{F-1}{F+1} \right)^2 = 1$$

Therefore,

$$\begin{aligned} k_o \text{ lower bound} &= T^2 + \frac{1}{T^2} - \left(T^2 + \frac{1}{T^2} \right) \frac{3}{(2)^2} \\ &= 0.25 \left(T^2 + \frac{1}{T^2} \right) \end{aligned} \tag{16}$$

Making these substitutions for A^* and A , the function F_2 (now a function of D^* and ϵ alone) can be expressed as follows:

$$F_2 = \frac{T^6 + T^2 + \frac{D^*}{2} [(T^4+1)^2 - (T^4-1)^2 \epsilon]}{T^2 \left\{ T^2 + \frac{D^*}{2} [(1-\epsilon)(1+T^4) - 2\epsilon D^* T^2] \right\}} \quad (14)$$

DB as a Function of N and F

Making use of the stiffnesses displayed by Tsai⁵ DB can be expressed as a simple function of N the (number of layers) and F the ratio of principal lamina stiffnesses.

$$DB = \frac{B_{11}}{D_{11}} \frac{B_{11}}{A_{11}}$$

$$DB = \frac{3}{N^2} \left(\frac{F-1}{F+1} \right)^2 \quad (15)$$

DB vs F is plotted in Fig. 1. The value of DB is less than 0.1 for six or more layers regardless of the value of F . Also for values of F greater than 0.5 the value of DB is less than 0.1 for any number of layers. However, for F less than 0.5 and 2 or 4 layers, the value of DB cannot be ignored.

Minimum Buckling Load

The minimum buckling coefficient $k_{o \min}$ is obtained by substituting $n=1$ in the expression for T and then searching through different m 's to get the minimum value of k_o . T for $n=1$ reduces as

$$T_{n=1} = \frac{a/b}{m}$$

and

$$DB = \frac{B_{11}}{D_{11}} \cdot \frac{B_{11}}{A_{11}} \quad (13)$$

Note that the first term in the equation (10) is the buckling load for the specially orthotropic laminate. And F2 which is a function of A, A*, and T only, is being multiplied per unit DB.

F2 in Terms of D* and ε

The function F2 can be expressed purely as a function of D* and the generalized Poissons ratio ε. Using the stiffness displayed by Tsai⁵ for antisymmetric cross-ply laminates with an even number of alternating 0 - 90 layers,

$$D^* = \frac{2(Q_{12} + 2Q_{66})}{(1+F)Q_{11}}$$

$$A^* = \frac{2(Q_{12} + Q_{66})}{(1+F)Q_{11}}$$

$$A = \frac{2Q_{66}}{(1+F)Q_{11}}$$

$$\epsilon = \frac{Q_{12}}{Q_{12} + 2Q_{66}}$$

Using the above relations, A* and A can be represented as functions of D* and ε:

$$A^* = \left(\frac{1+\epsilon}{2} \right) D^*$$

$$A = \left(\frac{1-\epsilon}{2} \right) D^*$$

$$\frac{\partial^4 w}{\partial x^4} + 2D^* \frac{\partial^4 w}{\partial x^2 \partial y^2} + \frac{\partial^4 w}{\partial y^4} + \frac{\bar{N}_x}{D_{11}} \frac{\partial^2 w}{\partial x^2} - D \left(\frac{\partial^3 u}{\partial x^3} - \frac{\partial^3 v}{\partial y^3} \right) = 0 \quad (6)$$

The following variations in deflections satisfy the B.C.'s for simply supported edge boundary condition S2:

$$u = U \cos \frac{m\pi x}{a} \sin \frac{n\pi y}{b}$$

$$v = V \sin \frac{m\pi x}{a} \cos \frac{n\pi y}{b}$$

$$w = W \sin \frac{m\pi x}{a} \sin \frac{n\pi y}{b}$$

Making these substitutions and defining $\frac{na}{mb} = T$, similarity parameter

the equations reduce to the following:

$$[1 + AT^2]U + [A^*T]V - \left[B\pi \left(\frac{m}{a} \right) \right] W = 0 \quad (7)$$

$$[A^*T]U + [A + T^2]V + \left[B\pi \left(\frac{n}{b} \right) T^2 \right] W = 0 \quad (8)$$

$$[-D]U + [DT^3]V + \pi \left(\frac{m}{a} \right) T^2 \left[T^2 + 2D^* + \frac{1}{T^2} - \frac{\bar{N}_x}{\pi^2 D_{11}} \left(\frac{b}{n} \right)^2 \right] W = 0 \quad (9)$$

The governing differential equation is exactly satisfied if:

$$k_o = \left[T^2 + 2D^* + \frac{1}{T^2} \right] - (F2) (DB) \quad (10)$$

where a buckling coefficient is defined as

$$k_o = \frac{\bar{N}_x}{\pi^2 D_{11}} \left(\frac{b}{n} \right)^2 \quad (11)$$

$$F2 = \frac{(1+AT^2)T^6 + 2A^*T^4 + A + T^2}{T^2[(1+AT^2)(A+T^2) - (A^*T^2)]} \quad (12)$$

II. Theory

Buckling

The new terms in the antisymmetric cross-ply laminate buckling differential equation in comparison to a specially orthotropic laminate are B_{11} and B_{22} . Because of this bending extension coupling, the buckling differential equations are coupled [4]:

$$A_{11} \frac{\partial^2 u}{\partial x^2} + A_{66} \frac{\partial^2 u}{\partial y^2} + (A_{12} + A_{66}) \frac{\partial^2 v}{\partial x \partial y} - B_{11} \frac{\partial^3 w}{\partial x^3} = 0 \quad (1)$$

$$(A_{12} + A_{66}) \frac{\partial^2 u}{\partial x \partial y} + A_{66} \frac{\partial^2 v}{\partial x^2} + A_{11} \frac{\partial^2 v}{\partial y^2} + B_{11} \frac{\partial^3 w}{\partial y^3} = 0 \quad (2)$$

$$D_{11} \frac{\partial^4 w}{\partial x^4} + 2(D_{12} + 2D_{66}) \frac{\partial^4 w}{\partial x^2 \partial y^2} + D_{22} \frac{\partial^4 w}{\partial y^4} - B_{11} \left(\frac{\partial^3 u}{\partial x^3} - \frac{\partial^3 v}{\partial y^3} \right) + \bar{N}_x \frac{\partial^2 w}{\partial x^2} = 0 \quad (3)$$

For the antisymmetric cross-ply laminates

$$A_{22} = A_{11} \quad B_{22} = -B_{11} \quad \text{and} \quad D_{22} = D_{11}$$

Defining:

$$\frac{A_{66}}{A_{11}} = A, \quad \frac{A_{12} + A_{66}}{A_{11}} = A^*, \quad \frac{B_{11}}{A_{11}} = B, \quad \frac{B_{11}}{D_{11}} = D, \quad \frac{D_{12} + 2D_{66}}{D_{11}} = D^*$$

Making the above substitutions the equations simplify to the following:

$$\frac{\partial^2 u}{\partial x^2} + A \frac{\partial^2 u}{\partial y^2} + A^* \frac{\partial^2 v}{\partial x \partial y} - B \frac{\partial^3 w}{\partial x^3} = 0 \quad (4)$$

$$A^* \frac{\partial^2 u}{\partial x \partial y} + A \frac{\partial^2 v}{\partial x^2} + \frac{\partial^2 v}{\partial y^2} + B \frac{\partial^3 w}{\partial y^3} = 0 \quad (5)$$

PART I

ANTISYMMETRIC CROSS-PLY

resulting partial differential equation contains only three materials constants; D^* called the generalized rigidity ratio; ϵ , called the generalized Poissons ratio; and F ; which is the ratio of the principal lamina stiffnesses. The number of layers is of course another variable which cannot be possibly absorbed into the constants.

Furthermore, the value of D^* is in the closed interval from 0 to 1 [2]. Other than the ratio of principal lamina stiffnesses the buckling and vibration solution are strongly dependent upon D^* . The generalized Poissons ratio, ϵ , is a weak parameter and influences the solutions slightly. The general range of ϵ for most modern composite materials is 0.15 to 0.35.

The thesis is divided into two parts, the first dealing with antisymmetric cross-ply and the second with antisymmetric angle-ply laminates. The vibration and buckling solutions for antisymmetric cross-ply are comparatively much simpler than those for antisymmetric angle-ply laminates where, in addition to the bending extension coupling stiffnesses B_{16} and B_{26} , the angle of orientation of principal material properties with respect to the laminate axes and the plate aspect ratio becomes another parameter.

many physical applications of laminated composites require non-symmetric laminates to achieve design requirements. For example, coupling is a necessary feature to make jet turbine fan blades with a pretwist.

Antisymmetric laminates have geometric symmetry and material property antisymmetry about the middle surface. Antisymmetric cross-ply laminates consist of an even number of orthotropic lamina laid on each other with principal material directions alternating at 0° and 90° to the laminate axes. Antisymmetric angle-ply laminates have lamina oriented at $+\theta$ degrees to the laminate coordinate axes on one side of the middle surface and corresponding equal thickness lamina oriented at $-\theta$ degrees on the other side. Because of the geometric symmetry and material property antisymmetry, certain stiffness simplifications are possible for antisymmetric laminates.

The known buckling and vibration solutions for antisymmetric cross-ply and antisymmetric angle ply rectangular laminates are few in number. These solutions do not give a good overview of how solutions depend on individual constants. The reason for this is the large number of constants associated with composite laminates.

The use of affine transformations [3] and similarity variable minimizes the number of parameters in the solutions, thus allowing one to see and predict solution trends with the variation of certain constants. Transformations of the form $x = Ax_0$ and $y = By_0$ transform the differential equations into an affine space, and the

SOLUTION TO EIGENVALUE PROBELMS OF ANTISYMMETRIC CROSS-PLY
AND ANTISYMMETRIC ANGLE-PLY LAMINATED PLATES
USING AFFINE TRANSFORMATIONS

I. Introduction

Laminated plates are an important structural element in both the aerospace and electronics industries. In aerospace applications where weight savings are of paramount importance, the advent of advanced fiber reinforced composite materials such as boron/epoxy and graphite/epoxy has resulted in dramatic increase in the use of laminated fiber-reinforced plates and other structural shapes. The composite materials are typically a combination of a usually light, weak, and flexible matrix material with a more dense, very strong, and stiff reinforcing material in fibrous or whisker form. Hence, high strength-to-weight and stiffness-to-weight ratios are readily obtained. Lamination asymmetry can result in coupling between bending and extension of the laminate. This phenomenon is evidenced by bending of a laminate that is subjected to only in-plane forces or extension of a laminate that is bent by application of moments only.

Symmetry of a laminate about the middle surface is often desirable to avoid coupling between bending and extension. However,

Abstract

Using affine transformations and suitably recasting the buckling and vibration differential equations, the eigenvalue problem of anti-symmetric cross-ply and antisymmetric angle-ply laminated rectangular plates has been reduced to a function of two strong material constants, the generalized rigidity ratio, whose range is in the closed interval from 0 to 1, and the ratio of principal lamina stiffnesses.

With the reduction in number of constants an exhaustive parameter study of buckling and vibration solution trends, is possible. The buckling coefficients decrease with decreasing value of generalized rigidity ratio for both antisymmetric cross-ply and antisymmetric angle-ply laminates. For a given aspect ratio, and ratio of principal lamina stiffnesses, the buckling and frequency coefficient for antisymmetric cross-ply laminates vary linearly with the value of the generalized rigidity ratio, so that one may accurately interpolate between the values of the generalized rigidity ratio.

The buckling and frequency coefficients increase with increasing value of the ratio of principal lamina stiffnesses for antisymmetric cross-ply laminates. No such trend could be established for anti-symmetric angle-ply laminates.

A simple and fairly accurate method has been established for estimating the buckling and vibration coefficients for anti-symmetric cross-ply laminates.

List of Tables

| Table | | Page |
|-------|-------------------------------|------|
| I | Material Properties | 49 |

noticed that G is asymptotic to $2 \left(\frac{1-2\varepsilon}{1-\varepsilon} \right) D^*$. The deviation of G from its asymptotic value is maximum at $T=1$ and is small otherwise. The deviation increases with increasing value of ε . If the value of the constant G is approximated by its asymptotic value then the error in the value of F_2 is of the order of 2% for $D^*=0.5$ at $T=1$ and $\varepsilon=0.25$, and 4.7% for $\varepsilon=0.35$. The error is even lesser for other values of T . Therefore, the error introduced in the value of F_2 by approximating G by its asymptotic value of $2 \left(\frac{1-2\varepsilon}{1-\varepsilon} \right) D^*$ is indeed negligible. It may also be remembered that F_2 is multiplied by DB , the value of which is less than one, thereby further reducing the total error in the buckling coefficient.

Vibration

Again the new terms here in comparison to a specially orthotropic laminate are B_{11} and B_{22} (B_{22} being equal to $-B_{11}$). Because of this bending-extension coupling, the vibration differential equations are coupled:

$$A_{11} \frac{\partial^2 u}{\partial x^2} + A_{66} \frac{\partial^2 u}{\partial y^2} + (A_{12} + A_{66}) \frac{\partial^2 v}{\partial x \partial y} - B_{11} \frac{\partial^3 w}{\partial x^3} = 0 \quad (22)$$

$$(A_{12} + A_{66}) \frac{\partial^2 u}{\partial x \partial y} + A_{66} \frac{\partial^2 v}{\partial x^2} + A_{11} \frac{\partial^2 v}{\partial y^2} + B_{11} \frac{\partial^3 w}{\partial y^3} = 0 \quad (23)$$

$$D_{11} \left(\frac{\partial^4 w}{\partial x^4} + \frac{\partial^4 w}{\partial y^4} \right) + 2(D_{12} + 2D_{66}) \frac{\partial^4 w}{\partial x^2 \partial y^2} - B_{11} \left(\frac{\partial^3 u}{\partial x^3} - \frac{\partial^3 v}{\partial y^3} \right) + \rho \frac{\partial^2 w}{\partial t^2} = 0 \quad (24)$$

As stated earlier antisymmetric cross-ply laminates have extensional stiffnesses A_{11} , A_{12} , $A_{22} = A_{11}$, and A_{66} , bending extension coupling stiffnesses B_{11} and $B_{22} = -B_{11}$, and bending stiffnesses D_{11} , D_{22} , $D_{22} = D_{11}$, and D_{66} .

Defining the constants A^* , A , B , D , D^* , and T in the same way as in the buckling differential equations and using variations in displacement:

$$\begin{aligned} u &= U \cos \frac{m\pi x}{a} \sin \frac{n\pi y}{b} e^{i\omega t} \\ v &= V \sin \frac{m\pi x}{a} \cos \frac{n\pi y}{b} e^{i\omega t} \\ w &= W \sin \frac{m\pi x}{a} \sin \frac{n\pi y}{b} e^{i\omega t} \end{aligned}$$

which satisfy simply supported edge boundary condition S2 at all times, the vibration differential equations reduce to the following form:

$$[1 + AT^2]U + [A^*T]V - B\pi \left(\frac{m}{a} \right) W = 0 \quad (25)$$

$$[A^*T]U + [A + T^2]V + B\pi \left(\frac{n}{b} \right) T^2 W = 0 \quad (26)$$

$$[-D]U + [DT^3]V + T^4 \left(\frac{m}{a} \right) \left[1 + \frac{2D^*}{T^2} + \frac{1}{T^4} - \frac{\rho\omega^2}{D_{11}\pi^4} \left(\frac{b}{n} \right)^2 \right] (W\pi) = 0 \quad (27)$$

$$\frac{\Omega_{mn}^2}{n^4} = \left\{ 1 + \frac{2D^*}{T^2} + \frac{1}{T^4} \right\} - \frac{(F2)(DB)}{T^2} \quad (28)$$

where

$$\Omega_{mn}^2 = \frac{\rho \omega_{mn}^2}{D_{11}} \left(\frac{b}{\pi} \right)^4 \quad (29)$$

and F2 and DB are the same as in the buckling case.

Again, it may be noted that the first term in the equation is the frequency coefficient for the specially orthotropic laminate and $F2/T^2$ is being multiplied per unit DB.

Lower Bound of Vibration Frequency

Again, the function F2 expressed as a function of D^* , ϵ and T is:

$$F2 = \frac{T^6 + T^2 + \frac{D^*}{2} [(T^4+1)^2 - (T^4-1)^2 \epsilon]}{T^2 \left\{ T^2 + \frac{D^*}{2} [(1-\epsilon)(1+T^4) - 2\epsilon D^* T^2] \right\}}$$

Since the range of generalized rigidity ratio D^* is the closed interval from 0 to 1, the minimum value of D^* gives the lowest vibration frequencies and thus the lower bound for

$$\left. \frac{F2}{T^2} \right)_{D^*=0} = 1 + \frac{1}{T^4} \quad (30)$$

and again DB can have a maximum value of 3/4 and hence:

$$\frac{\Omega_{mn}^2}{n^4} \text{ lower bound} = 0.25 \left(1 + \frac{1}{T^4} \right) \quad (31)$$

Approximation of F_2/T^2

In a manner similar to the buckling problem F_2/T^2 can be approximated by:

$$\frac{F_2}{T^2} = \left(\frac{\Omega_{mn}^2}{n} \right) SOT^{-2D^*} \left(\frac{1-2\epsilon}{1-\epsilon} \right) / T^2 \quad (32)$$

The above approximation gives an error of 4.7% in the value of F_2/T^2 and 3.3% in the value of Ω_{mn}^2/n^4 for $T = 1$, $D^* = .5$, $\epsilon = 0.35$ and $DB = 0.5$. In most cases the error would be much less than the above case.

III. Results and Discussion

The eigenvalue problem of antisymmetric cross-ply laminated plate has been reduced to a function of three material parameters D^* , F , and ϵ and the similarity parameter T . This has been done by simply recasting the equation in a suitable manner. An affine transformation was not necessary to reduce the number of constants because for this particular lay up $D_{11} = D_{22}$, and the simplification introduced by affine transformation can be obtained by simply dividing the transverse differential equations by D_{11} or D_{22} .

With the eigenvalue problem reduced to a function of two strong material parameters D^* and F , it is now possible to do an exhaustive parameter study of buckling and vibration solution trends.

There is an enormous payoff in using T as a parameter specially in the vibration solutions, because T has in it the variables m , n and aspect ratio a/b . For a given material, one curve of frequency vs. T gives the complete spectrum of vibration solutions.

Effect of Variation of D^*

a) Buckling

The effect of variation of D^* on the buckling solution can be studied by fixing a value of DB and then varying D^* . Once the value of DB is fixed, the buckling coefficient remains

a function of D^* and ϵ alone. ϵ is a weak parameter and it does effect the solution, but minimally, as will be shown later. The value of ϵ can however, be fixed to some nominal value, i.e., 0.2

The buckling coefficient decreases with decreasing D^* as shown in Figs. 5 and 6 for DB of 0.1 and 0.4 respectively. It is also noticed that for a given aspect ratio the $k_{o \min}$ vs. D^* curves vary almost linearly, so that one may accurately interpolate between the D^* values.

b) Vibration

For a fixed value of DB, the frequency decreases with decreasing value of D^* . Here again, for a given value of the similarity parameter, the $\frac{\Omega mn^2}{n^4}$ vs. T curves vary almost linearly, so that one may accurately interpolate between the D^* values. Figs. 7 and 8 show $\frac{\Omega mn^2}{n^4}$ vs. T curves for DB of 0.1 and 0.4 respectively.

Effect of Variation of F

a) Buckling

DB is related to F as follows:

$$DB = \frac{3}{N^2} \left(\frac{F-1}{F+1} \right)^2$$

The relationship between DB and F is graphically shown in Fig. 1. For a given number of layers the value of DB decreases with increasing value of F. And from Eqn. (10) a lower value of DB

means a higher buckling coefficient. Therefore, the buckling load increases with increasing value of F.

$k_{o \min}$ vs. F for a square plate with a D^* of 0.5 and ϵ of 0.2 is shown in Fig. 9.

b) Vibration

The effect of a variation of F on the frequency is similar to its effect on buckling coefficient. The frequency increases with increasing value of F. The frequency coefficient vs. F curve for an T of 1 is shown in Fig. 9. It may be noted that for a square plate, T=1 gives the minimum buckling coefficient and hence the same curves apply to vibration as well as buckling.

Lower Bound for Buckling

The lower bound for the buckling load is given by Eqn. (16) which transforms as follows for $n = 1$

$$k_{o \min \text{ lower bound}} = 0.25 \left[\left(\frac{a/b}{m} \right)^2 + \left(\frac{m}{a/b} \right)^2 \right] \quad (33)$$

The above equation solved for the lower bound envelope is shown in Fig. 10. This is a very significant result because the lower bound is material independent and thus forms the absolute minimum for any antisymmetric cross-ply laminated plate.

Lower Bound for Vibration

The lower bound envelope for vibration is given by Eqn. (31)

and is shown in Fig. 11 . This lower bound again is material independent. The lower bound is plotted vs. the similarity parameter because of the advantage of using T.

Approximation of Buckling Load

The function F2 can be approximated by

$$F2 = k_o \text{ SOT} - 2 \left(\frac{1-2\varepsilon}{1-\varepsilon} \right) D^*$$

Now if the specially orthotropic buckling coefficient is also approximated as $k_o)_{\min} \text{ SOT} = 2(D^* - 1) [1]$ then

$$k_o \text{ min} = 2D^* \left(1 - \frac{\varepsilon DB}{1-\varepsilon} \right) + 2(1-DB) \quad (34)$$

For a given material D^* , ε and F are known and a very good approximation of $k_o \text{ min}$ can be obtained using Equation (34). The error because of this approximation is indeed minimal.

For a square 2 layered Graphite Epoxy laminate [7] ($D^*=0.0609$, $\varepsilon=0.2003$, $F=0.025$, $\frac{t}{b}=0.01$) the above approximation underestimates the buckling stress by 0.527%. And for 4 layers the underestimation is only .055%.

As illustrated by this example, the approximation is fairly accurate and can be conveniently used to get a good estimate of the minimum buckling stress for a rectangular antisymmetric cross-ply laminated plate.

The approximation can also be used to get an estimate of the vibration frequency for a given material. In this case, however, there is no approximation for $\frac{\Omega_{mn}^2}{n^4} \Big|_{SOT}$ and this value will have to be calculated or read from a standard graph.

Effect of ϵ on k_o

As stated earlier, the generalized Poissons ratio is a weak parameter and its range for most modern composite materials is limited from 0.15 to 0.35. Within this range the effect of ϵ on buckling load is indeed minimal. For a given value of D^* and DB a variation in ϵ shifts the complete buckling solution up or down by almost a constant amount. The shift is of the order of only 0.5 - 1.5% of the value of the buckling coefficient. The $(k_o)_{\min}$ vs. aspect ratio for an ϵ of 0.15 and 0.35 is shown in Fig. 12.

Since ϵ occurs only in F2, the variation of F2 with ϵ was studied. The function F2 plotted vs. T for a fixed value of D^* and $\epsilon = 0.15, 0.35$ is shown in Fig. 13. It is noticed that F2 increases with increasing ϵ . And since F2 times DB is subtracted off from the specially orthotropic buckling coefficient, the higher the value of F2, the smaller will be the buckling coefficient for an anti-symmetric cross-ply. Therefore, k_o decreases with increasing ϵ . This is consistent with [1].

Also the constant G for a fixed value of D^* decreases with increasing value of ϵ . See Fig. 4 where G is plotted vs. T for

$D^* = 0.5$. From Eqn. (20) [$F_2 = k_o SOT - G$], the smaller the value of G , higher the value of F_2 and consequently the smaller the value of k_o .

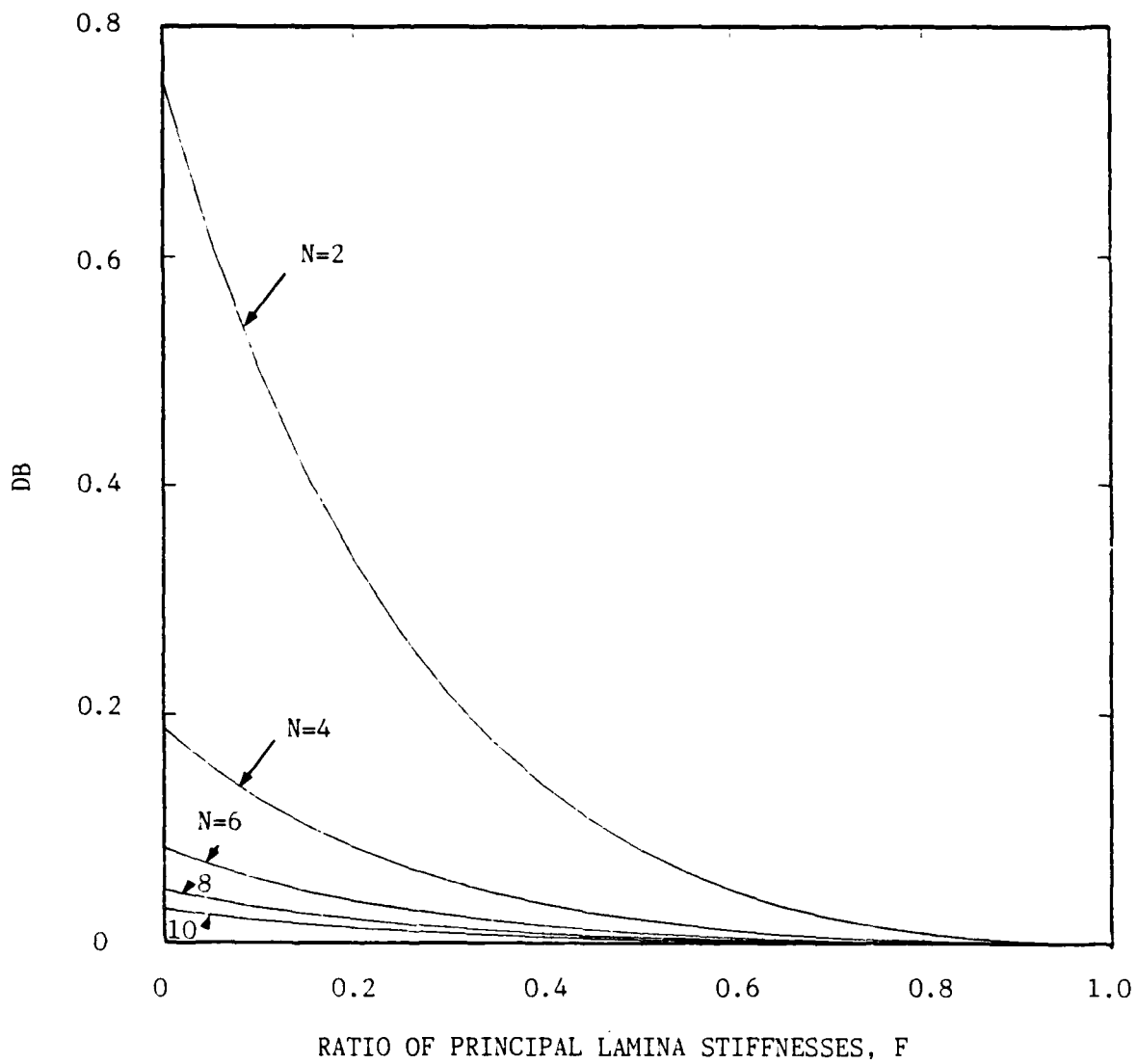


Fig. 1 . DB vs. Ratio of Principal Lamina Stiffnesses With Number of Layers as a Parameter

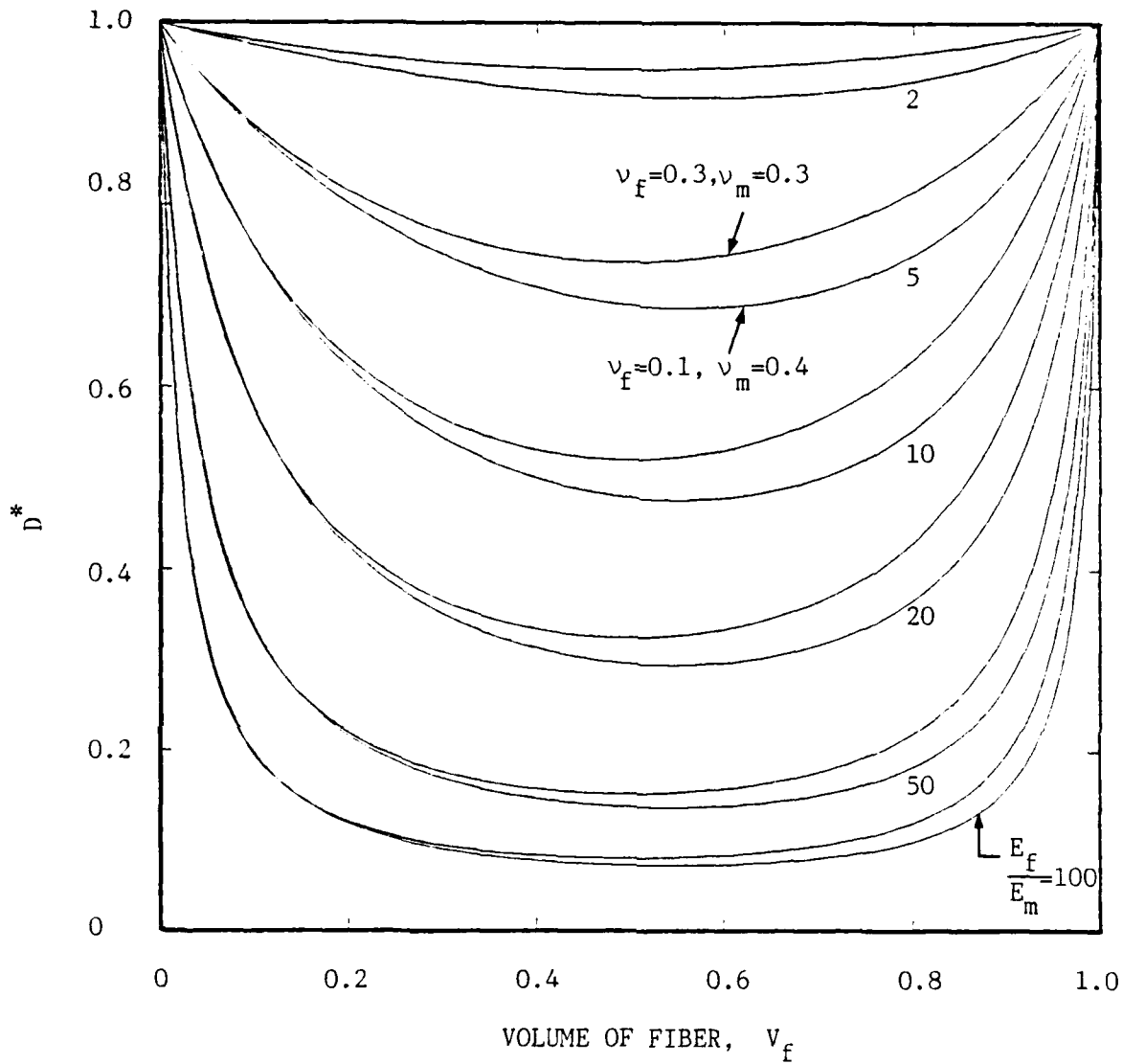


Fig. 2. D^* vs. Volume of Fiber with E_f/E_m as a Parameter

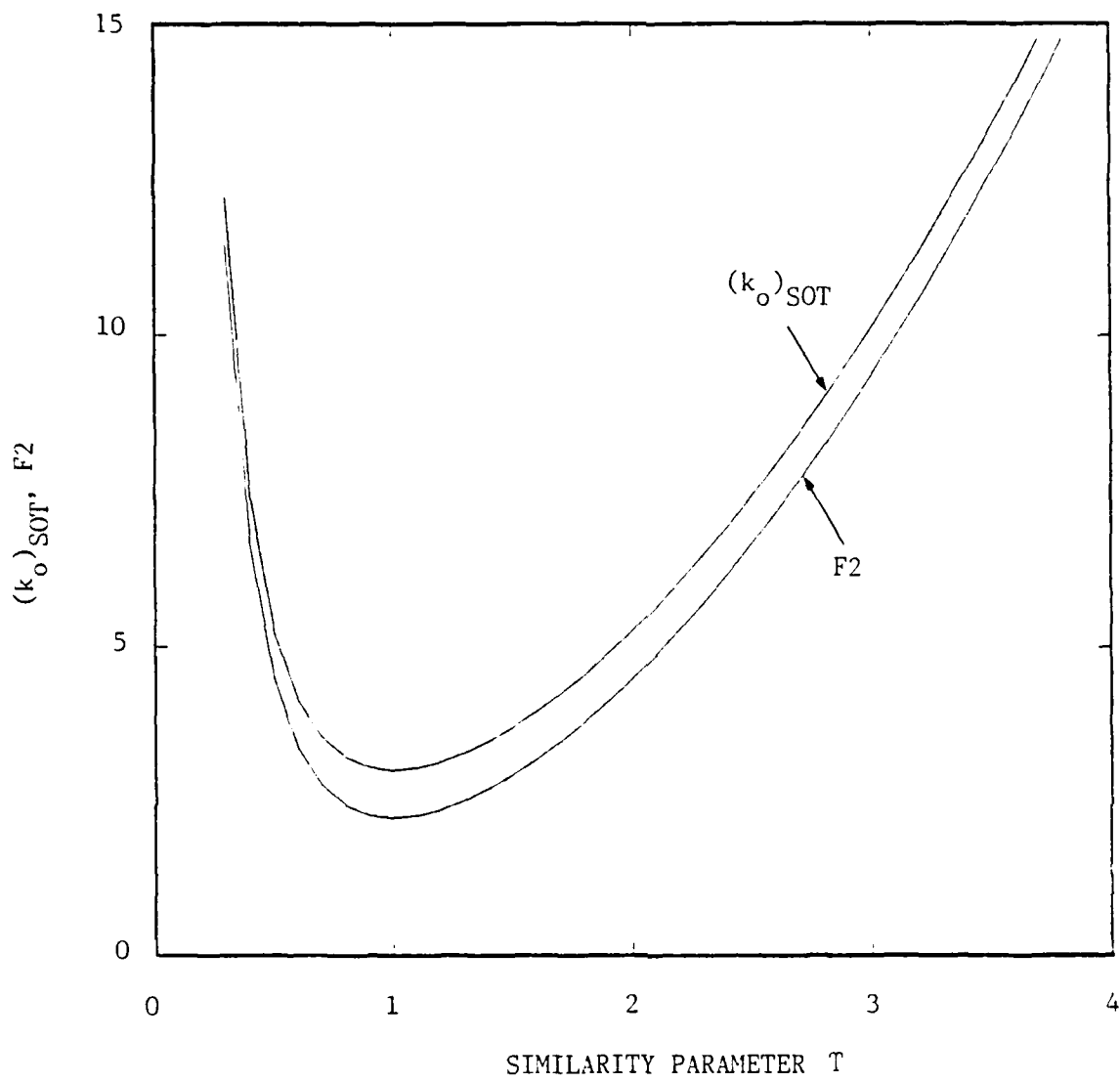


Fig. 3 . Specially Orthotropic Buckling Coefficient and F2 vs. Similarity Parameter, $D^*=0.5$

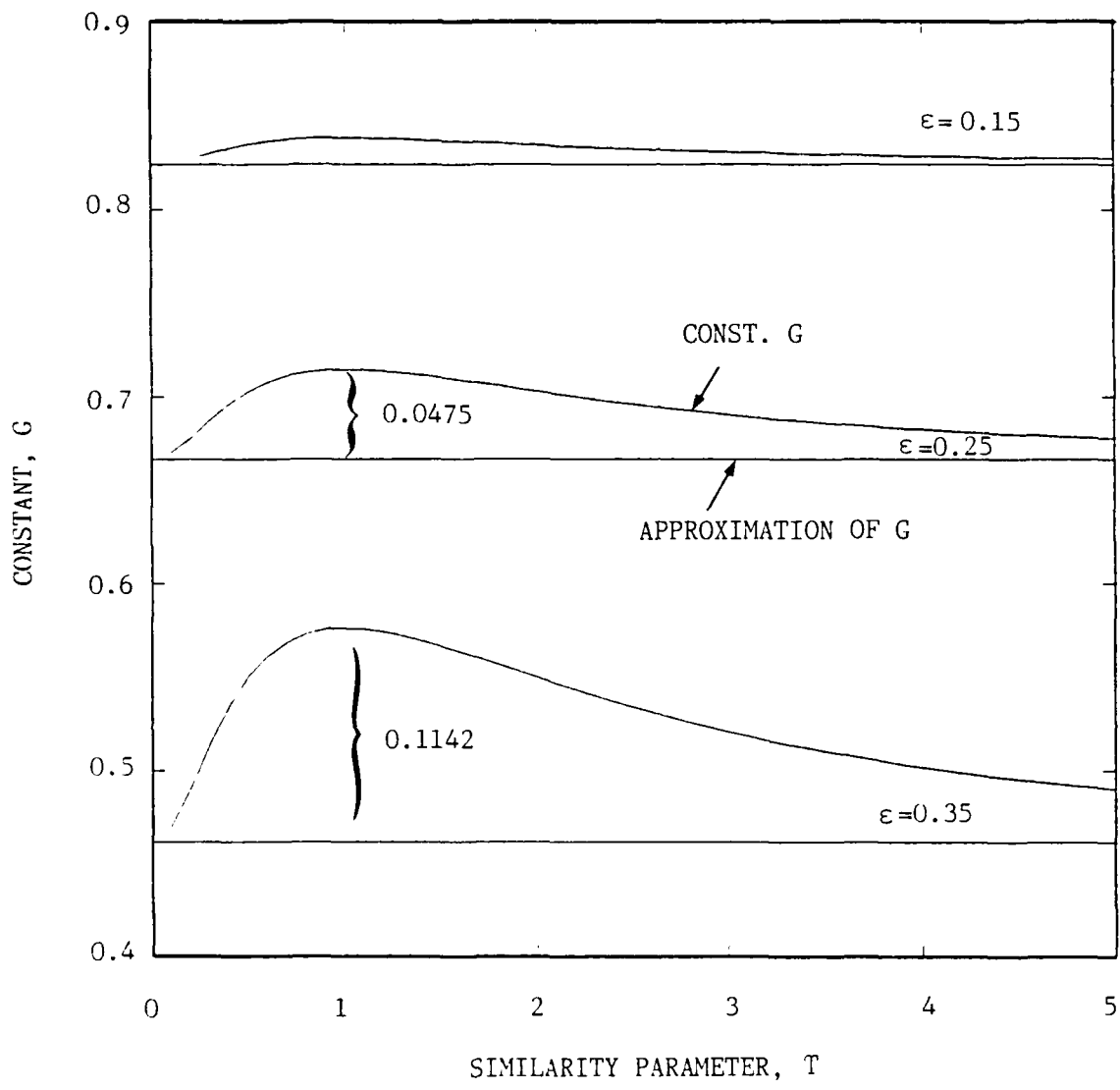


Fig. 4 . Constant G vs. Similarity Parameter with T as a Parameter $D^{**} = 0.5$

Using the stiffnesses displayed by Tsai [5]

$$A_{11}, A_{12}, A_{22}, A_{66} = t (\bar{Q}_{11}, \bar{Q}_{12}, \bar{Q}_{22}, \bar{Q}_{66})$$

$$B_{16}, B_{26} = -\frac{t^2}{2N} (\bar{Q}_{16}, \bar{Q}_{26})$$

$$D_{11}, D_{12}, D_{22}, D_{66} = \frac{t^3}{12} (\bar{Q}_{11}, \bar{Q}_{12}, \bar{Q}_{22}, \bar{Q}_{66})$$

and defining

$$D_o^* = \frac{D_{12} + 2D_{66}}{(D_{11}D_{22})^{\frac{1}{2}}}_{\theta=0} = \frac{Q_{12} + 2Q_{66}}{(Q_{11}Q_{22})^{\frac{1}{2}}}$$

$$D^* = \frac{D_{12} + 2D_{66}}{(D_{11}D_{22})^{\frac{1}{2}}}_{\theta=0} = \frac{\bar{Q}_{12} + 2\bar{Q}_{66}}{(Q_{11}Q_{22})^{\frac{1}{2}}}$$

$$\epsilon_o = \frac{D_{12}}{D_{12} + 2D_{66}}_{\theta=0} = \frac{Q_{12}}{Q_{12} + 2Q_{66}}$$

$$\epsilon = \frac{D_{12}}{D_{12} + 2D_{66}} = \frac{\bar{Q}_{12}}{Q_{12} + 2\bar{Q}_{66}}$$

$$K = \left(\frac{D_{11}}{D_{22}} \right)^{\frac{1}{2}}_{\theta=0} = \left(\frac{Q_{11}}{Q_{22}} \right)^{\frac{1}{2}} = \left(\frac{E_1}{E_2} \right)^{\frac{1}{2}}$$

$$S = (Q_{11}Q_{22})^{\frac{1}{2}}$$

Equations (7), (8), and (9) transform as follows:

$$\begin{aligned} -K^{\frac{1}{2}} \left[\frac{\bar{Q}_{11}}{Q_{11}} + \left(\frac{1-\epsilon}{2} \right) D^* T^2 \right] U_o - T \left[D^* \left(\frac{1+\epsilon}{2} \right) \right] V_o \\ - \left(\frac{n}{b} \right) \frac{Q_{22}^{\frac{1}{2}}}{N} \left[\frac{3\bar{Q}_{16}}{S} + \frac{\bar{Q}_{26}}{S} K T^2 \right] W_o = 0 \quad (10) \end{aligned}$$

and hence the plate dimensions a and b transform as

$$a = (D_{11})_{\theta=0}^{\frac{1}{2}} a_0, \quad b = (D_{22})_{\theta=0}^{\frac{1}{2}} b_0 \quad \text{so that the plate aspect ratio}$$

transforms as

$$a/b = (D_{11}/D_{22})_{\theta=0}^{\frac{1}{2}} (a_0/b_0).$$

Equations (4), (5), and (6) become

$$\begin{aligned} - \left[\frac{A_{11}}{(D_{11})_{\theta=0}^{\frac{1}{2}}} + \frac{A_{66}}{(D_{22})_{\theta=0}^{\frac{1}{2}}} T^2 \right] U - \left[\frac{(A_{12}+A_{66})}{(D_{11}D_{22})_{\theta=0}^{\frac{1}{2}}} T \right] V + \\ \frac{n\pi}{b_0} \left[\frac{3B_{16}}{(D_{11}^{\frac{3}{2}} D_{22}^{\frac{1}{2}})_{\theta=0}} + \frac{B_{26}}{(D_{22})_{\theta=0}^{3/4}} T^2 \right] W = 0 \quad (7) \end{aligned}$$

$$\begin{aligned} - \left[\frac{(A_{12}+A_{66})}{(D_{11}D_{22})_{\theta=0}^{\frac{1}{2}}} T \right] U - \left[\frac{A_{66}}{(D_{11})_{\theta=0}^{\frac{1}{2}}} + \frac{A_{22}}{(D_{22})_{\theta=0}^{\frac{1}{2}}} T^2 \right] V + \\ \frac{m\pi}{a_0} \left[\frac{B_{16}}{(D_{11})_{\theta=0}^{3/4}} + \frac{3B_{26}}{(D_{11}^{\frac{1}{2}} D_{22}^{\frac{3}{2}})_{\theta=0}} \right] W = 0 \quad (8) \end{aligned}$$

$$\begin{aligned} - \left\{ \frac{3B_{16}}{(D_{11}^{\frac{3}{2}} D_{22}^{\frac{1}{2}})_{\theta=0}} + \frac{B_{26}}{(D_{22})_{\theta=0}^{3/4}} T^2 \right\} U - \frac{1}{T} \left\{ \frac{B_{16}}{(D_{11})_{\theta=0}^{3/4}} + \frac{3B_{26}}{(D_{11}^{\frac{1}{2}} D_{22}^{\frac{3}{2}})_{\theta=0}} T^2 \right\} V \\ + \frac{\pi T}{a_0} \left\{ \frac{D_{11}}{(D_{11})_{\theta=0}} \frac{1}{T^2} + \frac{2(D_{12}+2D_{56})}{(D_{11}D_{22})_{\theta=0}} + \frac{D_{22}}{(D_{22})_{\theta=0}} T^2 \right. \\ \left. - \frac{\bar{N}_x}{\pi^2 (D_{11})_{\theta=0}^{\frac{1}{2}}} \left(\frac{b_0}{n} \right)^2 \right\} W = 0 \quad (9) \end{aligned}$$

satisfy the S3 boundry conditions and also satisfy the governing differential equation. Substituting these variations in displacements into the governing differential equation.

$$\begin{aligned}
 & - A_{11} \left(\frac{m\pi}{a}\right)^2 U - A_{66} \left(\frac{n\pi}{b}\right)^2 U - (A_{12} + A_{66}) \left(\frac{m\pi}{a}\right) \left(\frac{n\pi}{b}\right) V + \\
 & 3B_{16} \left(\frac{m\pi}{a}\right)^2 \left(\frac{n\pi}{b}\right) W + B_{26} \left(\frac{n\pi}{b}\right)^3 W = 0 \quad (4)
 \end{aligned}$$

$$\begin{aligned}
 & - (A_{12} + A_{66}) \left(\frac{m\pi}{a}\right) \left(\frac{n\pi}{b}\right) U - A_{66} \left(\frac{m\pi}{a}\right)^2 V - A_{22} \left(\frac{n\pi}{b}\right)^2 V \\
 & + B_{16} \left(\frac{m\pi}{a}\right)^3 W + 3B_{26} \left(\frac{m\pi}{a}\right) \left(\frac{n\pi}{b}\right)^2 W = 0 \quad (5)
 \end{aligned}$$

$$\begin{aligned}
 & D_{11} \left[\left(\frac{m\pi}{a}\right)^4 + 2(D_{12} + 2D_{66}) \left(\frac{m\pi}{a}\right)^2 \left(\frac{n\pi}{b}\right)^2 + D_{22} \left(\frac{n\pi}{b}\right)^4 \right] W \\
 & - B_{16} \left[3 \left(\frac{m\pi}{a}\right)^2 \left(\frac{n\pi}{b}\right) U + \left(\frac{m\pi}{a}\right)^3 V \right] - B_{26} \left[\left(\frac{n\pi}{b}\right)^3 U + 3 \left(\frac{m\pi}{a}\right) \left(\frac{n\pi}{b}\right)^2 V \right] \\
 & - \bar{N}_x \left(\frac{m\pi}{a}\right)^2 W = 0 \quad (6)
 \end{aligned}$$

Introducing

$$x \equiv (D_{11})_{\theta=0}^{\frac{1}{2}} \text{ deg. } x_0$$

$$y \equiv (D_{22})_{\theta=0}^{\frac{1}{2}} \text{ deg. } y_0$$

$$T = \frac{na_0}{mb_0}$$

IV. Theory

Buckling

Antisymmetric angle-ply laminates have extensional stiffnesses A_{11} , A_{12} , A_{22} and A_{66} , bending extension coupling stiffnesses B_{16} and B_{26} , and bending stiffnesses D_{11} , D_{12} , D_{22} and D_{66} . Thus, this type of laminate exhibits a different kind of bending extension coupling than does the antisymmetric cross-ply laminate.

The buckling differential equations are [7]:

$$A_{11} \frac{\partial^2 u}{\partial x^2} + A_{66} \frac{\partial^2 u}{\partial y^2} + (A_{12} + A_{66}) \frac{\partial^2 v}{\partial x \partial y} - 3B_{16} \frac{\partial^3 w}{\partial x^2 \partial y} - B_{26} \frac{\partial^3 w}{\partial y^3} = 0 \quad (1)$$

$$(A_{12} + A_{66}) \frac{\partial^2 u}{\partial x \partial y} + A_{66} \frac{\partial^2 v}{\partial x^2} + A_{22} \frac{\partial^2 v}{\partial y^2} - B_{16} \frac{\partial^3 w}{\partial x^3} - 3B_{26} \frac{\partial^3 w}{\partial x \partial y^2} = 0 \quad (2)$$

$$D_{11} \frac{\partial^4 w}{\partial x^4} + 2(D_{12} + 2D_{66}) \frac{\partial^4 w}{\partial x^2 \partial y^2} + D_{22} \frac{\partial^4 w}{\partial y^4} - B_{16} \left(3 \frac{\partial^3 u}{\partial x^2 \partial y} + \frac{\partial^3 v}{\partial x^3} \right) - B_{26} \left(\frac{\partial^3 u}{\partial y^3} + 3 \frac{\partial^3 v}{\partial x \partial y^2} \right) + \bar{N}_x \frac{\partial^2 w}{\partial x^2} = 0 \quad (3)$$

The following variations in displacements

$$u = U \sin \frac{m\pi x}{a} \cos \frac{n\pi y}{b}$$

$$v = V \cos \frac{m\pi x}{a} \sin \frac{n\pi y}{b}$$

$$w = W \sin \frac{m\pi x}{a} \sin \frac{n\pi y}{b}$$

PART II

ANTISYMMETRIC ANGLE-PLY LAMINATES

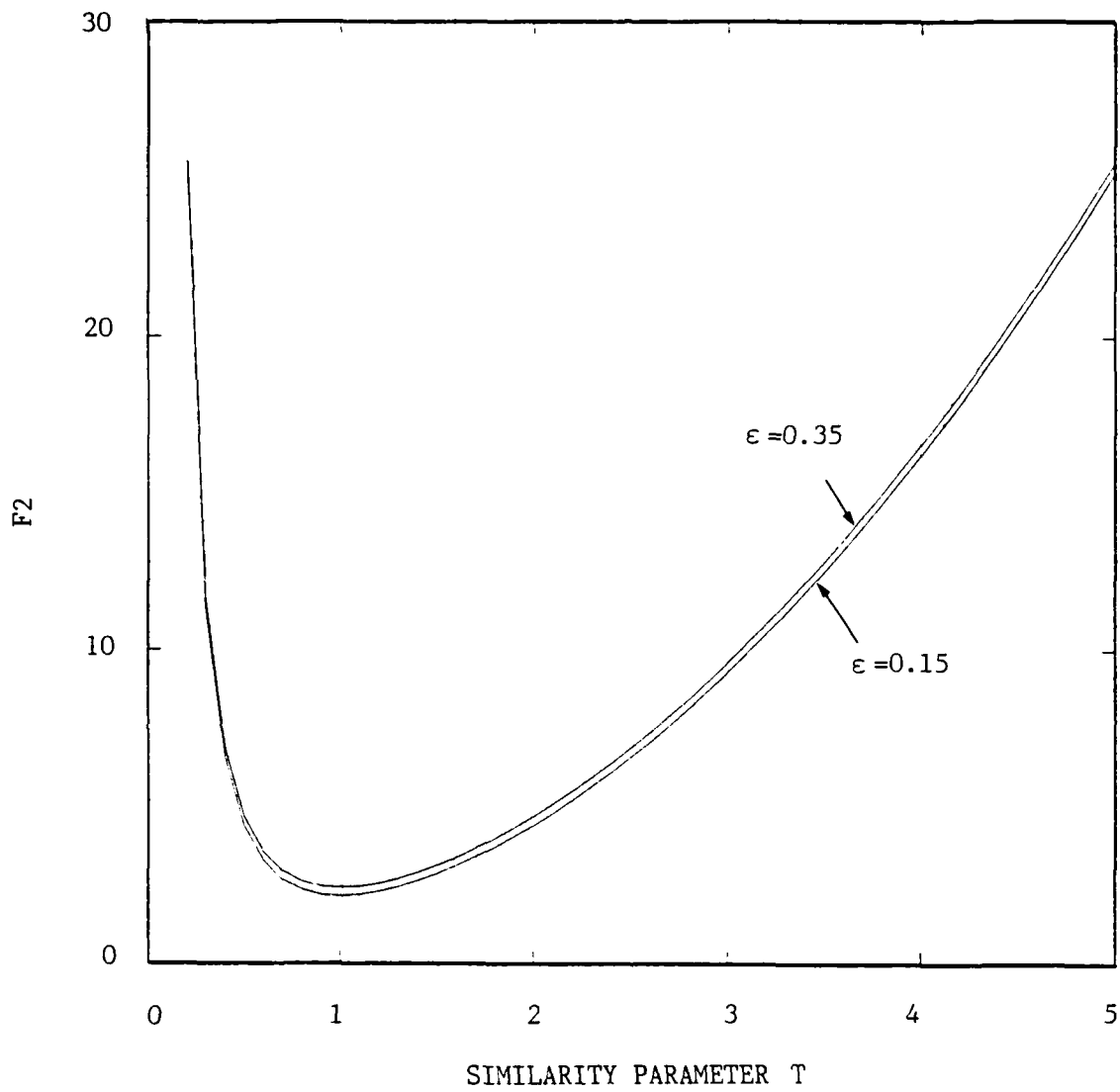


Fig. 13 . Function F2 vs. Similarity Parameter
 $D^* = 0.5$

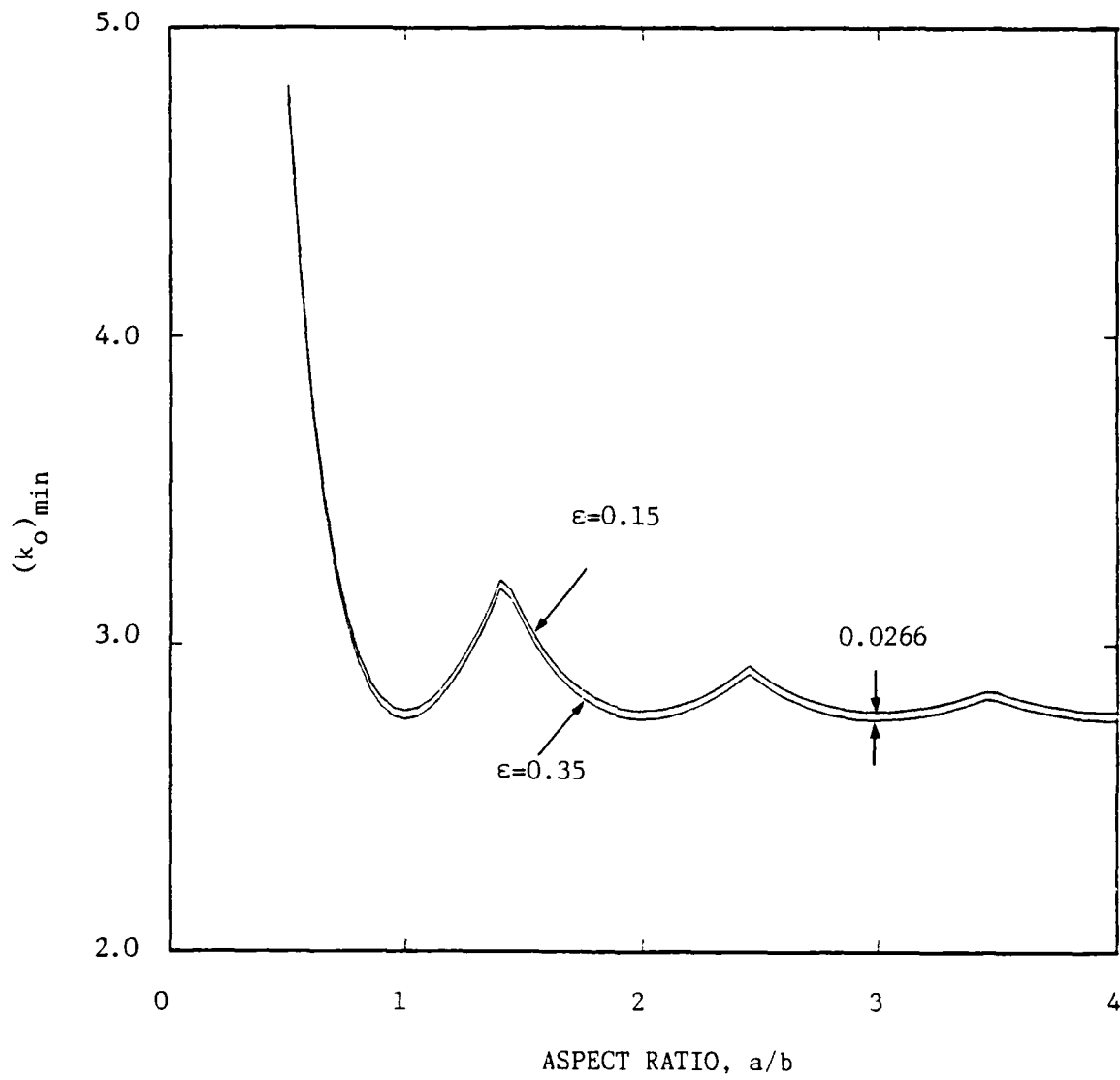


Fig. 12. Minimum Buckling Coefficient vs. Aspect Ratio
 $D^* = 0.5$, $DB = 0.1$

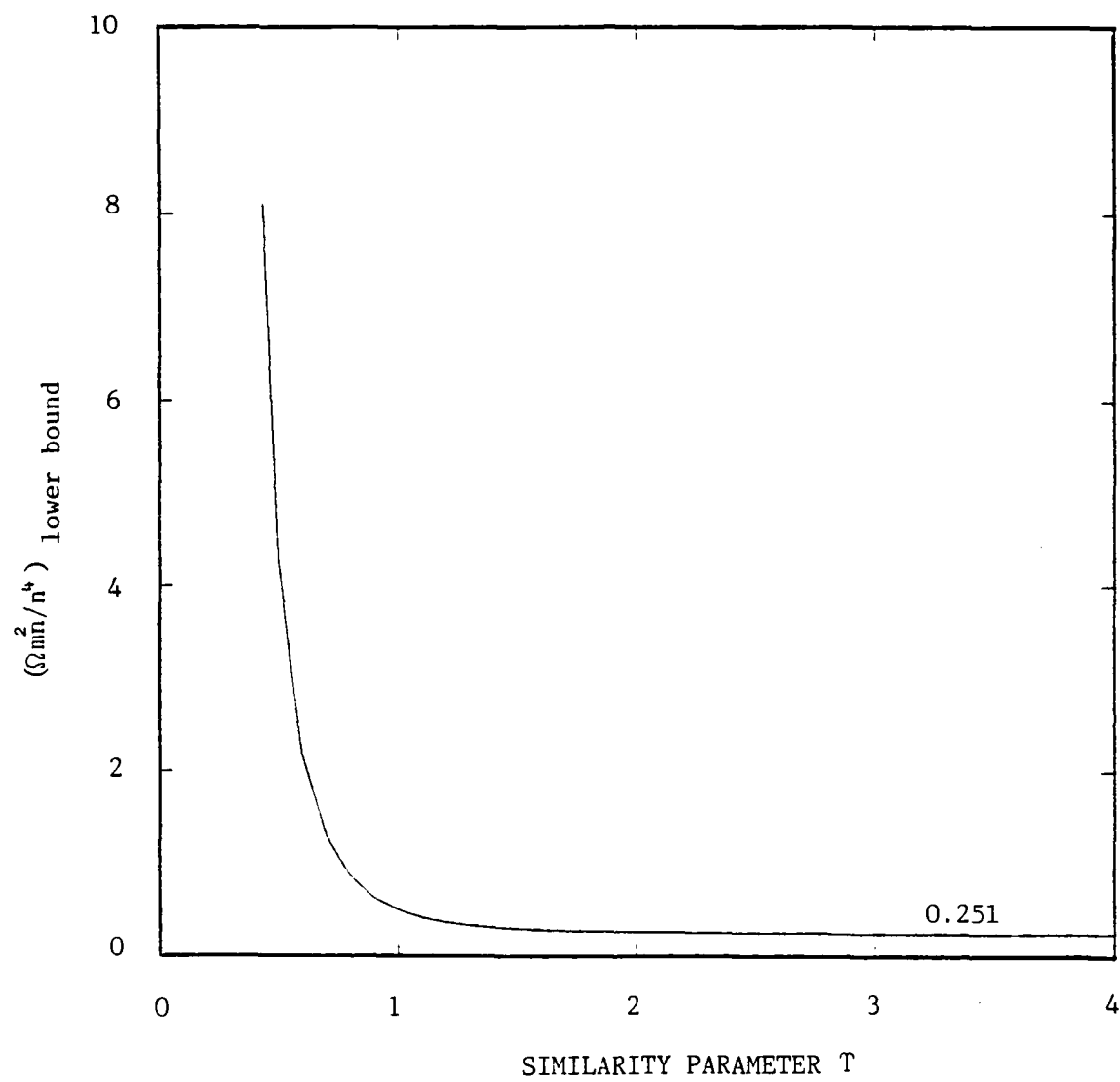


Fig. 11. Lower Bound of Frequency Coefficient vs. Similarity Parameter

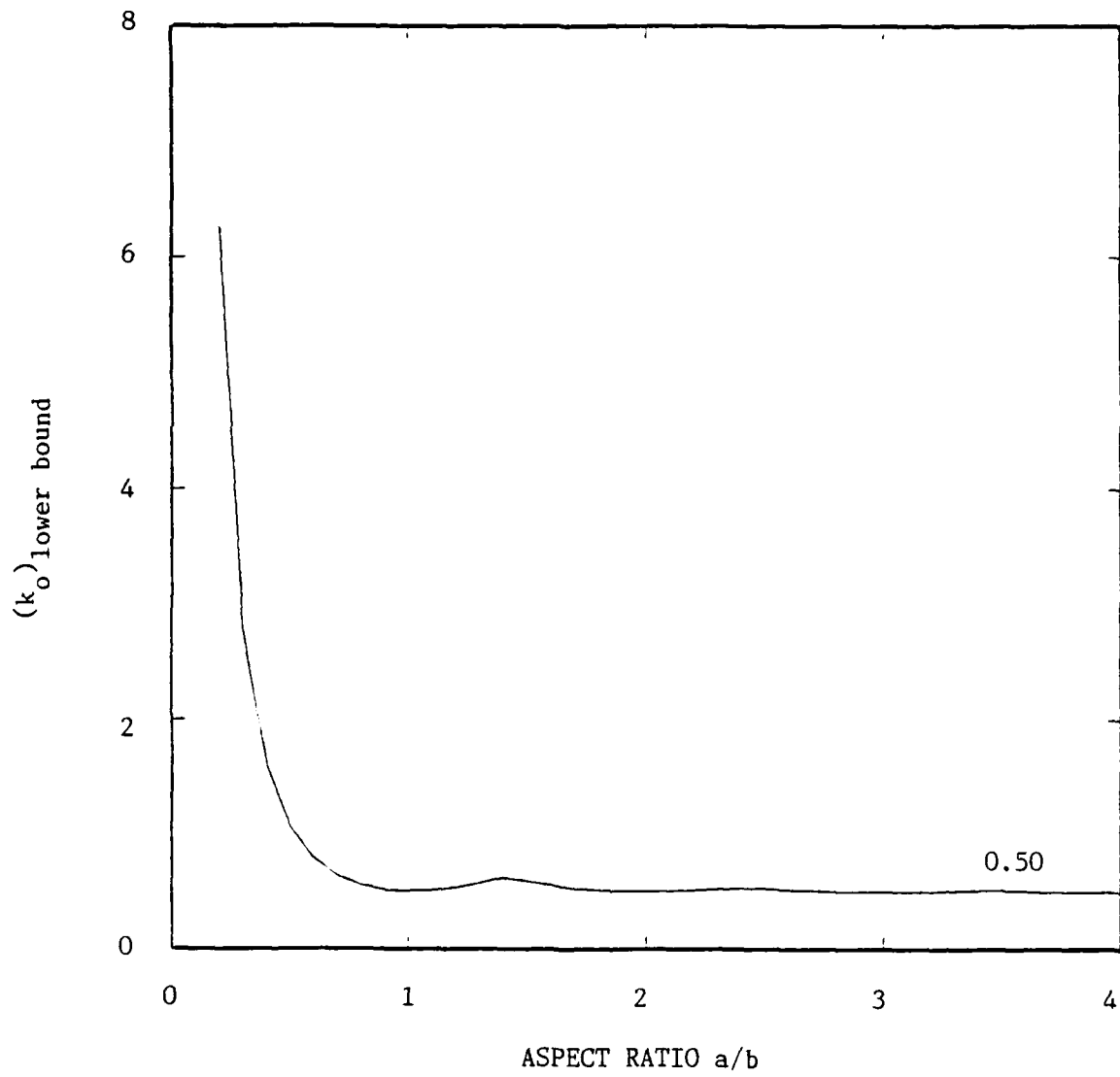


Fig. 10. Lower Bound for Buckling Coefficient vs. Aspect Ratio

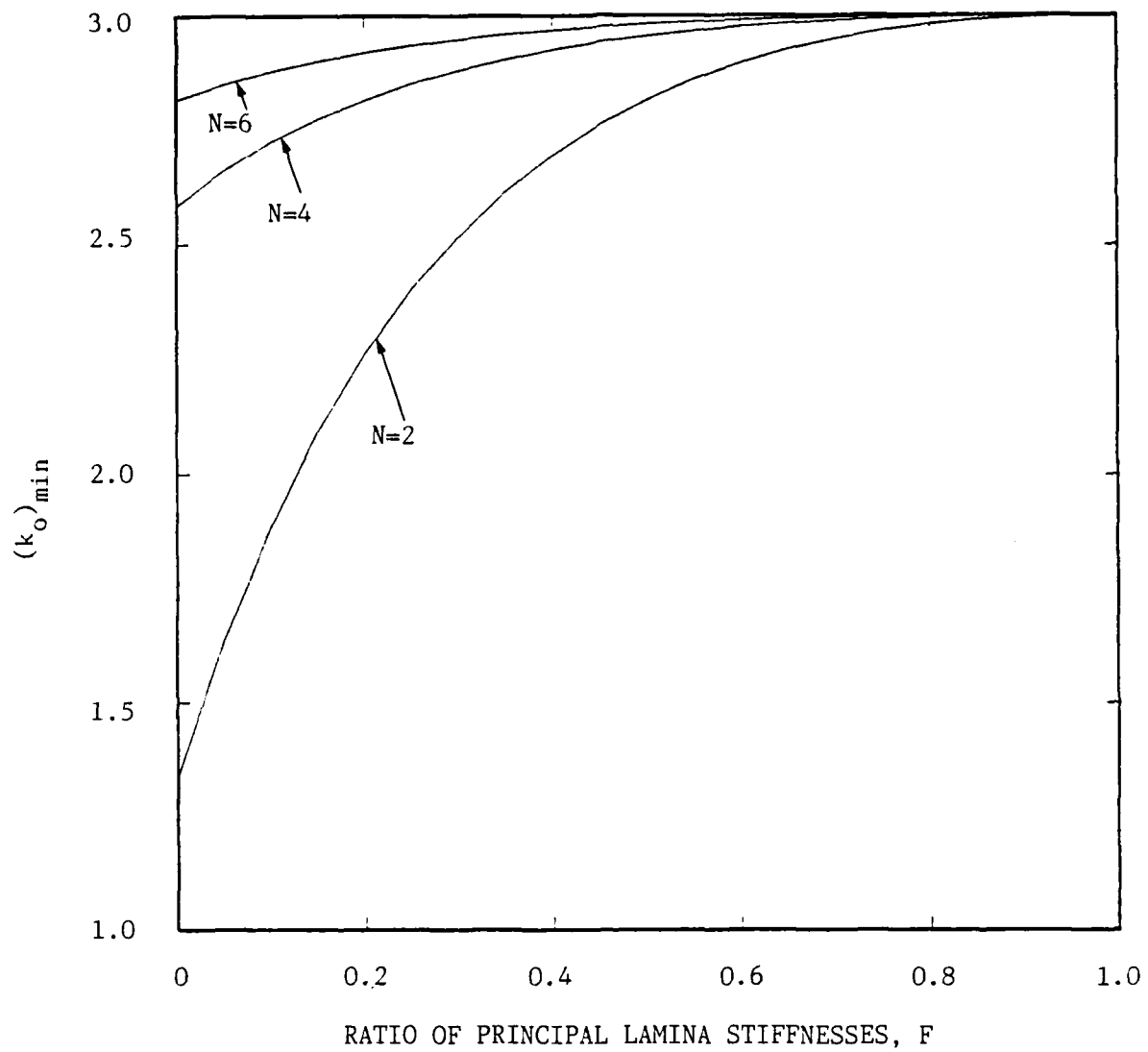


Fig. 9 . Minimum Buckling Coefficient vs. Ratio of Principal Lamina Stiffnesses, $D^* = 0.5$, Aspect Ratio = 1

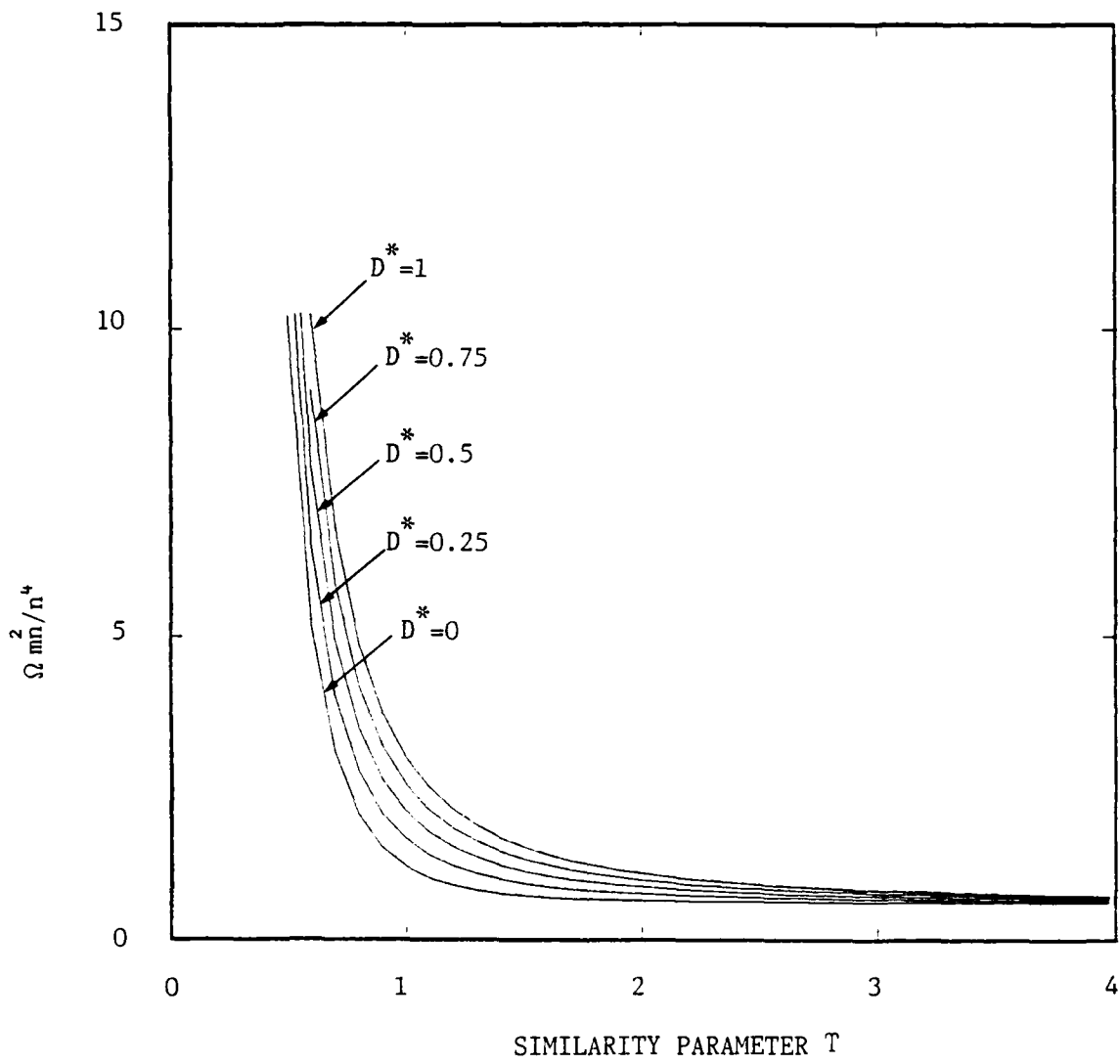


Fig. 8 . Frequency Coefficient vs. Similarity Parameter
 DB=0.4, $\epsilon=0.2$

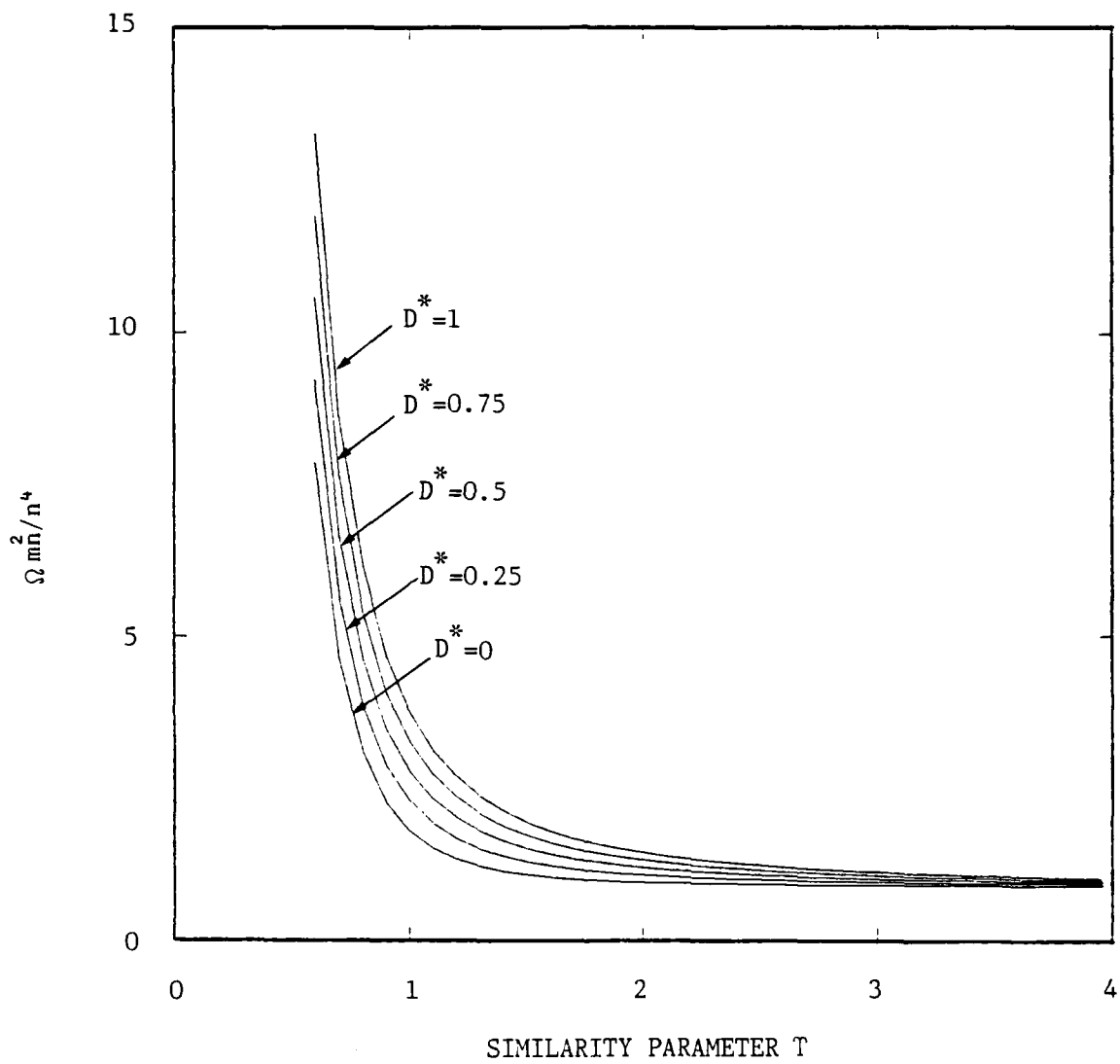


Fig. 7 . Frequency Coefficient vs. Similarity Parameter
 $DB=0.1, \epsilon=0.2$

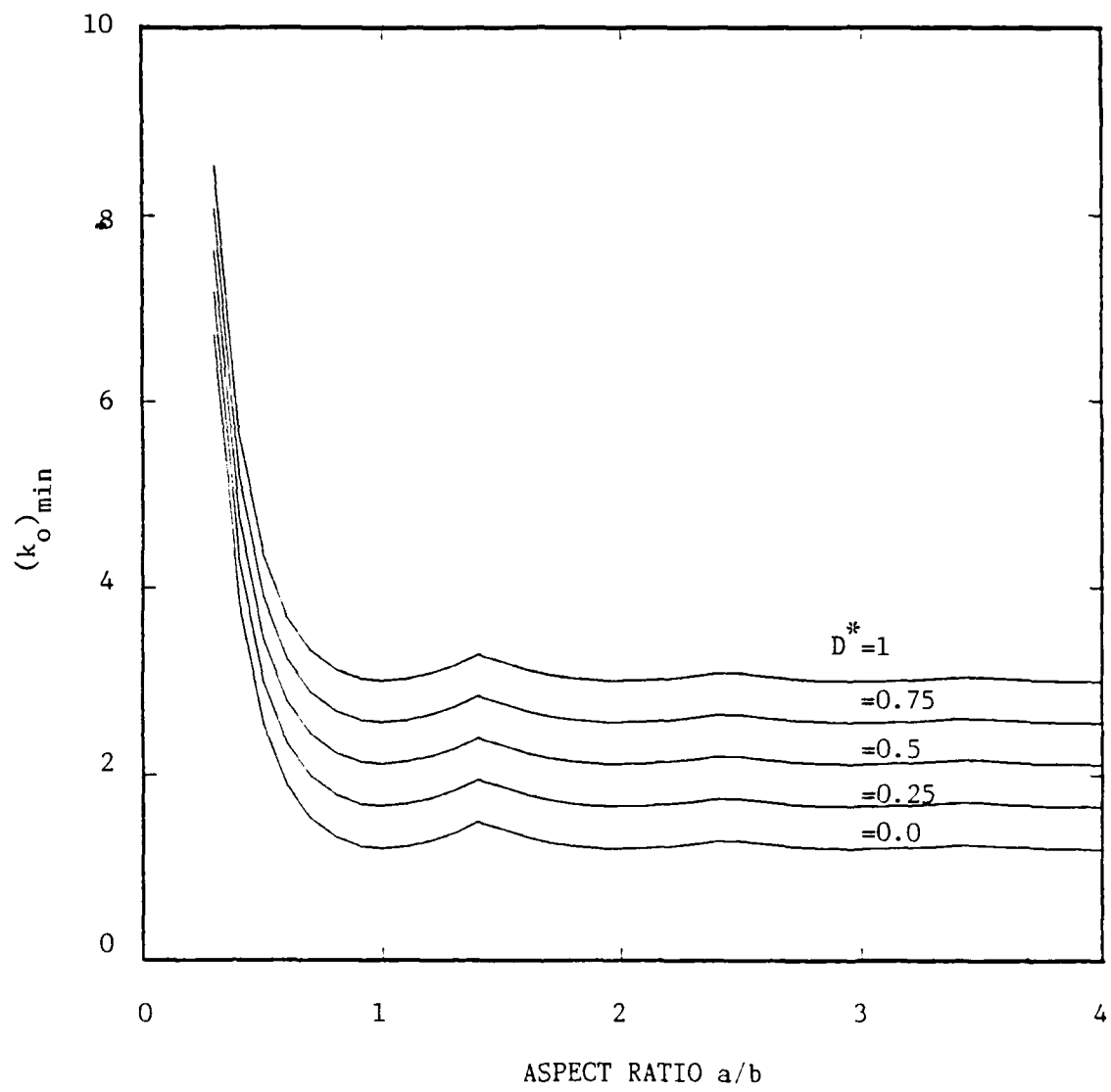


Fig. 6 . Minimum Buckling Coefficient vs. Aspect Ratio
 $DB=0.4, \epsilon=0.2$

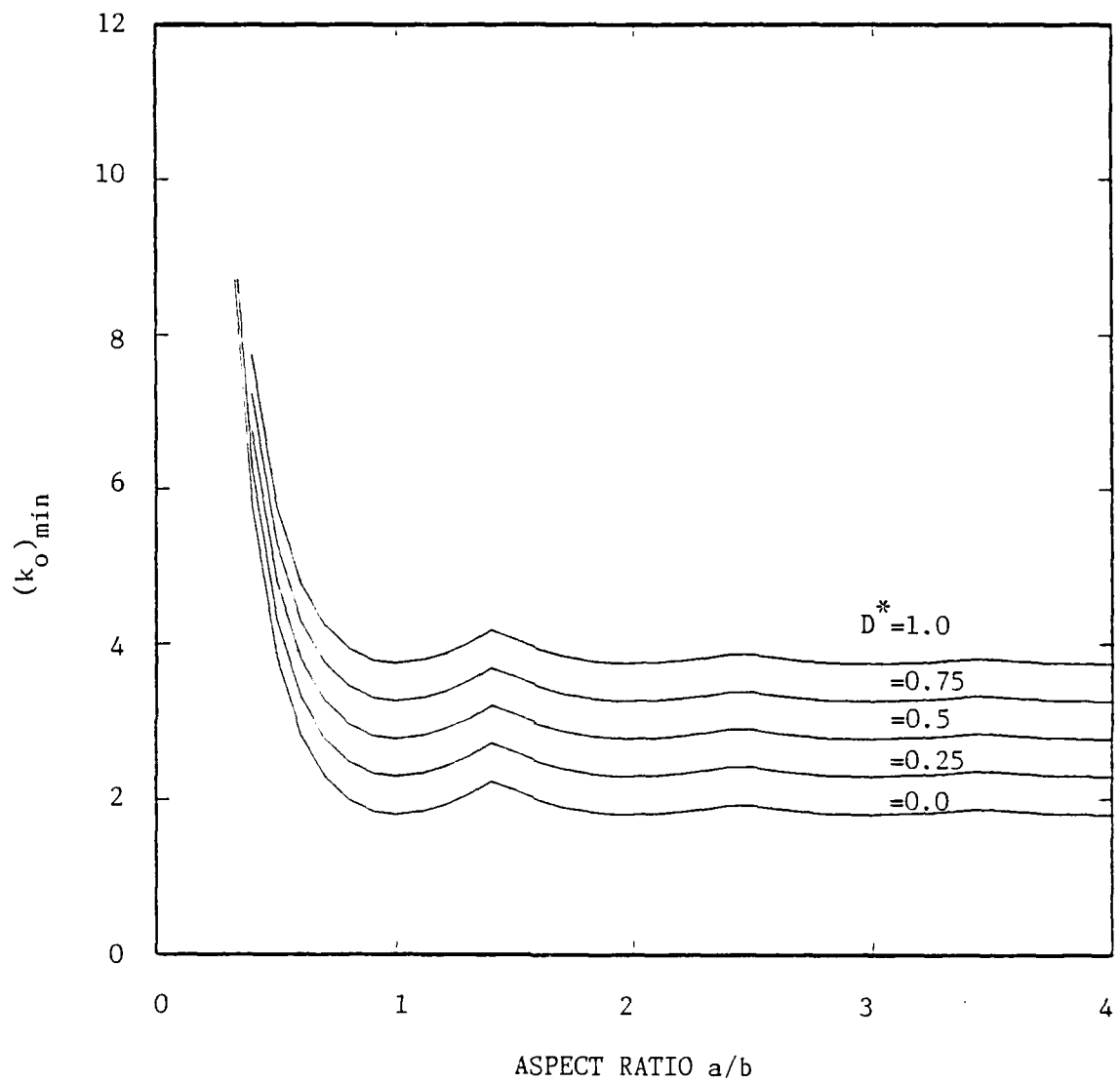


Fig. 5 . Minimum Buckling Coefficient vs. Aspect Ratio
 DB=0.1, $\epsilon=0.2$

$$- \left\{ T D^* \left(\frac{1+\epsilon}{2} \right) \right\} U_o - K^{-\frac{1}{2}} \left\{ \left(\frac{1-\epsilon}{2} \right) D^* + \frac{\bar{Q}_{22}}{Q_{22}} T^2 \right\} V_o - \left(\frac{m}{a} \right) \frac{\bar{Q}_{11}^{\frac{1}{4}}}{N} \left\{ \frac{\bar{Q}_{16}}{S} K^{-\frac{1}{2}} + \frac{3\bar{Q}_{26}}{S} \right\} W_o = 0 \quad (11)$$

$$\frac{3}{N} \frac{1}{Q_{11}^{\frac{1}{4}}} \left\{ \frac{3\bar{Q}_{16}}{S} + \frac{\bar{Q}_{26}}{S} K T^2 \right\} U_o + \frac{3}{N} \frac{1}{(Q_{22})^{\frac{1}{4}}} \frac{1}{T} \left\{ \frac{\bar{Q}_{16}}{S} K^{-\frac{1}{2}} + \frac{3\bar{Q}_{26}}{S} T^2 \right\} V_o + \left(\frac{m}{a} \right) T \left\{ \frac{\bar{Q}_{11}}{Q_{11}} \frac{1}{T^2} + 2D^* + \frac{\bar{Q}_{22}}{Q_{22}} T^2 - \frac{\bar{N}_x}{\pi^2 (D_{11} D_{22})^{1/2}} \left(\frac{b}{n} \right)^2 \right\} W_o = 0 \quad (12)$$

where

$$U_o = \left[\begin{array}{c} (D_{11} D_{22})^{\frac{1}{4}}_{\theta=0} \\ \frac{12}{t^2} \end{array} \right] U$$

$$V_o = \left[\begin{array}{c} (D_{11} D_{22})^{\frac{1}{4}}_{\theta=0} \\ \frac{12}{t^2} \end{array} \right] V$$

$$W_o = \left[\begin{array}{c} \frac{6\pi}{12^{\frac{1}{4}} t^{\frac{1}{4}}} \end{array} \right] W$$

and the buckling coefficient is given as

$$k_o = (k_o)_{SOT} - \frac{3}{N} F3 \quad (13)$$

where

$$k_o \text{ SOT} = \frac{\bar{Q}_{11}}{Q_{11}} \frac{1}{T^2} + 2D^* + \frac{\bar{Q}_{22}}{Q_{22}} T^2 \quad (14)$$

$$\begin{aligned}
F3 &= \frac{\bar{Q}_{11}}{Q_{11}} \left(\frac{\bar{Q}_{16}}{S} \right)^2 K^{-1} + \left\{ 6 \frac{\bar{Q}_{11}}{Q_{11}} \frac{\bar{Q}_{16}\bar{Q}_{26}}{S} - 2 \frac{\bar{Q}_{16}^2 D^*}{S K} (-1+4\epsilon) \right\} T^2 \\
&+ \left\{ 9 \left(\frac{\bar{Q}_{16}}{S} \right)^2 \frac{\bar{Q}_{22}}{Q_{22}} \frac{1}{K} + \left(\frac{\bar{Q}_{26}}{S} \right)^2 K \frac{\bar{Q}_{11}}{Q_{11}} \right\} T^4 - \left\{ 4D^* (1+4\epsilon) \frac{\bar{Q}_{16}\bar{Q}_{26}}{S^2} \right\} T^4 \\
&+ \left\{ 6 \frac{\bar{Q}_{16}\bar{Q}_{26}}{S^2} \frac{\bar{Q}_{22}}{Q_{22}} - 2D^* (-1+4\epsilon) \left(\frac{\bar{Q}_{26}}{S} \right)^2 K \right\} T^6 + \left\{ \left(\frac{\bar{Q}_{26}}{S} \right)^2 K \frac{\bar{Q}_{22}}{Q_{26}} \right\} T^8 \quad (15)
\end{aligned}$$

$$k_o = \frac{\bar{N}_x}{\pi^2 (D_{11} D_{22})^{\frac{1}{2}}} \left(\frac{b}{n} \right)^2 \quad (16)$$

$\frac{\bar{Q}_{11}}{Q_{11}}, \frac{\bar{Q}_{22}}{Q_{22}}, \frac{\bar{Q}_{16}}{S}, \frac{\bar{Q}_{26}}{S}, D^*$ and ϵ can all be expressed as a function of D_o^* , ϵ_o and K . To illustrate the procedure $\frac{\bar{Q}_{16}}{S}$ is explicitly solved for as follows:

$$\begin{aligned}
\bar{Q}_{16} &= (Q_{11} - Q_{12} - 2Q_{66}) \sin\theta \cos^3\theta + (Q_{12} - Q_{22} + 2Q_{66}) \sin^3\theta \cos\theta \\
\frac{\bar{Q}_{16}}{(Q_{11}Q_{22})^{\frac{1}{2}}} &= \left[\left(\frac{Q_{11}}{Q_{22}} \right)^{\frac{1}{2}} - \frac{(Q_{12} + 2Q_{66})}{(Q_{11}Q_{22})^{\frac{1}{2}}} \right] \sin\theta \cos^3\theta + \left[\frac{Q_{12} + 2Q_{66}}{(Q_{11}Q_{22})^{\frac{1}{2}}} - \left(\frac{Q_{22}}{Q_{11}} \right)^{\frac{1}{2}} \right] \sin^3\theta \cos\theta \\
\frac{\bar{Q}_{16}}{S} &= (K - 2D_o^*) \sin\theta \cos^3\theta + \left(D_o^* - \frac{1}{K} \right) \sin^3\theta \cos\theta
\end{aligned}$$

Similarly each of the other terms can be expressed as a function of D_o^* , ϵ_o and k .

$$\frac{\bar{Q}_{11}}{Q_{11}} = \cos^4\theta + \frac{2D_o^*}{K} \sin^2\theta \cos^2\theta + \frac{\sin^4\theta}{K^2} \quad (17)$$

$$\frac{\bar{Q}_{22}}{Q_{22}} = K^2 \sin^4\theta + 2D_o^* K \sin^2\theta \cos^2\theta + \cos^4\theta \quad (18)$$

$$\frac{\bar{Q}_{16}}{S} = (K - D_o^*) \sin\theta \cos^3\theta + (D_o^* - \frac{1}{K}) \sin^3\theta \cos\theta \quad (19)$$

$$\frac{\bar{Q}_{26}}{S} = (K - D_o^*) \sin^3\theta \cos\theta + (D_o^* - \frac{1}{K}) \sin\theta \cos^3\theta \quad (20)$$

$$D^* = 3 \sin^2\theta \cos^2\theta \left[\left(\frac{K+1}{K} \right) - 2D_o^* \right] + D_o^* \quad (21)$$

$$\epsilon = \frac{\sin^2\theta \cos^2\theta \left[\left(\frac{K+1}{K} \right) - 2D_o^* \right] + D_o^* \epsilon_o}{3 \sin^2\theta \cos^2\theta \left[\left(\frac{K+1}{K} \right) - 2D_o^* \right] + D_o^*} \quad (22)$$

Using the above expressions the buckling coefficient K_o can be expressed as a function of D_o^* (generalized rigidity ratio at $\theta=0$ deg.), K (square root of the ratio of the principal lamina stiffnesses), ϵ_o (generalized poissons ratio at $\theta=0$ deg.), T (similarity parameter) and θ (the ply layup angle).

D_o^* and K are the strong parameters and ϵ_o is a weak parameter. The range of K for most materials is from 1-7.

By recasting the buckling differential equations in the affine plane the buckling coefficient has been reduced to a function of basically two material parameters D_o^* and K and now it is possible to do an exhaustive parameter study of buckling solution trends, i.e., by varying D_o^* in the range of 0-1 and observing its effect on buckling

coefficient for various values of K and similarly varying K and observing its effect on buckling coefficient.

Minimum Buckling Load.

The minimum buckling coefficient $k_{o \text{ min}}$ can be obtained by substituting $n = 1$ in the equation for the buckling coefficient. The similarity parameter T reduces as follows:

$$T = \frac{na_o}{mb_o}$$

$$T)_{n=1} = \frac{a_o/b_o}{m}$$

The minimum buckling coefficient for a given affine aspect ratio can now be computed by searching through $m = 1, 2, 3 \dots$. One value of m will give the minimum buckling coefficient.

Relationship Between Real and Affine Aspect Ratio.

The real aspect ratio is related to the affine aspect ratio through the ratio of the principal lamina stiffnesses:

$$\frac{a}{b} = \left(\frac{D_{11}}{D_{22}} \right)_{\theta=0}^{\frac{1}{4}} \frac{a_o}{b_o}$$

Again using stiffnesses displayed by Tsai

$$\frac{a}{b} = \left(\frac{Q_{11}}{Q_{22}} \right)^{\frac{1}{4}} \frac{a_o}{b_o}$$

$$= (K)^{\frac{1}{2}} \frac{a_o}{b_o}$$

$$\frac{a}{b} = \left(\frac{E_1}{E_2} \right)^{\frac{1}{4}} \frac{a_o}{b_o}$$

This relationship is graphically shown in Figure 1.

V. Results and Discussion

The buckling coefficient for antisymmetric angle-ply has been reduced to a function of basically two strong material parameters, the generalized rigidity ratio at zero degrees and the ratio of the principal lamina stiffnesses. In addition to these two material properties, the buckling coefficient is also a strong function of the angle of orientation of the principal material properties with respect to the laminate axes, and the plate aspect ratio.

Since there are four variables, it is only possible to see the trends by holding two of the variables constant and varying the other two.

In addition to the effect of these four parameters on the buckling coefficient, a few other interesting observations were also made which are also discussed in this section.

Effect of Aspect Ratio

Before going into the effects of aspect ratio on the buckling coefficient, it is important to understand the relationship between real and affine aspect ratio and also the effect of real aspect ratio on the specially orthotropic solution for zero ply orientation angle.

The real and affine aspect ratio are related through the following:

$$\begin{aligned}\frac{a}{b} &= \left(\frac{D_{11}}{D_{22}} \right)_{\theta=0}^{\frac{1}{2}} \frac{a_0}{b_0} \\ &= \sqrt{K} \frac{a_0}{b_0}\end{aligned}$$

and the buckling coefficient for specially orthotropic laminate ($\theta = 0$ deg.) is given by

$$k_{oSOT} \Big|_{\theta=0 \text{ deg.}} = \frac{1}{T^2} + 2D_o^* + T^2 \quad (23)$$

for the minimum buckling load $n=1$ and

$$k_{oSOT} \Big|_{\theta=0 \text{ deg.}} = \frac{m^2}{(a_o/b_o)^2} + 2D_o^* + \frac{(a_o/b_o)^2}{m^2} \quad (24)$$

Substituting $\frac{a/b}{\sqrt{k}}$ for a_o/b_o

$$k_{oSOT} \Big|_{\theta=0 \text{ deg.}} = \frac{m^2 K}{(a/b)^2} + 2D_o^* + \frac{(a/b)^2}{m^2 K} \quad (25)$$

or

$$k_{oSOT} \Big|_{\theta=0 \text{ deg.}} - 2D_o^* = \frac{m^2 K}{(a/b)^2} + \frac{(a/b)^2}{m^2 K} \quad (26)$$

Therefore, the minimum buckling coefficient for a specially orthotropic laminate is truly a function of D_o^* , K and the real aspect ratio. The effect of the variation of real aspect ratio and K needs to be studied, D_o^* merely steps the solution up or down as indicated by Eqn. (26).

Eqn. (26) solved for $k_{oSOT} \Big|_{\min \theta=0} - 2D_o^*$ is shown in Figure 2.

It is immediately noticed that up to a real aspect ratio of 1.6 a higher value of K means a higher buckling coefficient, but for a real aspect ratio higher than 1.6, $K=2$ becomes higher than $K=4$ and at a real aspect ratio of 2, $K=2$ gives the highest buckling coefficient.

It is also noticed that the effect of K is most pronounced for real aspect ratios less than 1.8. The effect of K rapidly dies out for aspect

ratios greater than 1.8 and the buckling coefficient becomes truly a function of D_o^* alone and the expression for $k_{o \min}$ reduces to

$$k_{o \min} = 2(D_o^* + 1)$$

It may be remembered that for ply orientation angle = 0 deg., $D^* = D_o^*$ and the above equation takes the same form as given by E. J. Brunelle and G. A. Oyibo in [1].

For antisymmetric angle-ply laminates the effect of aspect ratio over the entire range of θ is more pronounced for materials with a higher value of K . A comparative study for graphite epoxy ($K=6.324$) and glass epoxy ($K=1.732$) confirms this observation. Figures 3, 4, and 5 show this effect for 2 layers. The buckling load for glass epoxy varies much less with θ as compared to Graphite Epoxy.

The effect of aspect ratio is most pronounced in the range of $\theta = 0 - 45$ deg. For ply orientation angle greater than 45 deg. the effect of aspect ratio is almost negligible compared to 0-45 deg. range. This is true for 2, 4, 6 and infinite numbers of layers. Figures 6 and 7 show this effect for graphite epoxy and Figures 8 and 9 show this effect for boron epoxy for 2 and 4 layers respectively.

Another interesting observation in this regard is that for some materials the minimum buckling coefficient remains unchanged with aspect ratio for a certain range of θ . For graphite epoxy for $\theta = 35 - 55$ deg. $k_{o \min}$ is the same for a real aspect of 1 and 2 for 4 layers. Similarly for boron epoxy for $\theta = 30 - 55$ deg. the $k_{o \min}$ is

the same for a real aspect ratio of 1 and 2. This observation is shown in Figures 10 and 11 for graphite and boron epoxy respectively.

Effect of D_o^*

To observe the effect of variation of D_o^* on the minimum buckling coefficient it was necessary to fix K and the real aspect ratio. Increasing D_o^* increased $k_{o \min}$. Three different real aspect ratios were considered and the effect is the same for the complete range of θ i.e., 0 - 90 deg. $k_{o \min}$ for $K = 5$ and real aspect ratio = 1, 1.5 and 2 is shown in Figures 12, 13, and 14. It was also noticed that for real aspect ratios of 1 and 2 at $\theta = 45$ deg. $k_{o \min}$ becomes independent of D_o^* . For a real aspect ratio of 1.5 this is clearly not the case and as can be seen in Figure 13 at $\theta = 45^\circ$ $D_o^* = 1.0$ is clearly higher than $D_o^* = 0.75$ and so on. The same effect is observed for layers more than 2 as shown in Figures 15, 16, and 17.

To illustrate this effect, two materials with approximately the same value of K but with different values of D_o^* were considered. The properties for Graphite Epoxy T300/5208 with a D_o^* of 0.425 and Graphite Epoxy AS/3501 with a D_o^* of 0.297 are listed in Table I. The properties for boron epoxy and Graphite Epoxy [7] are also listed in the table as they will be required later.

Table I

| Material | E_1 | E_2 | G_{12} | ν_{12} | D_o^* | K | ϵ_o |
|--------------------------|-------|-------|----------|------------|---------|-------|--------------|
| Boron Epoxy | 30.0 | 3.0 | 1.0 | 0.30 | 0.304 | 3.16 | 0.312 |
| Graphite Epoxy AS/3501 | 21.0 | 1.4 | 0.6 | 0.30 | 0.297 | 3.87 | 0.260 |
| Graphite Epoxy T300/5208 | 22.9 | 1.5 | 1.04 | 0.28 | 0.425 | 3.90 | 0.169 |
| Graphite Epoxy [7] | 30.0 | 0.75 | 0.375 | 0.25 | 0.197 | 6.324 | 0.20 |

As can be seen from Table I, the values of K for both materials is approximately the same. The ϵ_o values are different, but as will be shown later, the variation of ϵ_o has minimal effect of $k_{o \min}$. $k_{o \min}$ for both materials is plotted in Figure 18 and 19 for an aspect ratio of 1 and 2 for 2 layers. It is noticed that the $k_{o \min}$ for Graphite Epoxy T300/5208 is higher than Graphite Epoxy AS/3501 for the complete range of θ . The same effect is observed for 4 and infinite number of layers as shown in Figures 20 and 21.

The $k_{o \min}$ was also plotted vs. real aspect ratio for a fixed K and θ and the same effect was observed, as shown in Figures 22 and 23.

Effect of ϵ_o

The effect of ϵ_o on buckling coefficient is indeed minimal. To study the effect of variation in ϵ_o , D_o^* and K were fixed and ϵ_o

was varied from 0.15 to 0.35. This is shown in Figure 29. The effect of ϵ is clearly negligible compared to the value of $k_{o \min}$.

Effect of K

No specific trends for the buckling coefficient with the variation of the ratio of the principal lamina stiffnesses could be established as was the case in specially orthotropic laminates at zero degrees. The real aspect ratio becomes another strong variable. For a given ply orientation and aspect ratio a higher value of K may give a higher $k_{o \min}$ whereas for a different aspect ratio and the same ply orientation a higher value of K may give a lesser $k_{o \min}$. This effect is more pronounced for the 2 layered solution.

Again to observe the effect of variation of K, D_o^* and real aspect ratio are fixed and K is varied. Figures 25 and 26 show this effect for a real aspect ratio of 1 and 2 for 2 layers. For a real aspect ratio of 1 $k_{o \min}$ for K = 6 is highest for almost the entire range of θ but for a real aspect ratio of 2 for $\theta = 0 - 20$ deg. K = 2 gives the highest value of $k_{o \min}$.

As the number of layers is increased the trend becomes consistent. A higher value of K means a higher $k_{o \min}$ for almost the entire range of θ i.e., 0 - 90 deg. Figures 27 and 28 show this effect for infinite number of layers and a real aspect ratio of 1 and 2.

This effect is more readily seen if the minimum buckling load

is plotted vs. real aspect ratio for a given angle and various values of K . Figures 29 and 30 best illustrate the presence of aspect ratio as a strong parameter. At $\theta = 60$ deg. from Figure 29, no standard conclusion can be drawn about the influence of K on minimum buckling load. Similarly at $\theta = 45$ deg. from Figure 30. $K = 6$ gives a higher buckling load for the entire range of aspect ratio whereas $K = 2$ gives a higher buckling load than $K = 4$.

To illustrate this effect again, two materials with approximately the same value of D_o^* but different values of K were considered. Graphite Epoxy AS/3501 and Boron Epoxy have D_o^* of 0.297 and 0.304 respectively but their K values are quite different. The detailed properties of these two materials are listed in Table I. For a real aspect ratio of 1 and 2 layers, Graphite Epoxy with a higher value of K has a higher $k_{o \min}$ from $\theta = 0$ to 60 deg., but beyond 60 deg. Boron Epoxy has a higher $k_{o \min}$. For a real aspect ratio of 2 and 2 layers Boron Epoxy with a smaller value of K has a higher $k_{o \min}$. Figures 31 and 32 illustrate the above.

For 4, 6 and infinite number of layers Graphite Epoxy has a higher $k_{o \min}$ for almost the entire range of θ i.e., 0 - 90 deg. as shown in Figures 33 and 34.

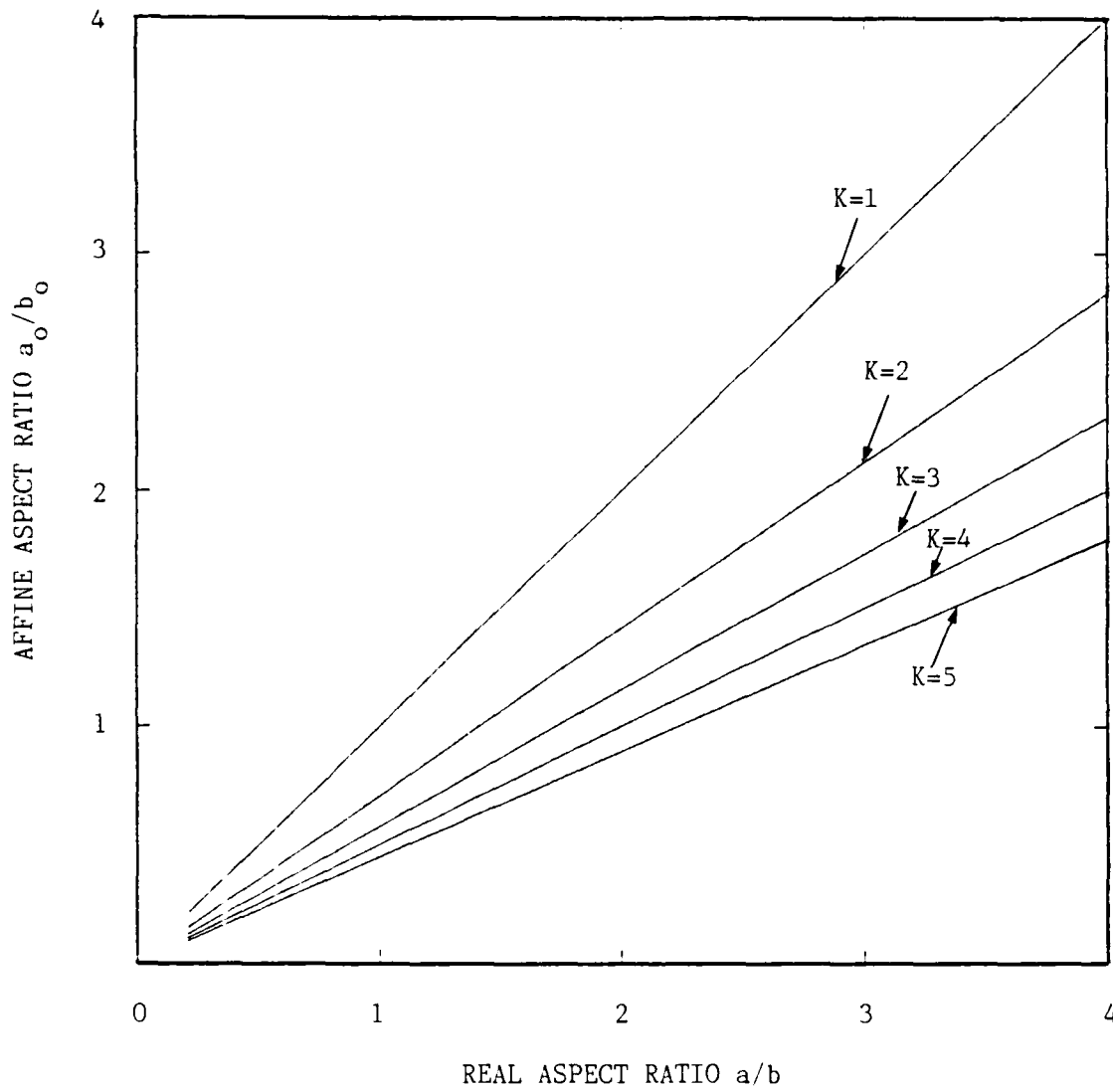


Fig. 1 . Real Aspect Ratio vs. Affine Aspect Ratio

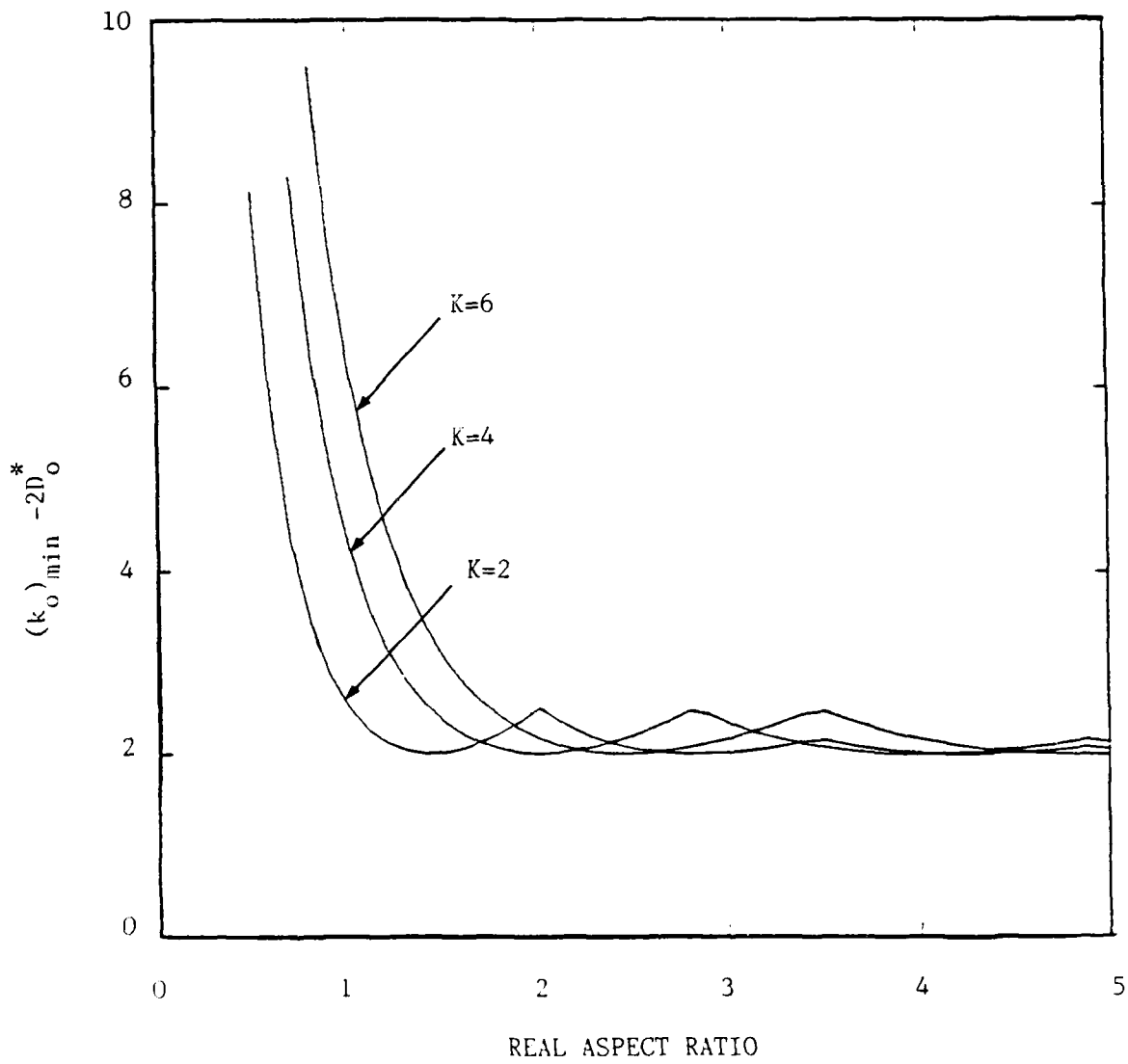


Fig. 2. Minimum Buckling Coefficient $-2D_0^*$ vs. Real Aspect Ratio Specially Orthotropic Laminate

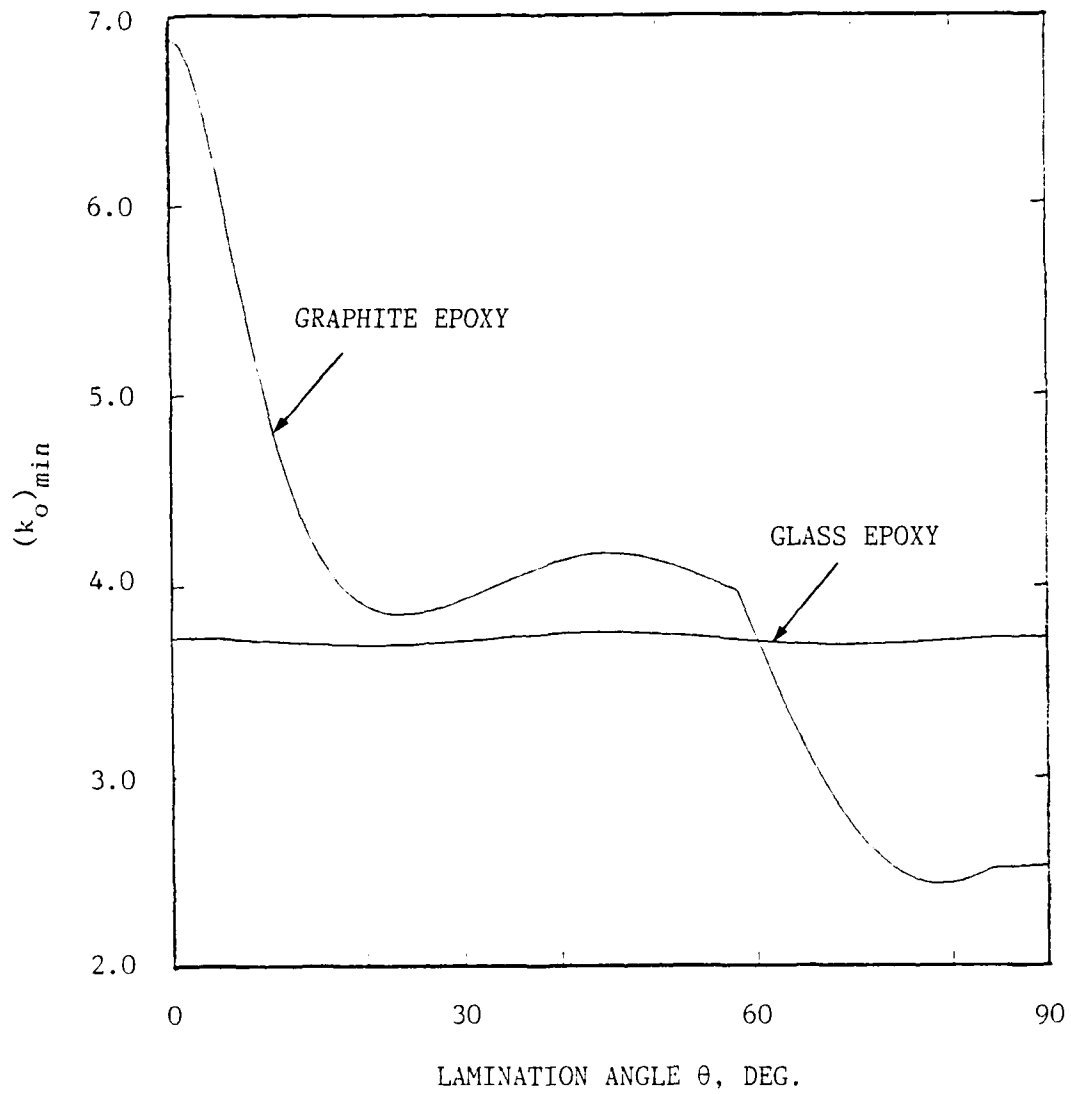


Fig. 3 . Minimum Buckling Coefficient vs. Lamination Angle
 Real Aspect Ratio = 1, No. of Layers = 2

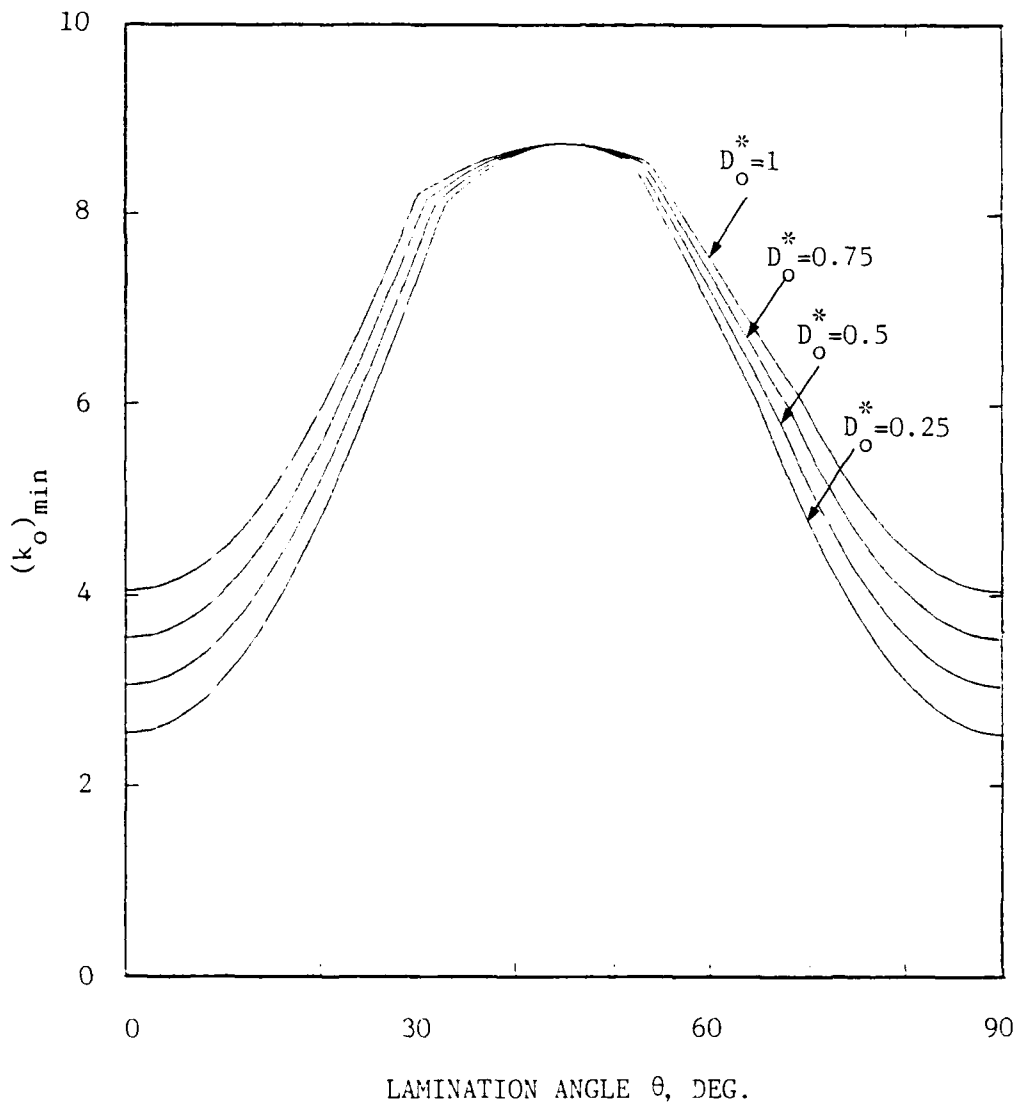


Fig. 17. Minimum Buckling Coefficient vs. Lamination Angle
 Real Aspect Ratio = 2, $K = 5$, No. of Layers = 4

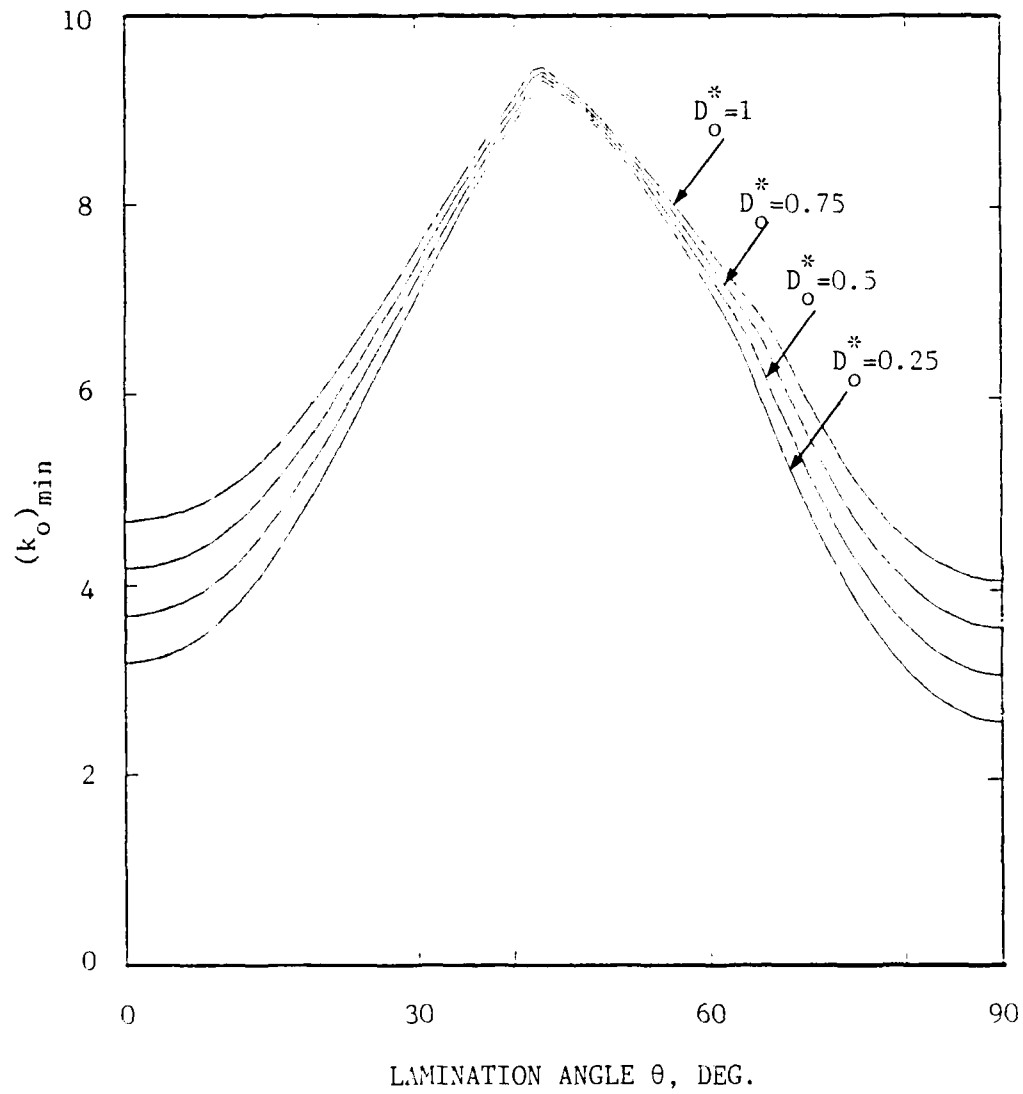


Fig. 16 . Minimum Buckling Coefficient vs. Lamination Angle
 Real Aspect Ratio = 1.5, $K = 5$, No. of Layers = 4

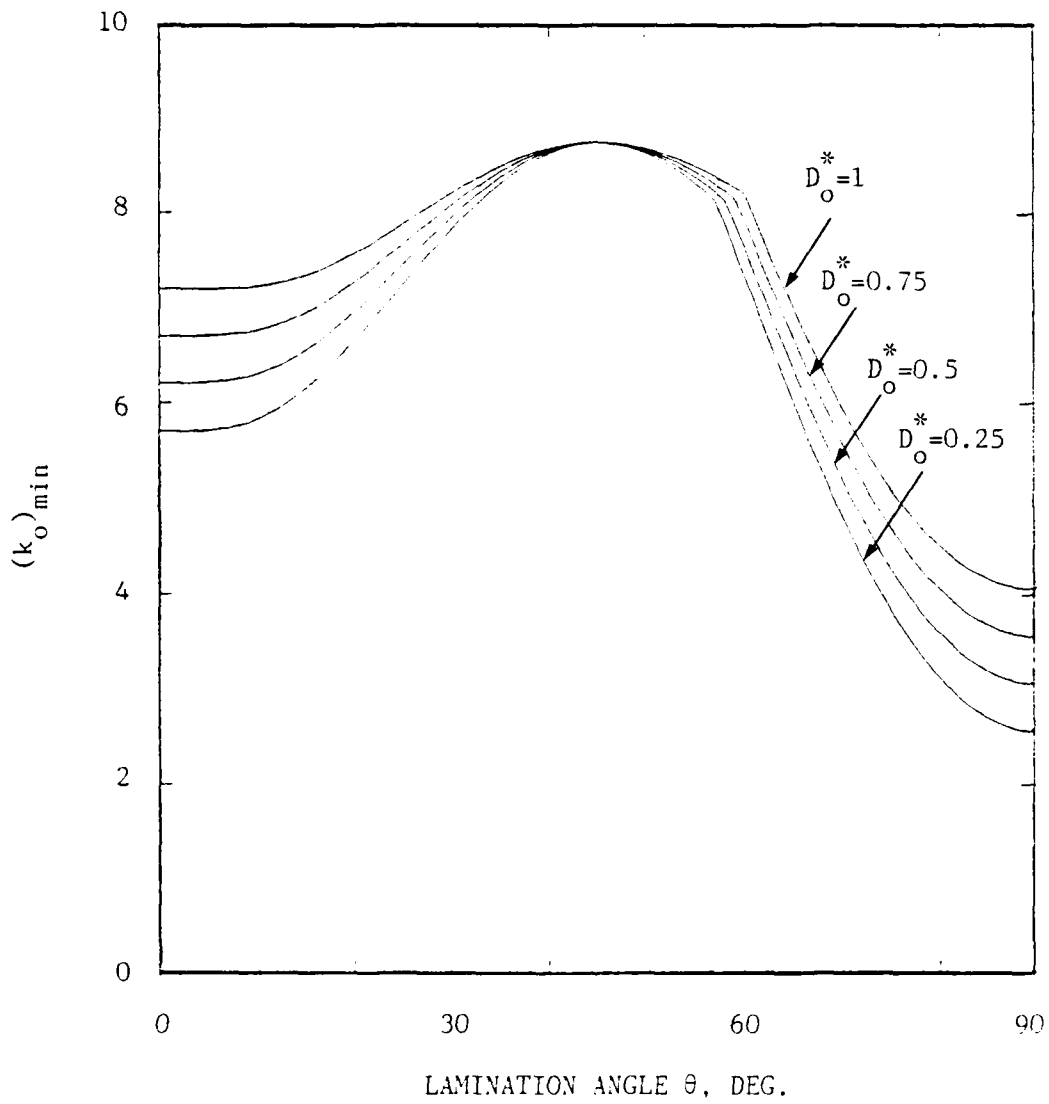


Fig. 15. Minimum Buckling Coefficient vs. Lamination Angle
 Real Aspect Ratio = 1, No. of Layers = 4, $K = 5$

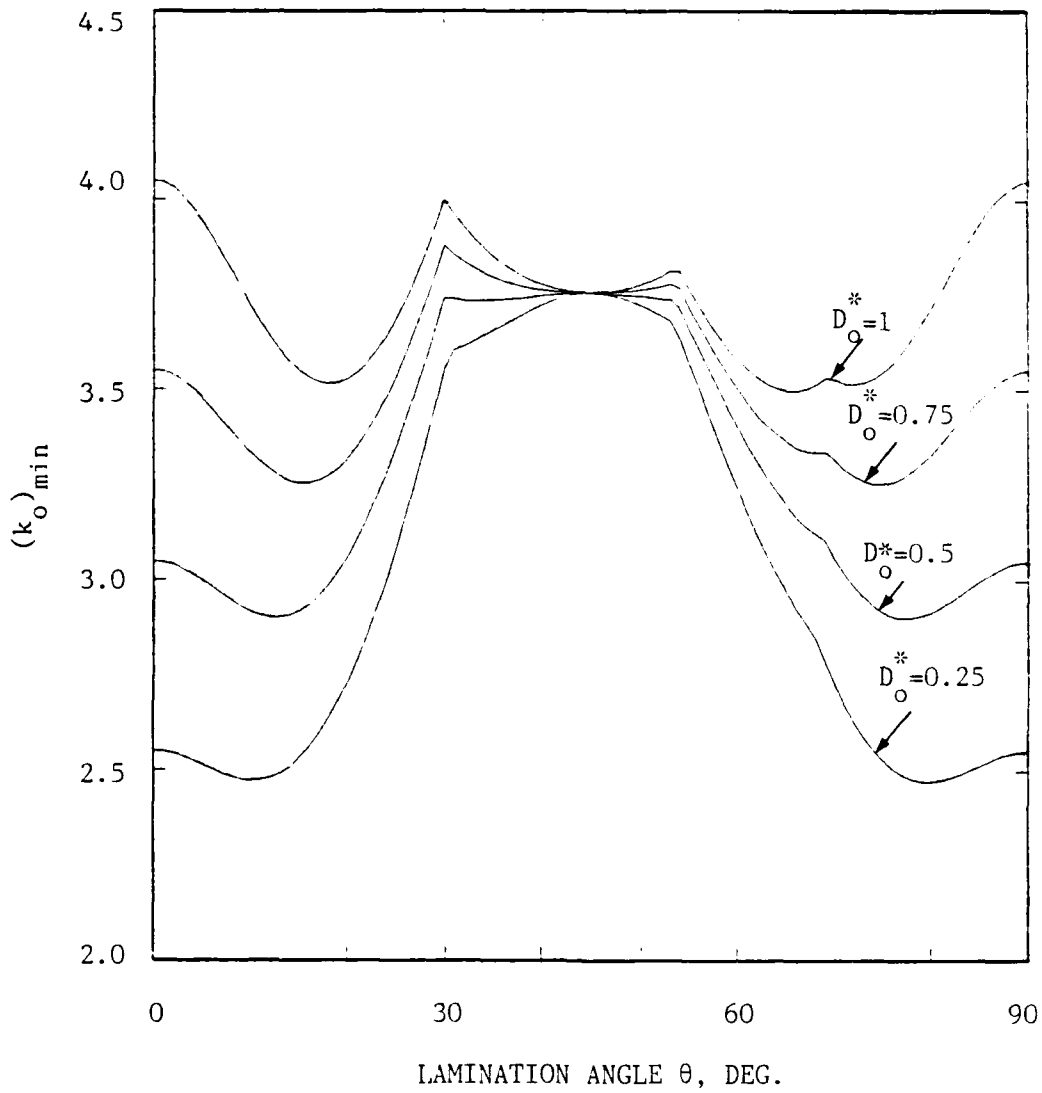


Fig. 14. Minimum Buckling Coefficient vs. Lamination Angle
 Real Aspect Ratio = 2, $K = 5$, No. of Layers = 2

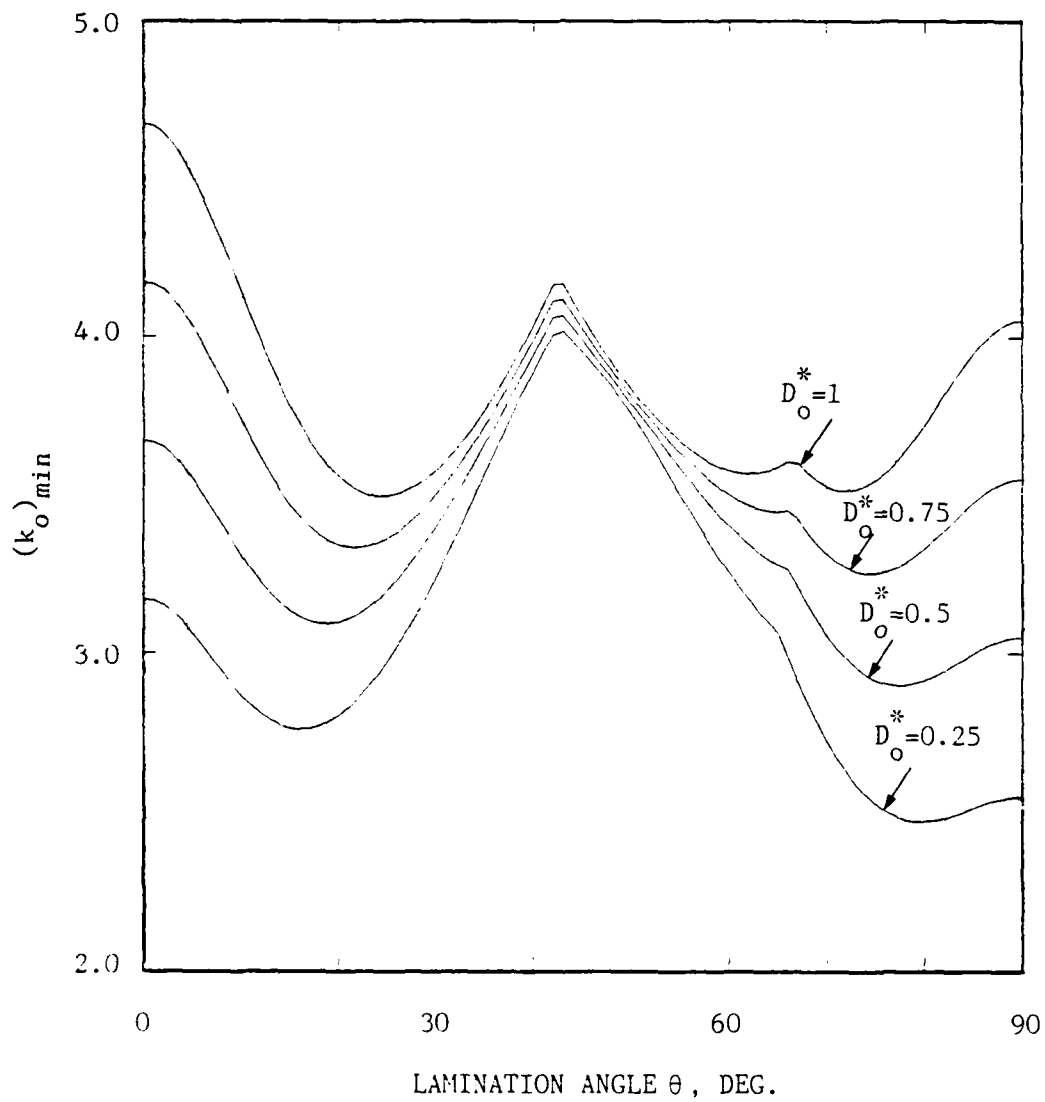


Fig. 13. Minimum Buckling Coefficient vs. Lamination Angle
 Real Aspect Ratio = 1.5, $K=5$, No. of Layers = 2

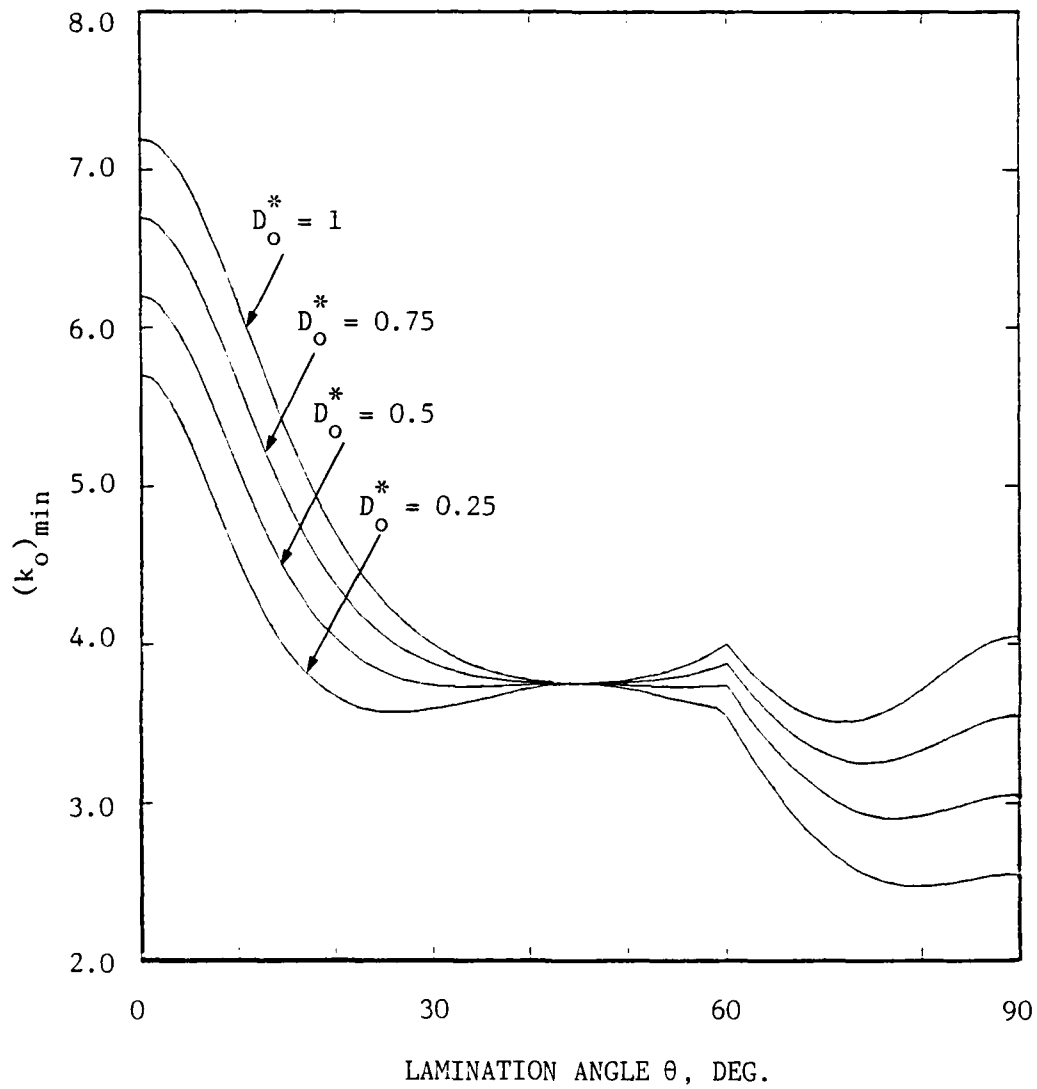


Fig. 12 . Minimum Buckling Coefficient vs. Lamination Angle
 Real Aspect Ratio = 1, $K = 5$, No. of layers = 2

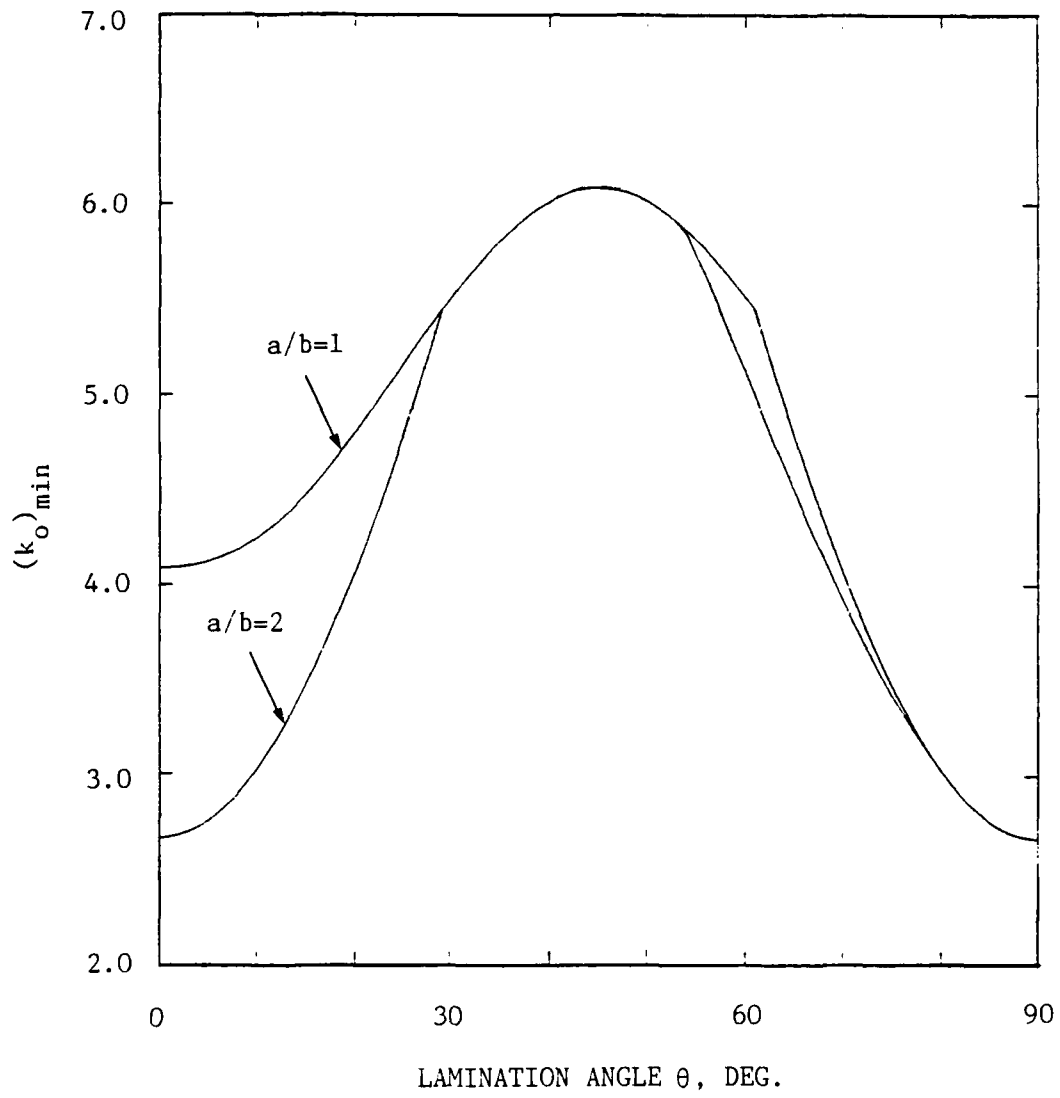


Fig. 11. Minimum Buckling Coefficient vs. Lamination Angle
 Boron Epoxy, No. of Layers = 4

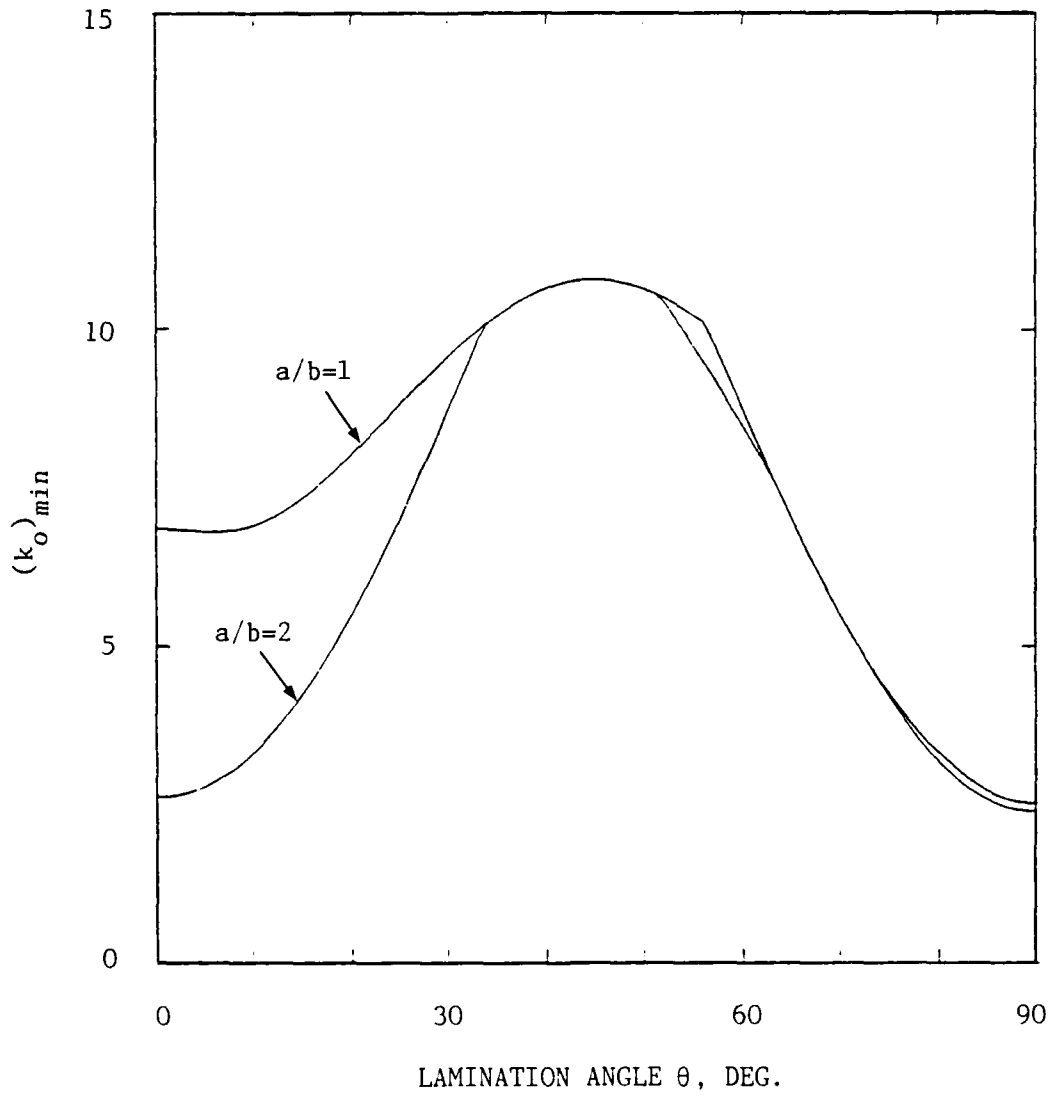


Fig. 10 . Minimum Buckling Coefficient vs. Lamination Angle
Graphite Epoxy, No. of Layers = 4

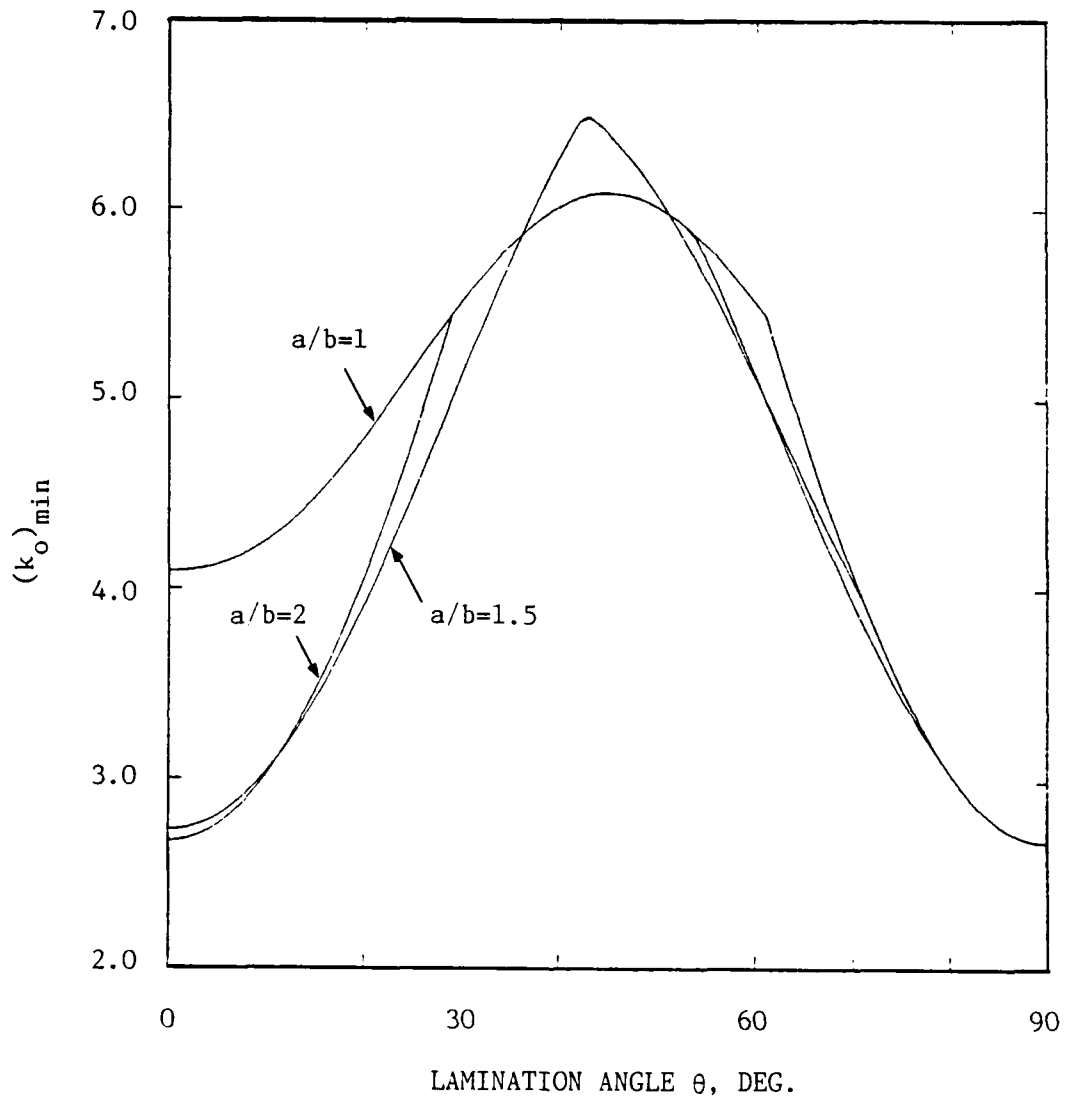


Fig. 9 . Minimum Buckling Coefficient vs. Lamination Angle
 Boron Epoxy No. of Layers = 4

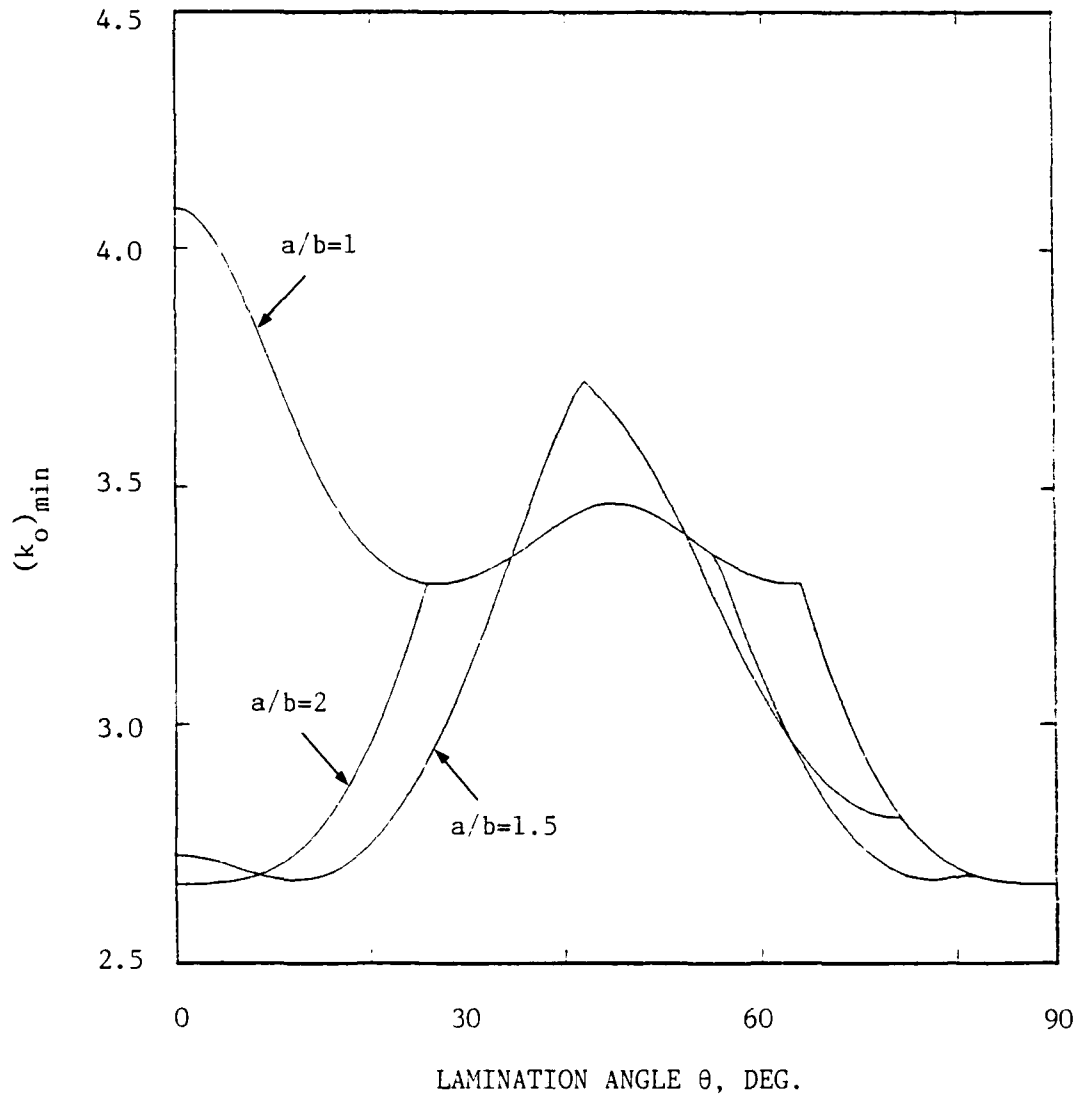


Fig. 8 . Minimum Buckling Coefficient vs. Lamination Angle
 Boron Epoxy, No. of Layers = 2

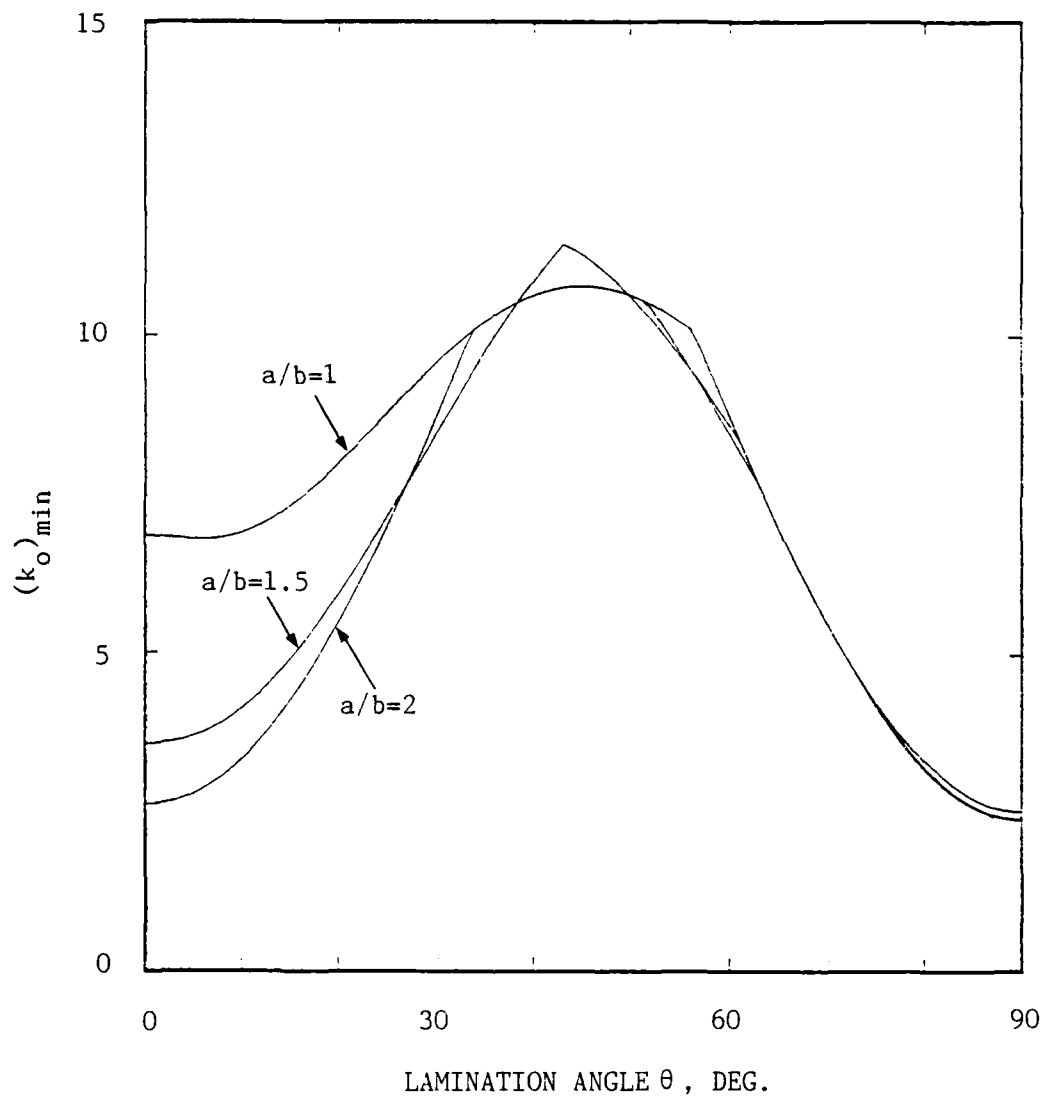


Fig. 7 . Minimum Buckling Coefficient vs. Lamination Angle
Graphite Epoxy, No. of Layers = 4

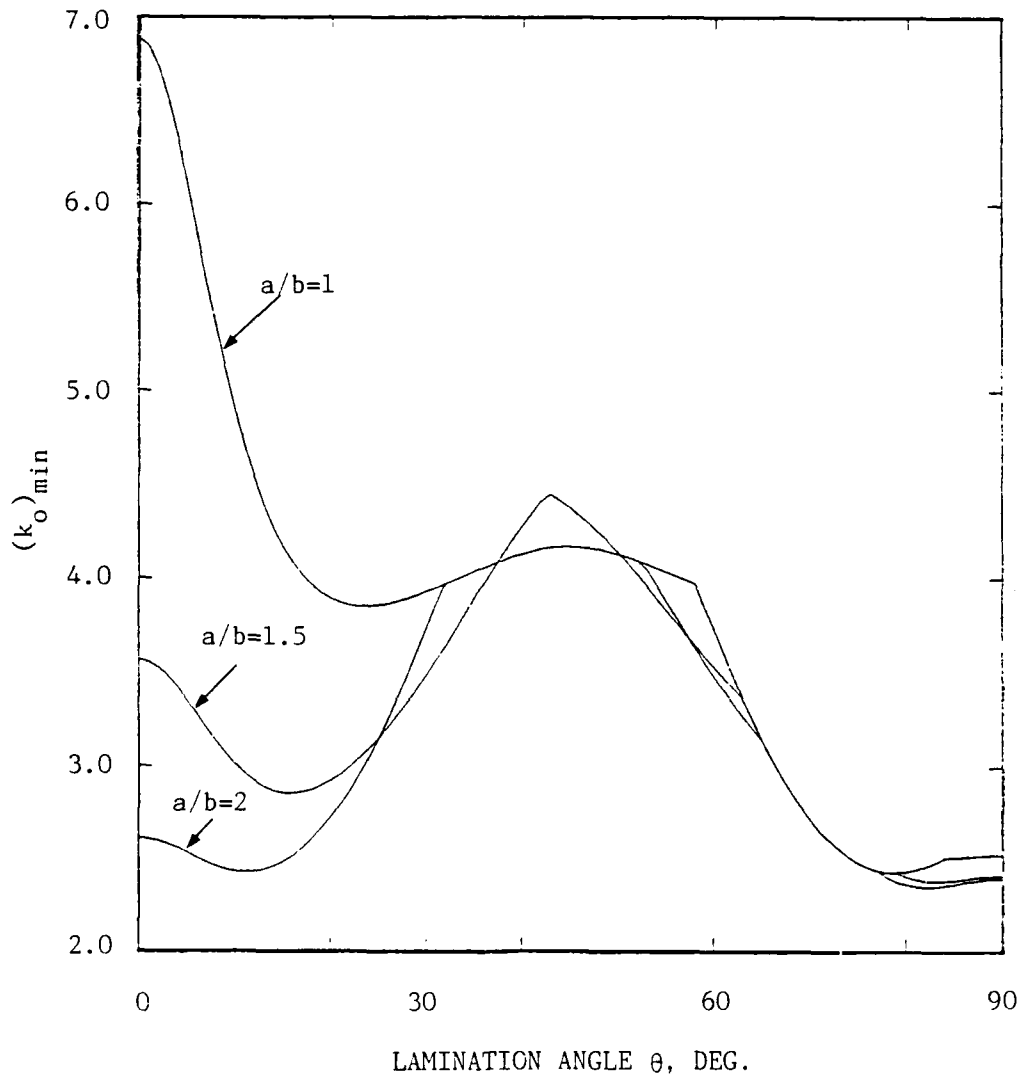


Fig. 6 . Minimum Buckling Coefficient vs. Lamination Angle
Graphite Epoxy, No. of Layers = 2

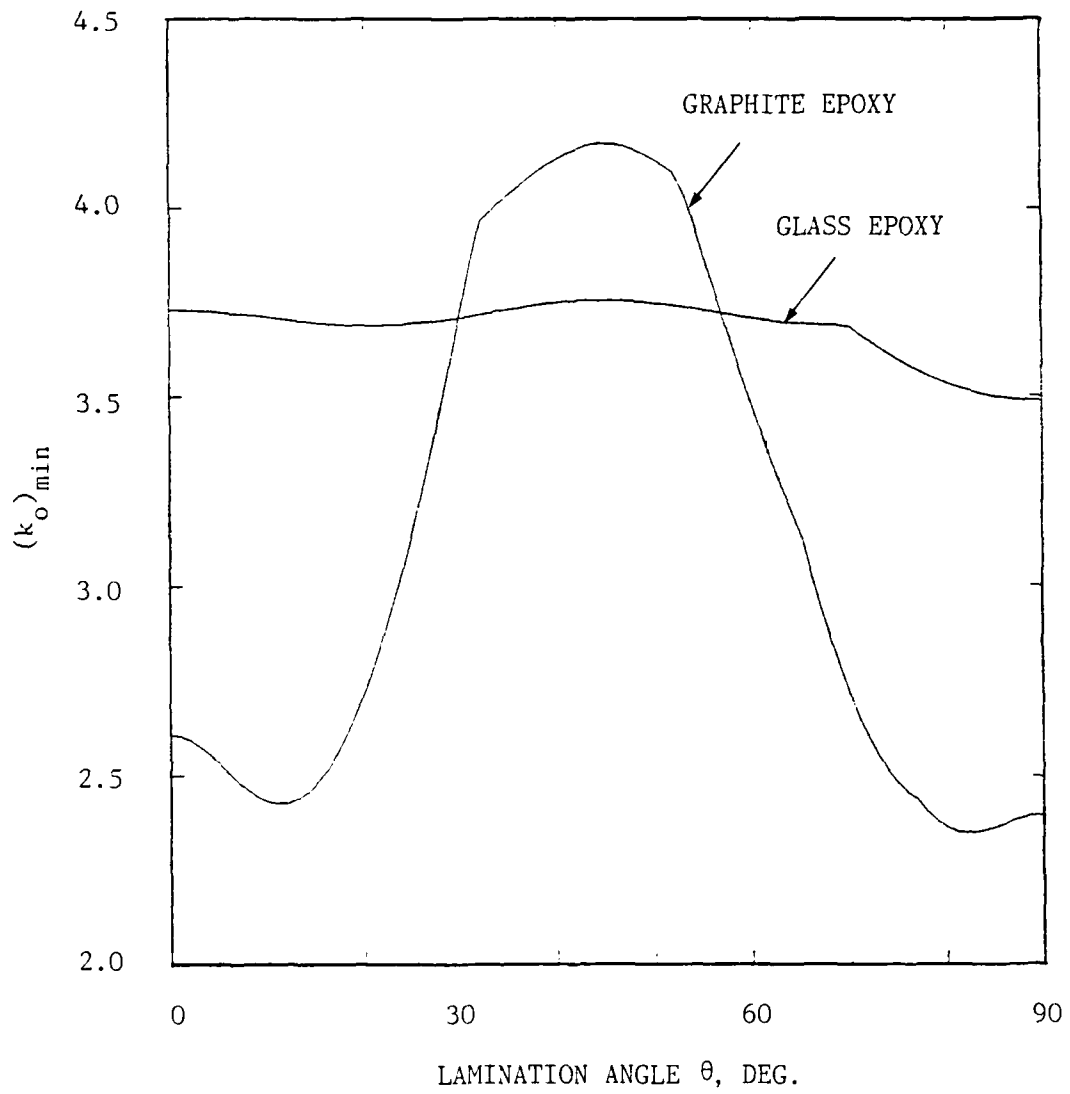


Fig. 5 . Minimum Buckling Coefficient vs. Lamination Angle
 Real Aspect Ratio = 2, No. of Layers = 2

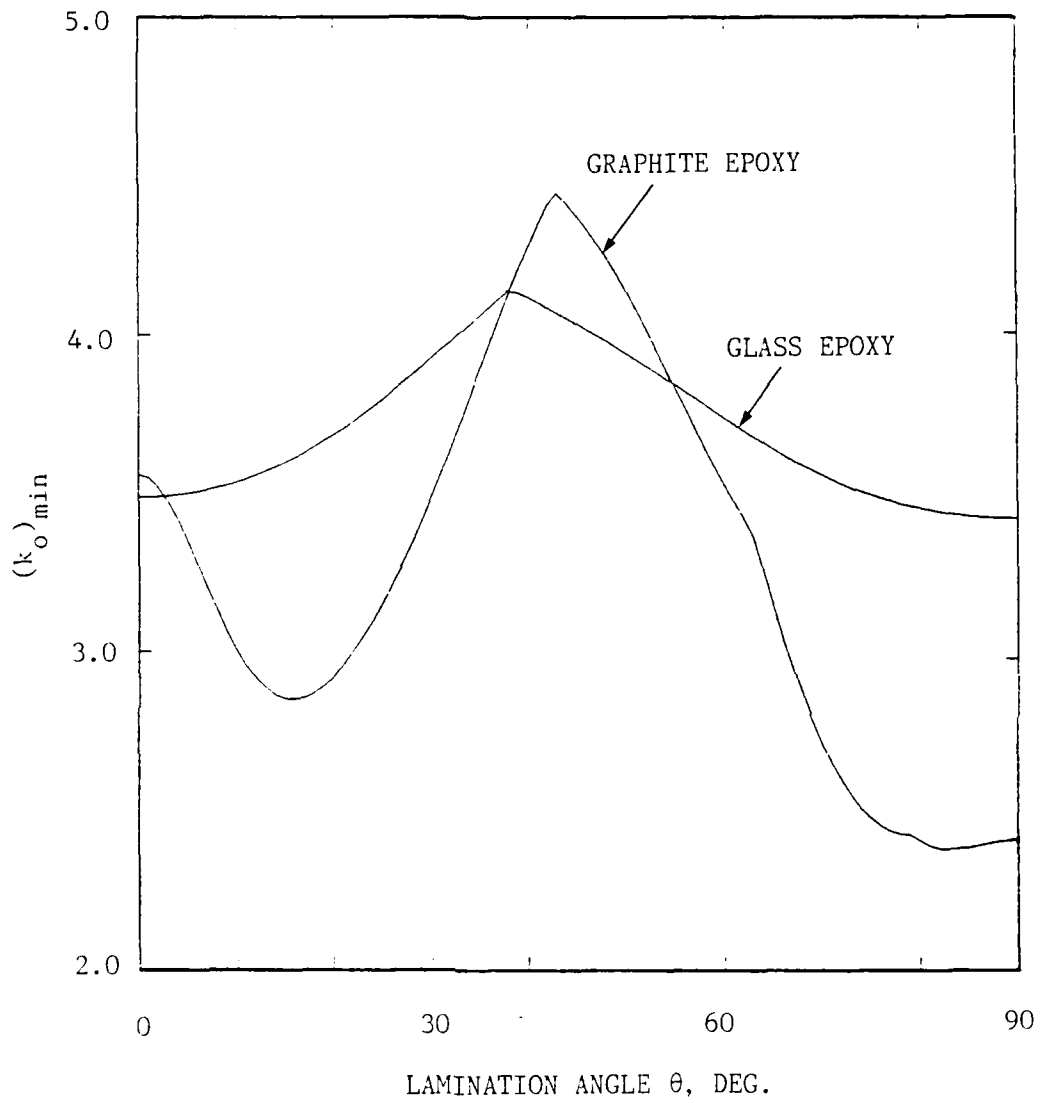


Fig. 4 . Minimum Buckling Coefficient vs. Lamination Angle
 Real Aspect Ratio = 1.5, No. of Layers = 2

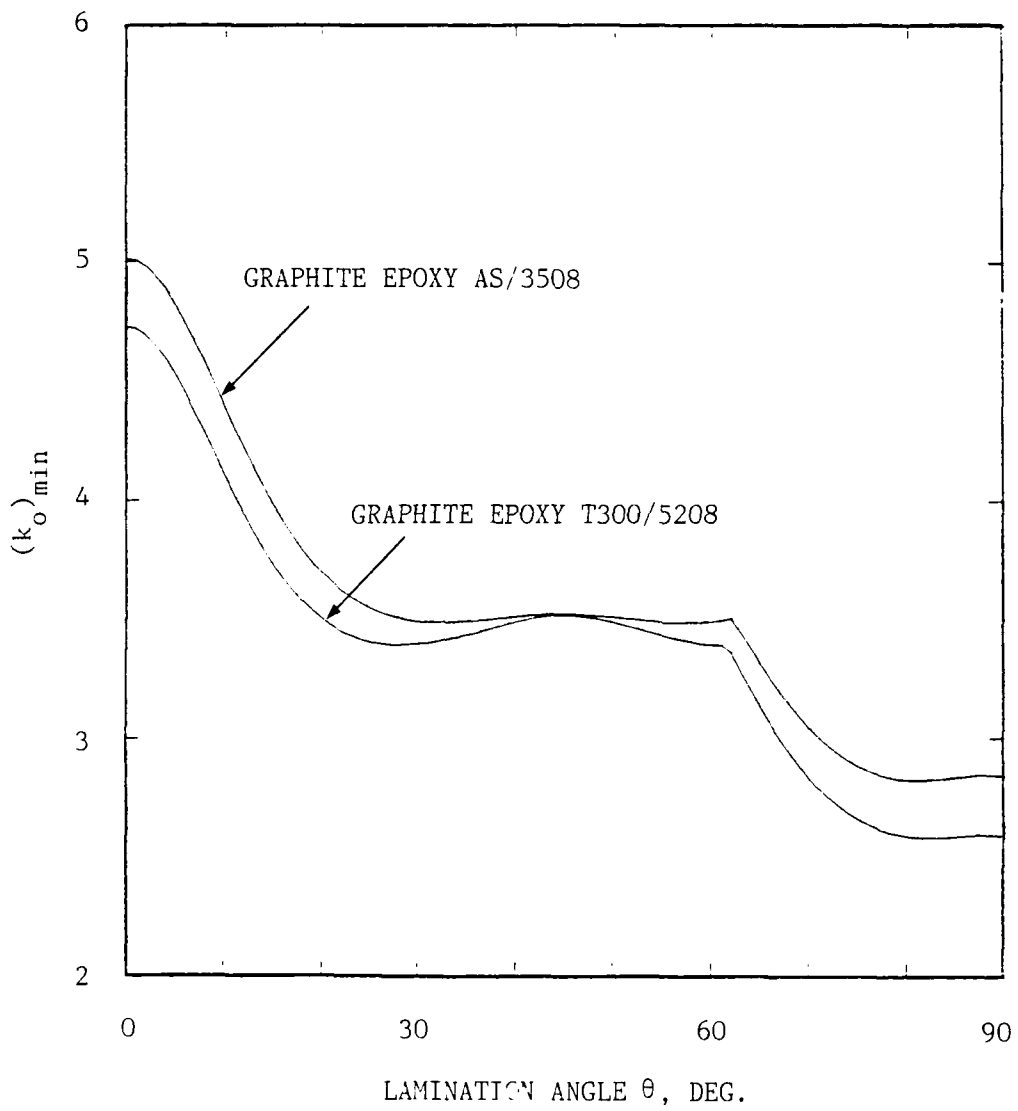


Fig. 18. Minimum Buckling Coefficient vs. Lamination Angle Real Aspect Ratio = 1, No. of Layers = 2

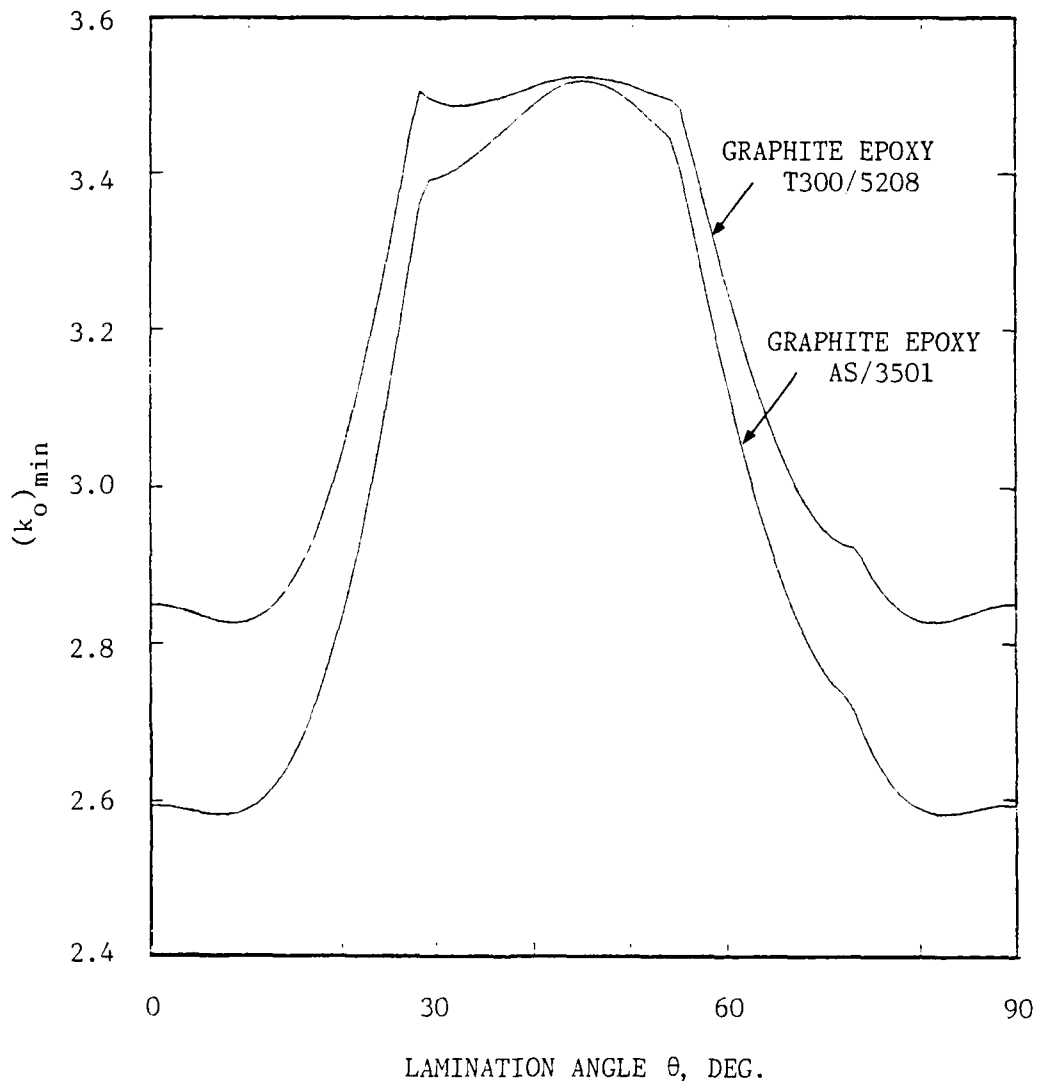


Fig. 19. Minimum Buckling Coefficient vs. Lamination Angle
Real Aspect Ratio = 2, No. of Layers = 2

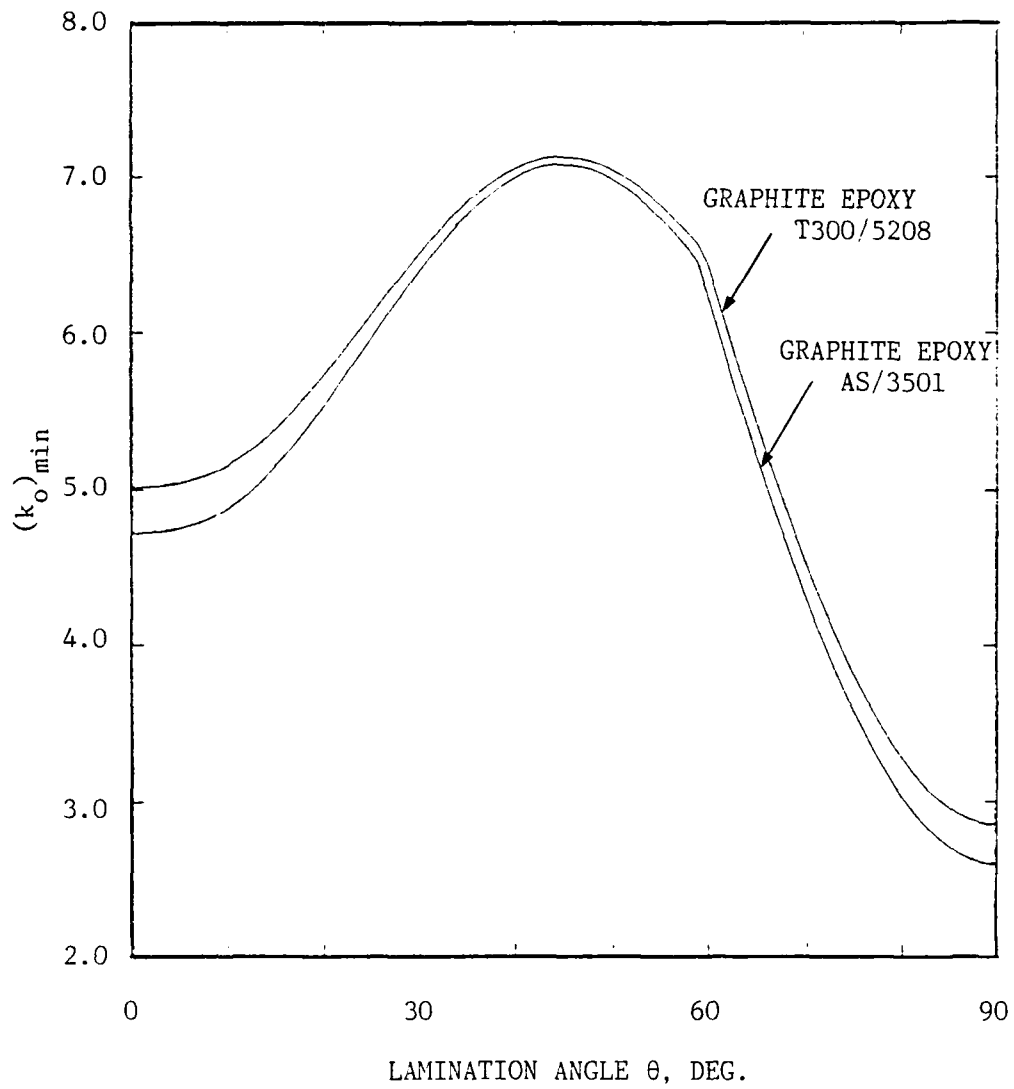


Fig. 20 . Minimum Buckling Coefficient vs. Lamination Angle
Real Aspect Ratio = 1, No. of Layers = 4

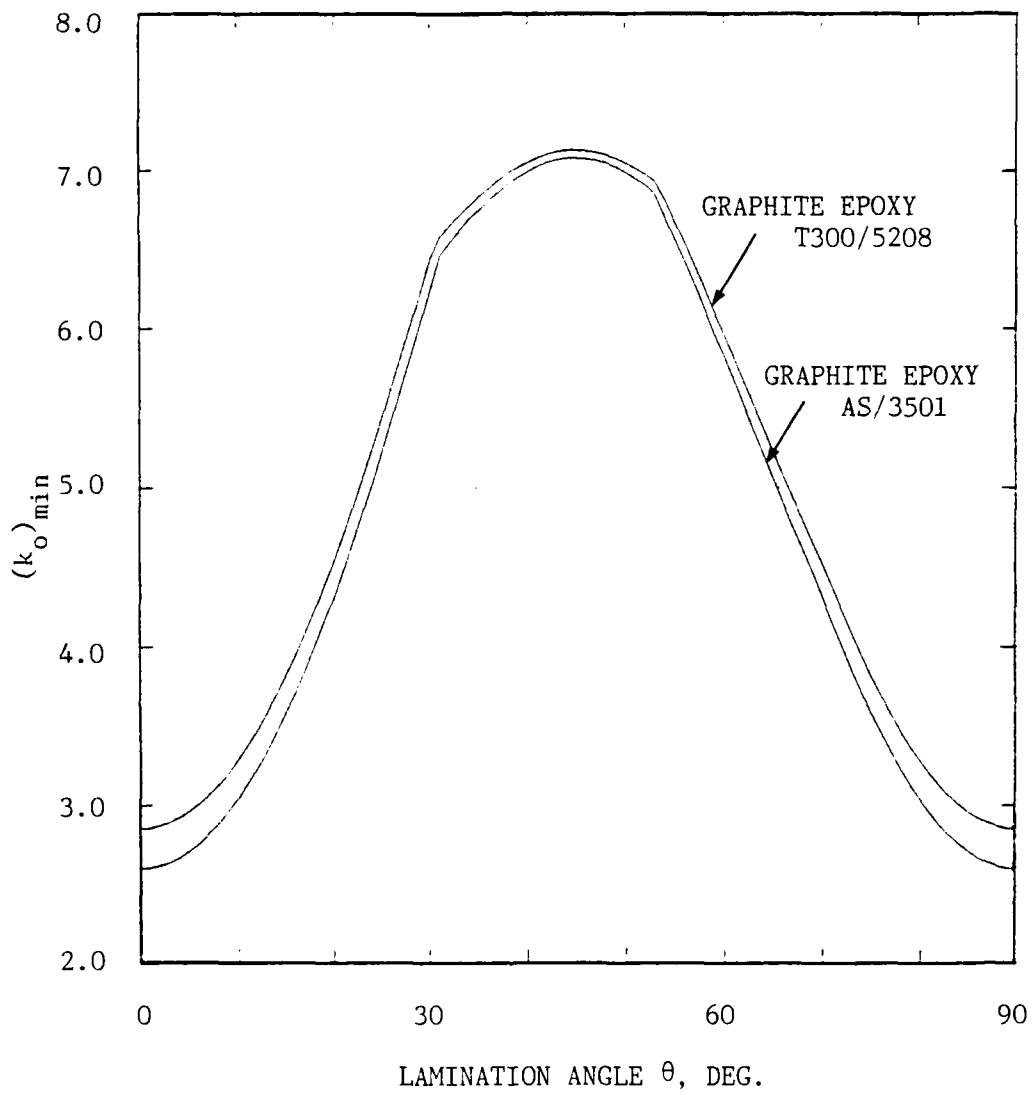


Fig. 21 . Minimum Buckling Coefficient vs. Lamination Angle
 Real Aspect Ratio = 2, No. of Layers = 4

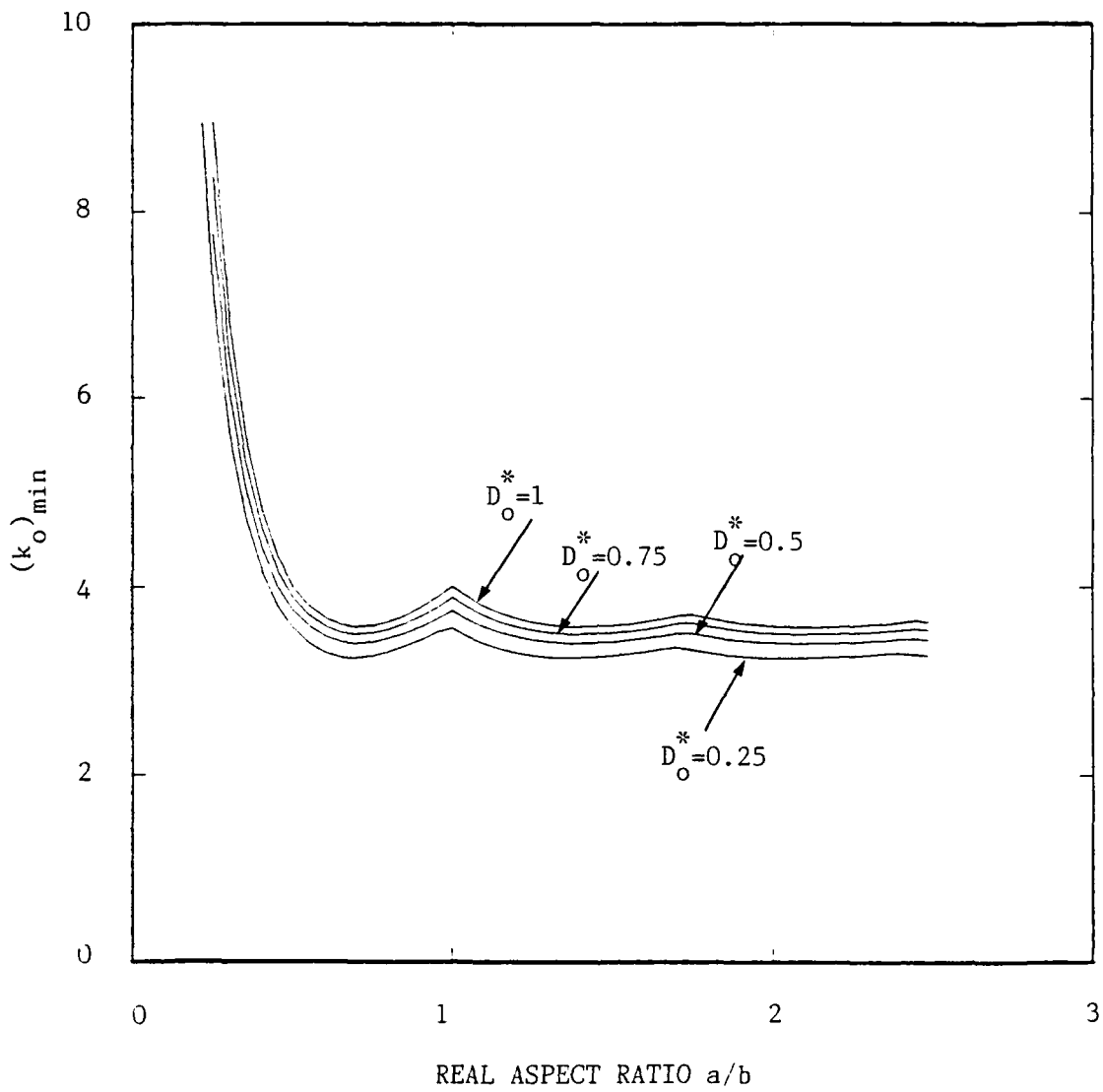


Fig. 22. Minimum Buckling Coefficient vs. Real Aspect Ratio
 Lamination Angle $\theta = 60$ deg., $K = 5$, No. of Layers = 2

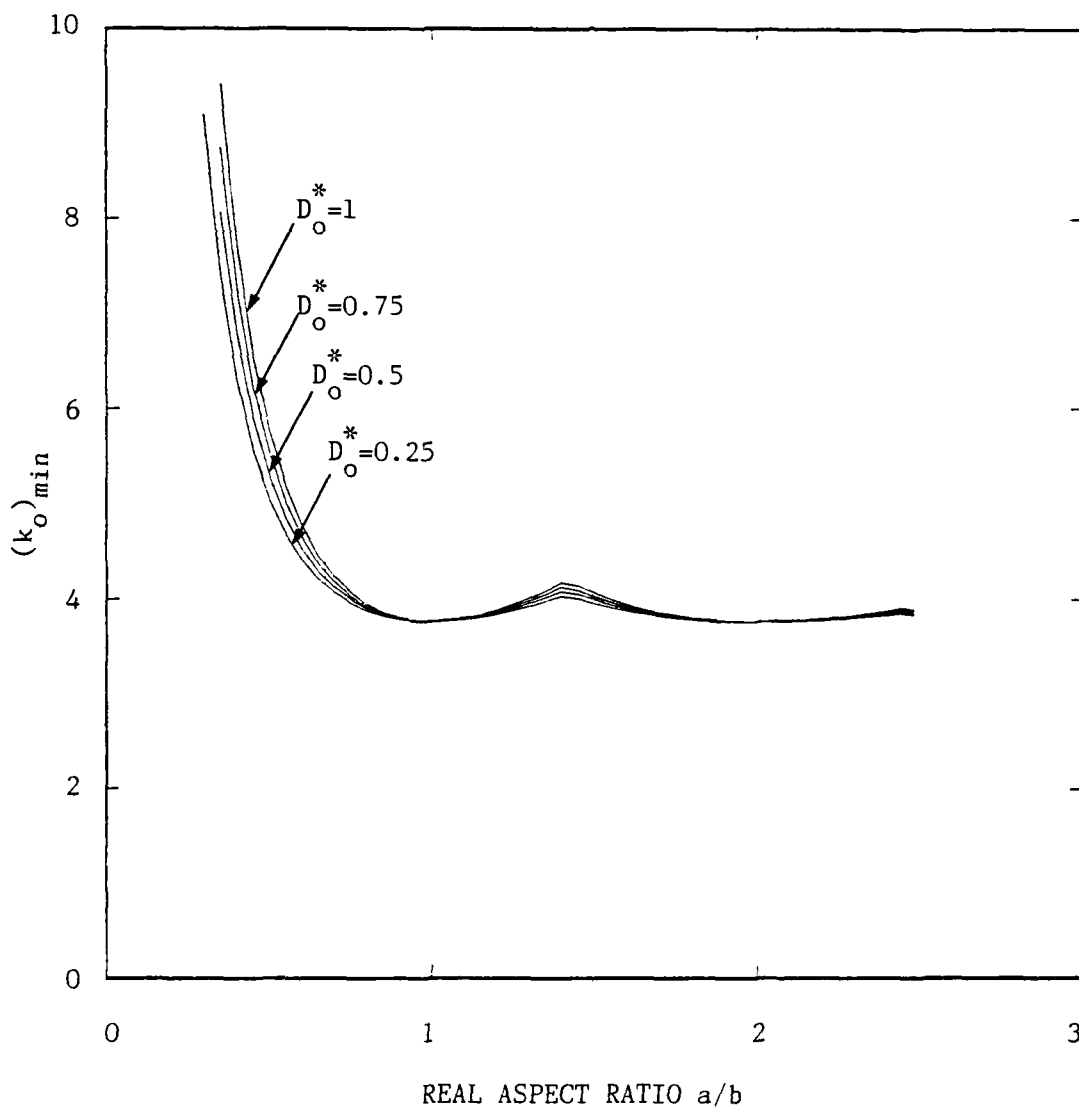


Fig. 23 . Minimum Buckling Coefficient vs. Real Aspect Ratio
 Lamination Angle $\theta = 45$ deg., No. of Layers = 2

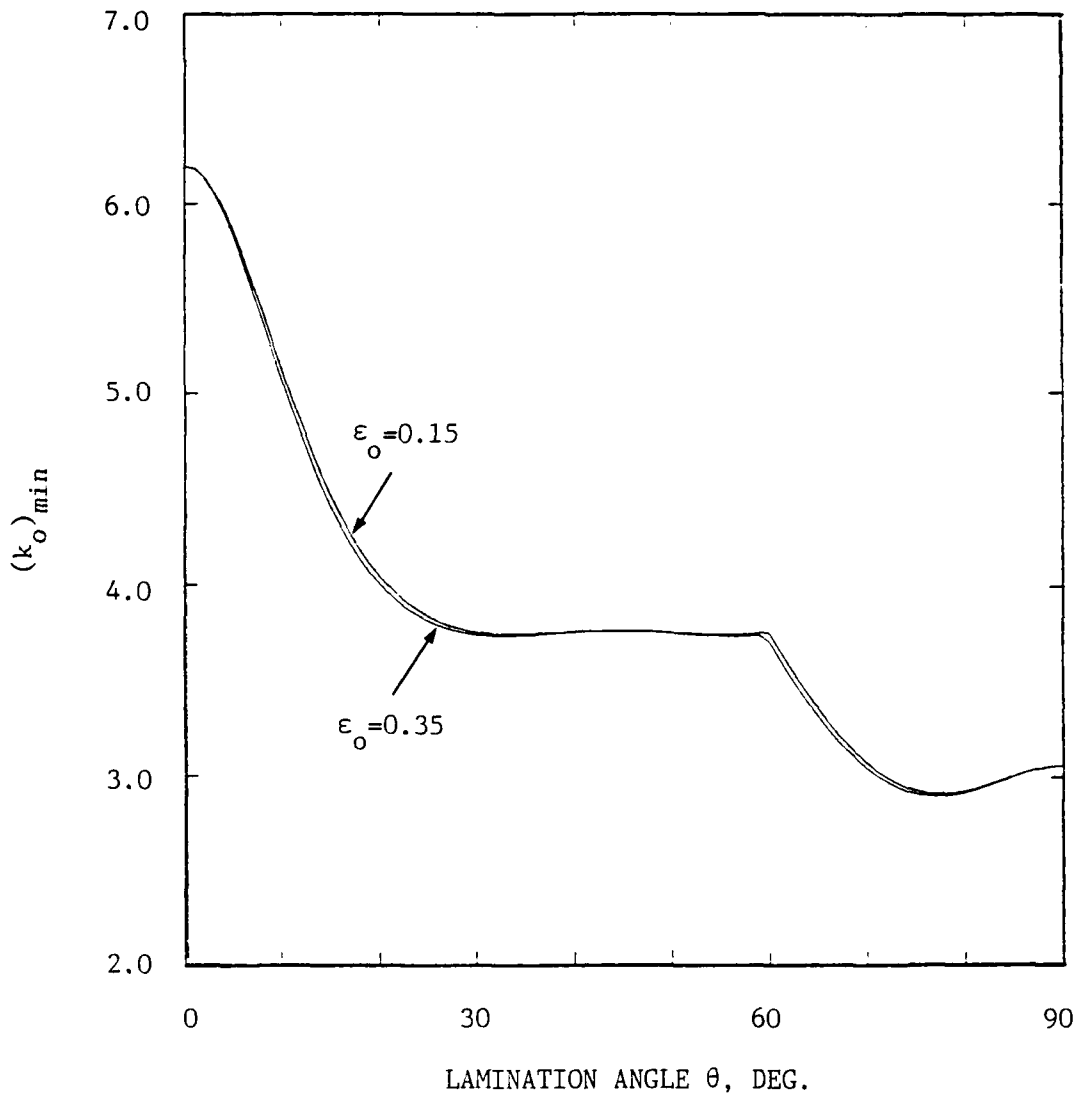


Fig. 24 . Minimum Buckling Coefficient vs. Lamination Angle
 $D_o^* = 0.5$, $K = 5.0$, Real Aspect Ratio = 1

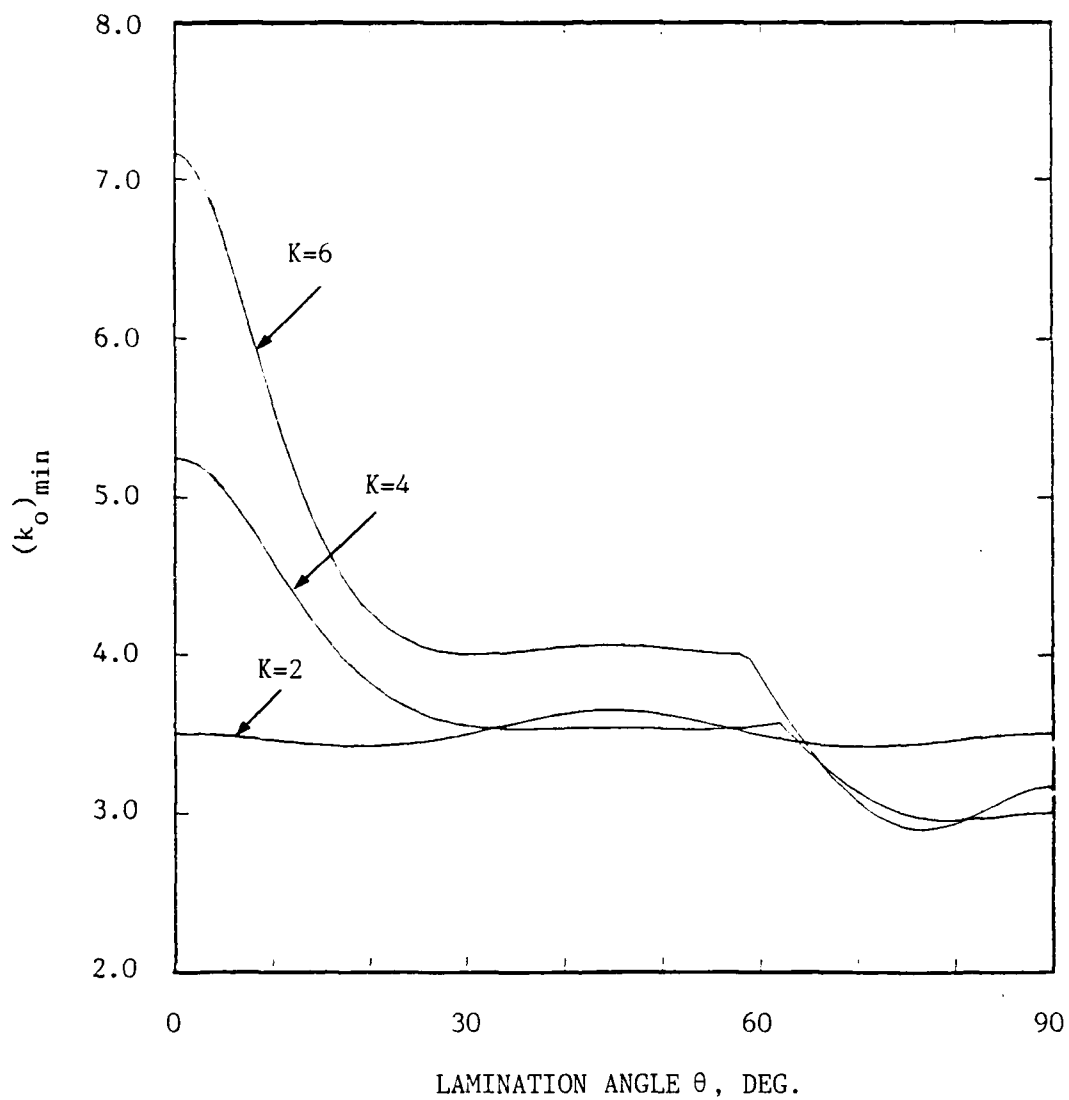


Fig. 25. Minimum Buckling Coefficient vs. Lamination Angle $D_o^* = 0.5$, Real Aspect Ratio = 1.0

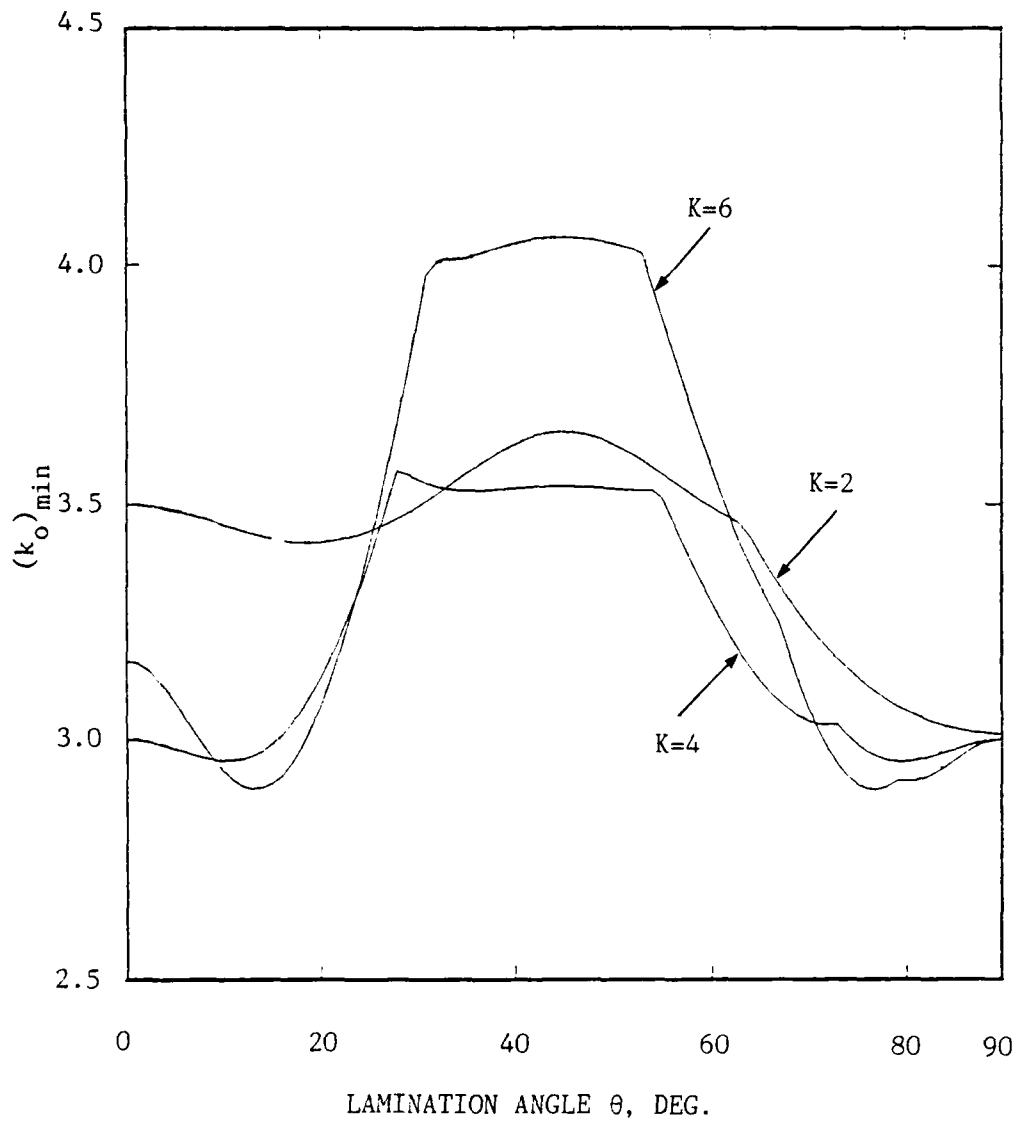


Fig. 26. Minimum Buckling Coefficient vs. Lamination Angle
 $D_0^* = 0.5$, Real Aspect Ratio = 2, No. of Layers = 2

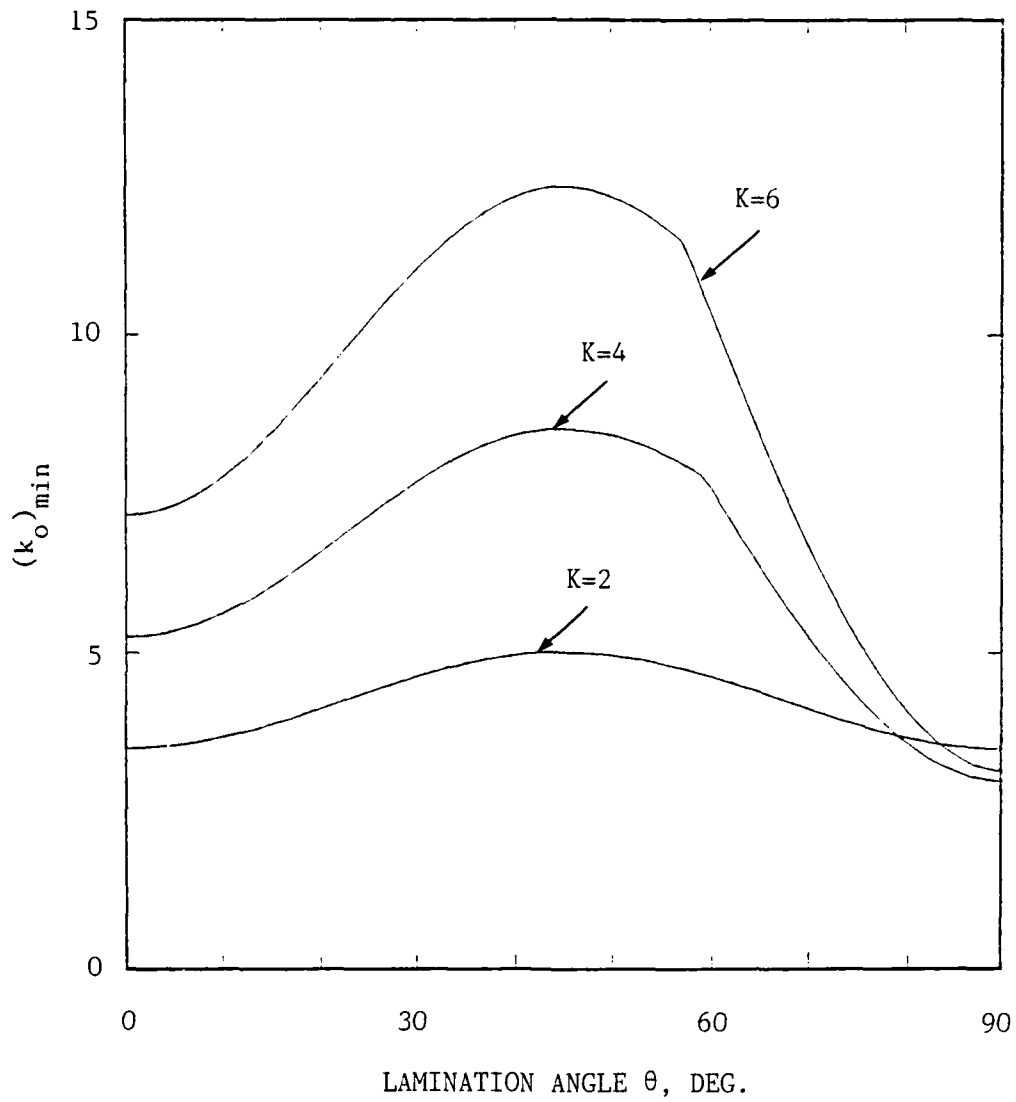


Fig. 27. Minimum Buckling Coefficient vs. Lamination Angle
 $D_o^* = 0.5$, Real Aspect Ratio = 1, No. of Layers = Infinite

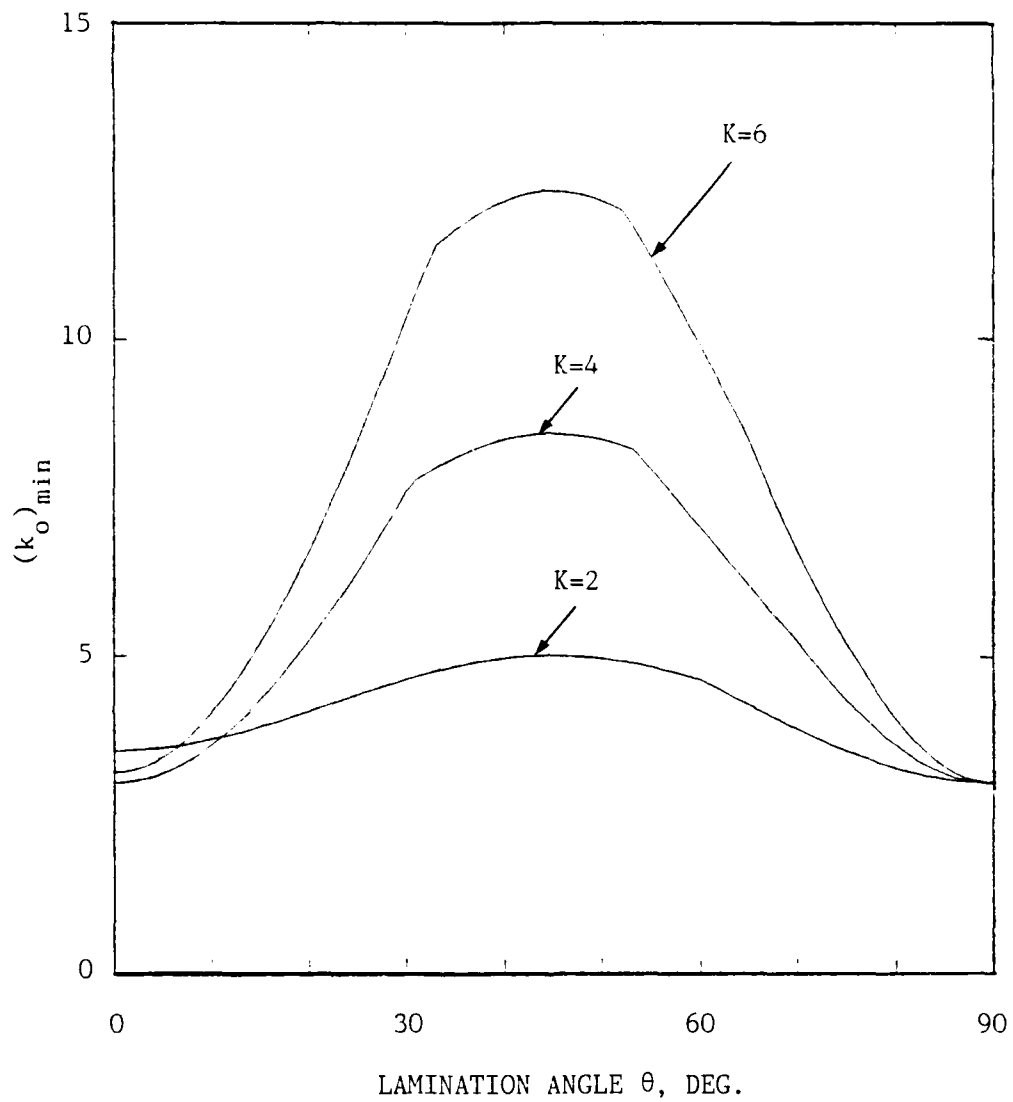


Fig. 28. Minimum Buckling Coefficient vs. Lamination Angle
 $D_o^* = 0.5$, Real Aspect Ratio = 2, No. of Layers = Infinite

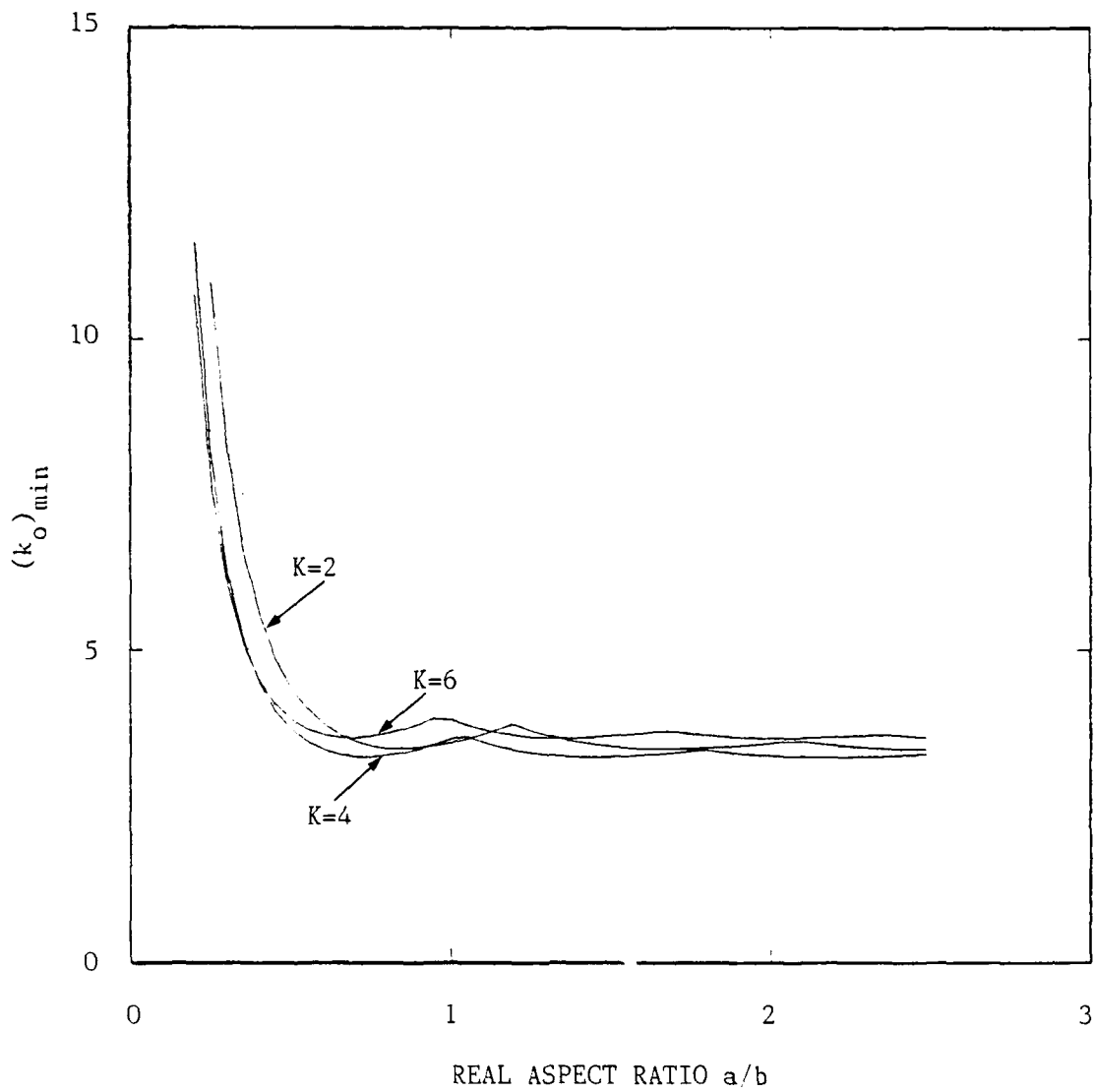


Fig. 29 . Minimum Buckling Coefficient vs. Real Aspect Ratio
 $D_0^* = 0.5$, Lamination Angle $\theta = 60$ deg., No. of Layers = 2

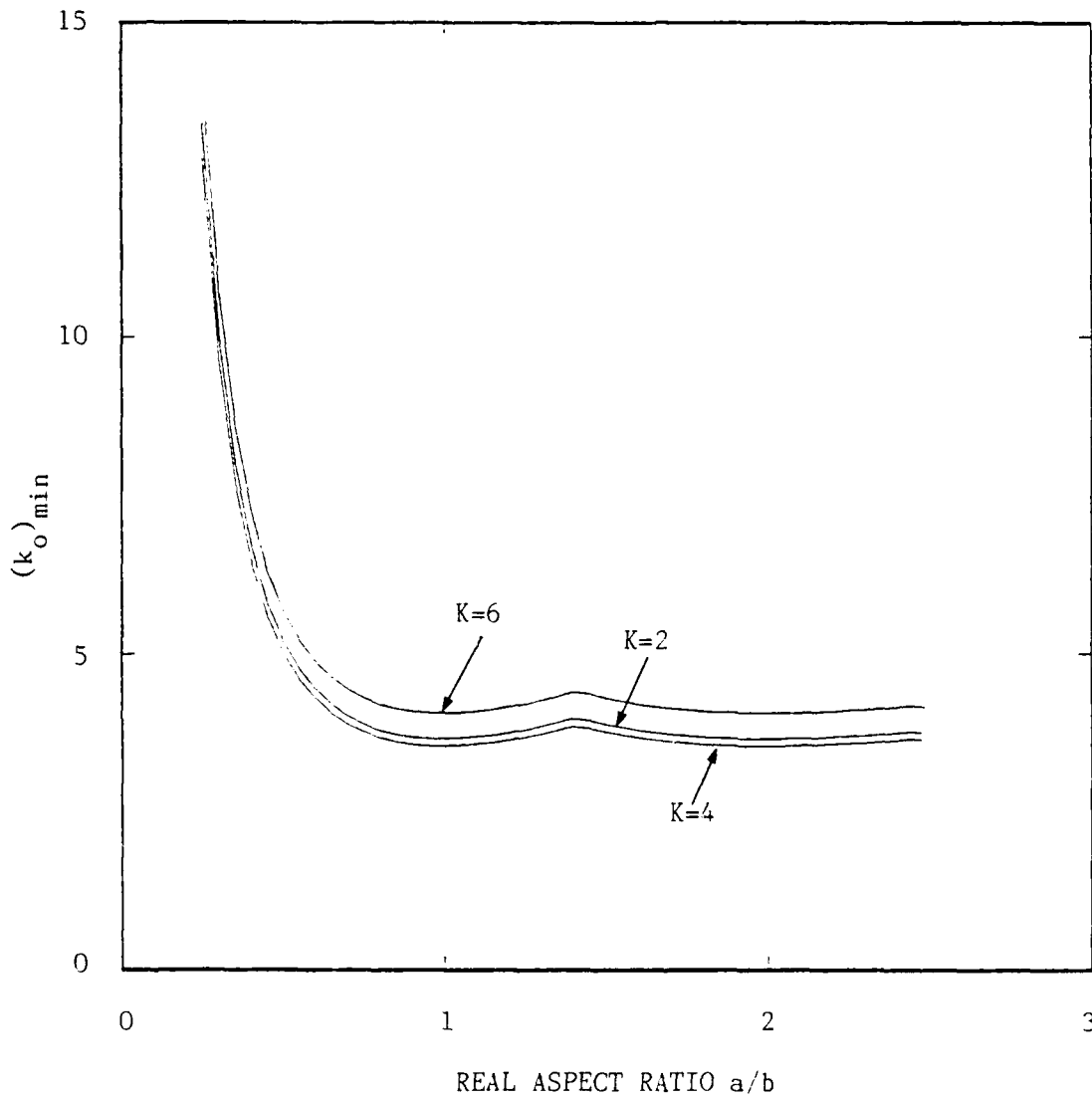


Fig. 30. Minimum Buckling Coefficient vs. Real Aspect Ratio
 $D_o^* = 0.5$, Lamination Angle $\theta = 45$ deg., No. of Layers = 2

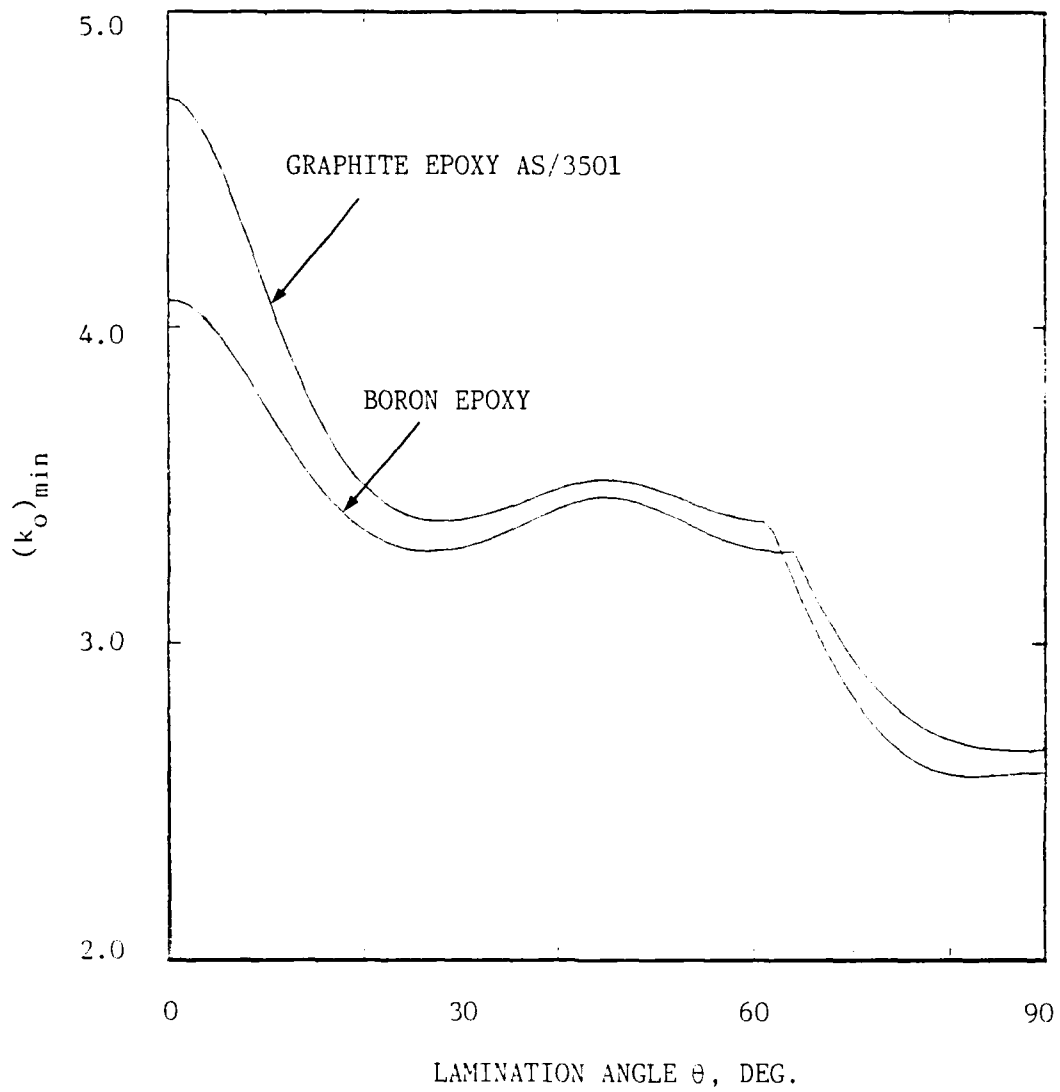


Fig. 31. Minimum Buckling Coefficient vs. Lamination Angle
Real Aspect Ratio = 1.0, No. of Layers = 2

AD-A153 040

SOLUTION TO EIGENVALUE PROBLEMS OF ANTISYMMETRIC
CROSS-PLY AND ANTISYMMET. (U) AIR FORCE INST OF TECH
WRIGHT-PATTERSON AFB OH SCHOOL OF ENGI.. Z A CHAUDHRY
DEC 84 AFIT/GAE/AA/84D-5 F/G 1374

2/2

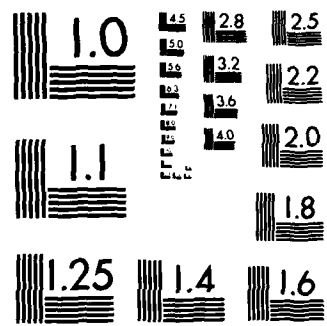
UNCLASSIFIED

NL

END

FILMED

DTIC



MICROCOPY RESOLUTION TEST CHART
NATIONAL BUREAU OF STANDARDS-1963-A

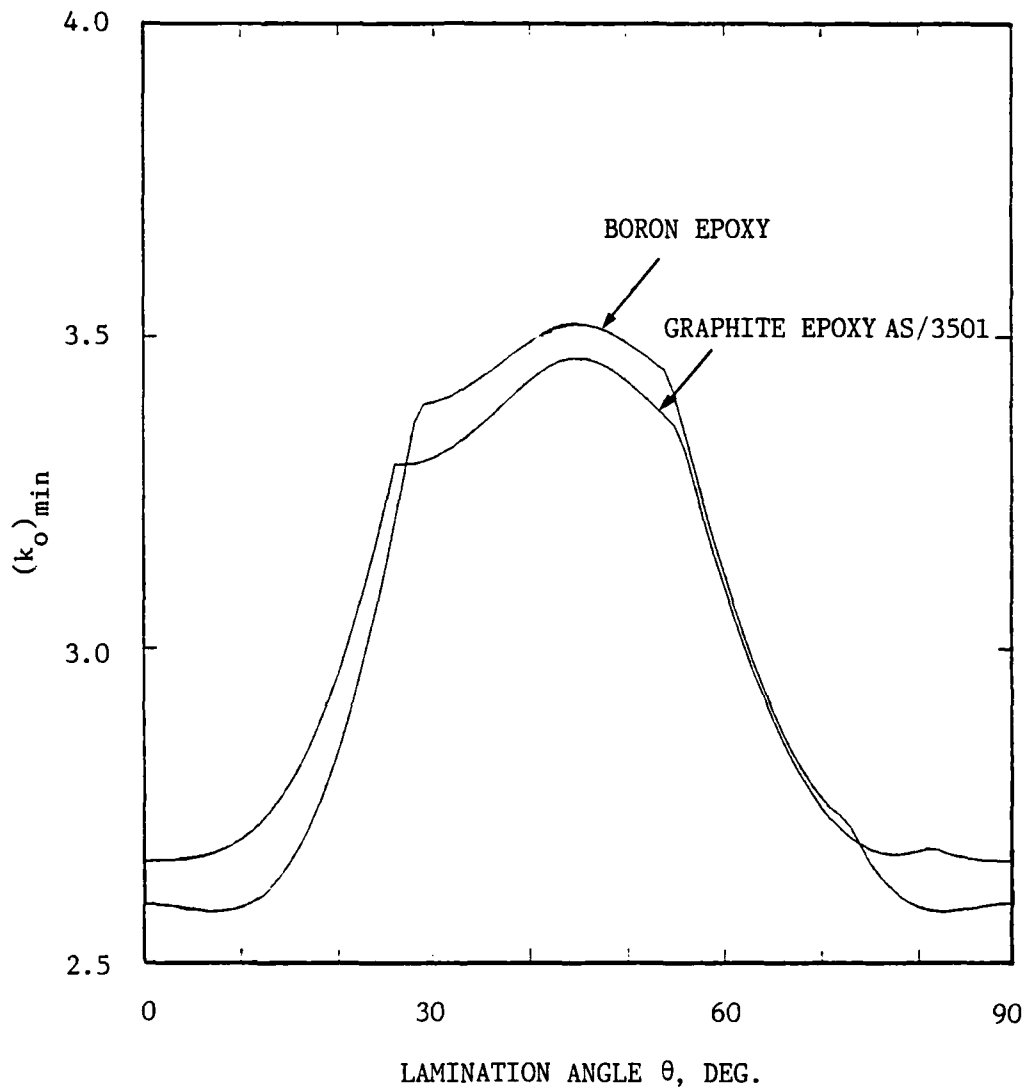


Fig. 32. Minimum Buckling Coefficient vs. Lamination Angle
 Real Aspect Ratio = 2, No. of Layers = 2

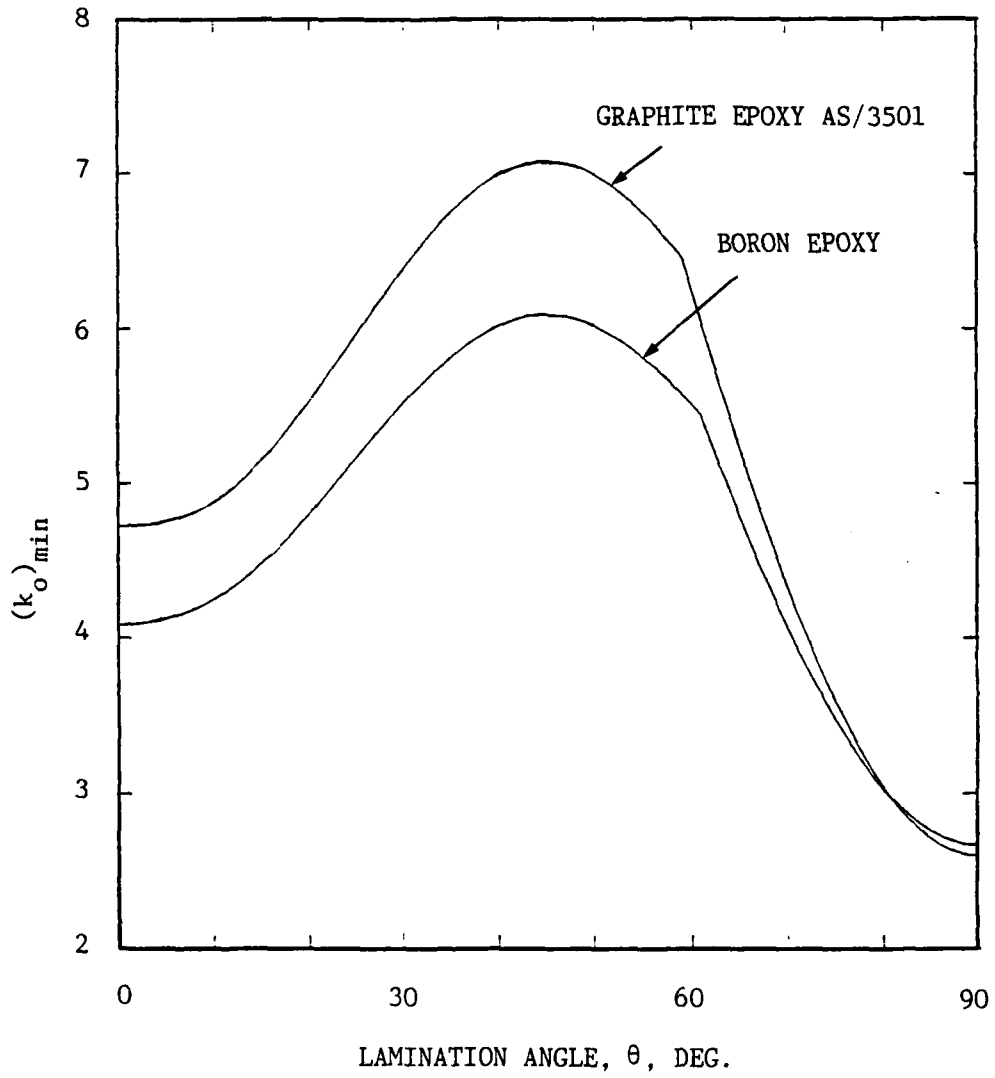


Fig. 33. Minimum Buckling Coefficient vs. Lamination Angle
Real Aspect Ratio = 1, No. of Layers = 4

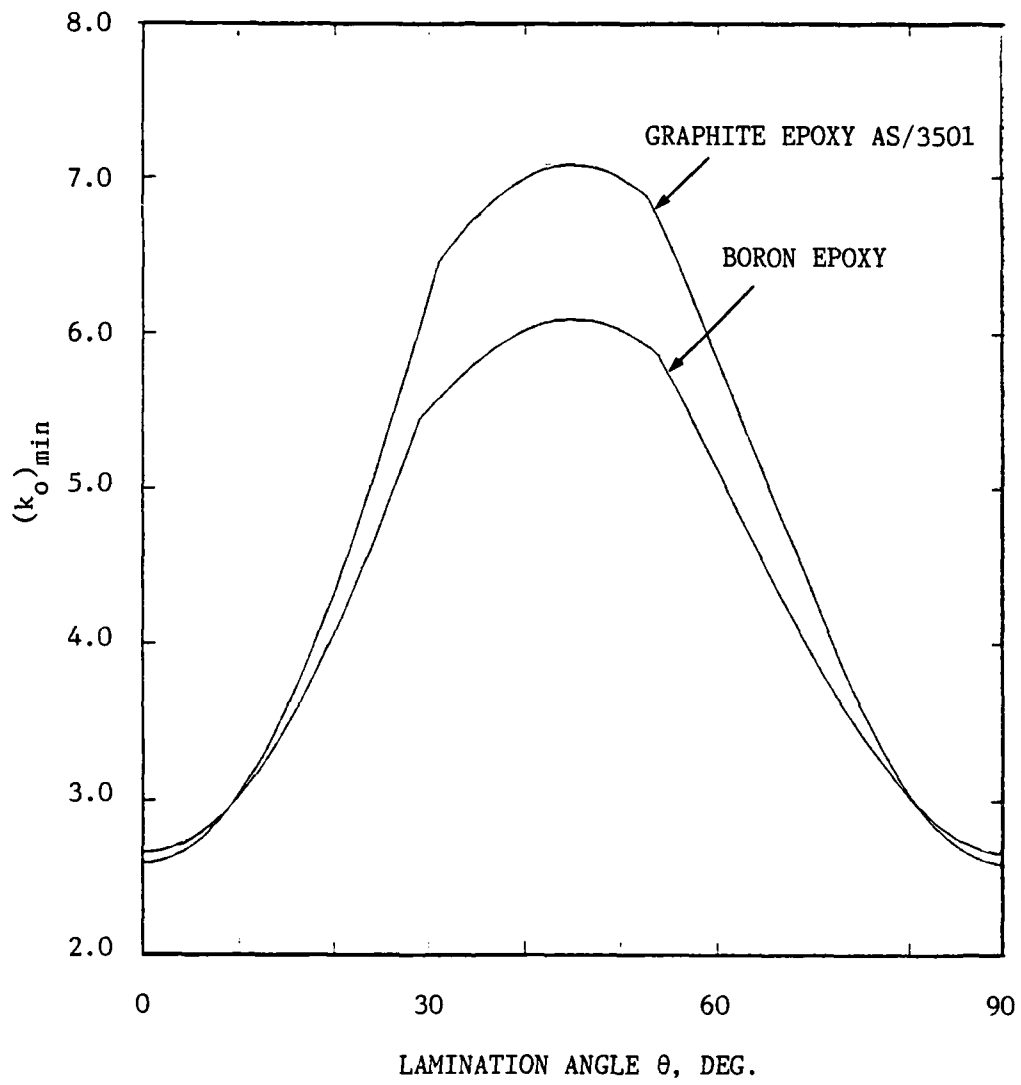


Fig. 34 . Minimum Buckling Coefficient vs. Lamination Angle
Real Aspect Ratio = 2, No. of Layers = 4

VI. Conclusions

Antisymmetric Cross-Ply Laminates

This presentation demonstrates the enormous pay off for recasting the buckling and vibration differential equations. The pay off is that the buckling and vibration coefficients have been reduced to a function of two strong material constants D^* and F . With the reduction in number of constants one can do an exhaustive parameter study of buckling and vibration solution trends. The buckling and vibration coefficients decrease with decreasing D^* . It is also noticed that for a given aspect ratio $k_{o \min}$ vs. D^* curves vary linearly, so that one may accurately interpolate between the D^* values. The buckling and vibration coefficient increase with increasing value of F .

The lower bound envelope for buckling and vibration is also presented. Since these lower bounds are material independent, they form the absolute minimum for any antisymmetric cross-ply laminate plate.

A simple and accurate method for approximating the buckling and vibration coefficients has been presented, and discussed.

Antisymmetric Angle-Ply Laminates

Using affine transformations the buckling differential equation has been reduced to a function of two strong material constants, D_o^* and K . The presence of aspect ratio as another strong parameter influencing the buckling load, is presented and discussed.

The effect of variation of D_o^* on the buckling coefficient is consistent with previous work [1], k_o decreases with decreasing D_o^* .

Like the specially orthotropic laminate, no specific trends for the buckling coefficient with the variation of K could be established. Materials with a higher value of K exhibit more sensitivity to the ply lamination angle.

The aspect ratio strongly influences the buckling coefficient in the range of $\theta = 0$ to 45 deg. For θ greater than 45 deg. the effect of aspect ratio is small.

Bibliography

1. Brunelle, E. J., and Oyibo, G. A., "Generic Buckling Curves for Specially Orthotropic Rectangular Plates", AIAA Journal, Volume 21, Number 8, August 1983, Page 1150.
2. Brunelle, E. J., "The Fundamental Constants of Orthotropic Affine Plate/Slab Equations". Paper presented at the 10th Annual Mini-Symposium on Aerospace Science and Technology, March 1984.
3. Brunelle, E. J., "The Use of Affine Transformation in the Solution of Composite Structures Problems". Paper presented at the Seventeenth Annual Meeting of the Society of Engineering Science, Inc., December 1980.
4. Jones, Robert M., "Buckling and Vibration of Rectangular Unsymmetrically Laminated Cross-Ply Plates". AIAA Journal, December, 1973, pp. 1626 - 1632.
5. Tsai, Stephen W., "Structural Behavior of Composite Materials". NASA CR-71, July 1964.
6. Whitney, J. M., "Bending-Extension Coupling in Laminated Plates Under Transverse Loading", Journal of Composite Materials, January 1969, pp. 20 - 28.
7. Jones, Robert M., Mechanics of Composite Materials, New York: McGraw-Hill Book Company, 1975.

VITA

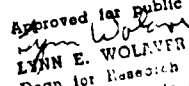
Flight Lieutenant Zaffir A. Chaudhry was born on 16 April, 1955 in Karachi, Pakistan. He graduated from Forman Christian College in Lahore, Pakistan, in 1972 and joined the Pakistan Air Force. He attended the PAF College of Aeronautical Engineering and received the degree of Bachelor of Science in Aerospace Engineering in January 1977. Upon graduation, he was commissioned in the Pakistan Air Force as a Flying Officer. He was employed as a Maintenance Engineering officer in the Pakistan Air Force until entering the School of Engineering, Air Force Institute of Technology in June 1983.

Permanent Address: 134-C, Model Town
Lahore-14
Pakistan

Unclassified

SECURITY CLASSIFICATION OF THIS PAGE

REPORT DOCUMENTATION PAGE

| | | | |
|---|--|---|--------------------------------|
| 1a. REPORT SECURITY CLASSIFICATION Unclassified | | 1b. RESTRICTIVE MARKINGS | |
| 2a. SECURITY CLASSIFICATION AUTHORITY | | 3. DISTRIBUTION/AVAILABILITY OF REPORT Approved for public release; distribution unlimited. | |
| 2b. DECLASSIFICATION/DOWNGRADING SCHEDULE | | | |
| 4. PERFORMING ORGANIZATION REPORT NUMBER(S) AFIT/GAE/AA/84D-5 | | 5. MONITORING ORGANIZATION REPORT NUMBER(S) | |
| 6a. NAME OF PERFORMING ORGANIZATION School of Engineering Air Force Institute of Technology AFIT/EN | 6b. OFFICE SYMBOL (If applicable) | 7a. NAME OF MONITORING ORGANIZATION | |
| 6c. ADDRESS (City, State and ZIP Code) Wright Patterson AFB Dayton, Ohio 45433 | | 7b. ADDRESS (City, State and ZIP Code) | |
| 8a. NAME OF FUNDING/SPONSORING ORGANIZATION | 8b. OFFICE SYMBOL (If applicable) | 9. PROCUREMENT INSTRUMENT IDENTIFICATION NUMBER | |
| 8c. ADDRESS (City, State and ZIP Code) | | 10. SOURCE OF FUNDING NOS. | |
| | | PROGRAM ELEMENT NO. | PROJECT NO. |
| | | TASK NO. | WORK UNIT NO. |
| 11. TITLE (Include Security Classification) See Box 19 | | | |
| 12. PERSONAL AUTHOR(S) Zaffir A. Chaudhry, B.S., Flt. Lt., Pakistan Airforce | | | |
| 1a. TYPE OF REPORT MS Thesis | 13b. TIME COVERED FROM _____ TO _____ | 14. DATE OF REPORT (Yr., Mo., Day) 1984 November DEC. | 15. PAGE COUNT 102 |
| 16. SUPPLEMENTARY NOTATION | | | |
| 17. COSATI CODES | | 18. SUBJECT TERMS (Continue on reverse if necessary and identify by block number) | |
| FIELD | GROUP | Composite Materials, Laminates, Buckling, Vibration. | |
| 11 | 04 | | |
| 20 | 11 | | |
| 19. ABSTRACT (Continue on reverse if necessary and identify by block number) | | | |
| Title: Solution to Eigenvalue Problems of Antisymmetric Cross-Ply and Antisymmetric Angle-Ply Laminated Plates Using Affine Transformations | | | |
| Thesis Advisor: E. J. Brunelle, Prof. | | | |
| <p style="text-align: right;">Approved for public release: 1AW AFR 190-17.  LYNN E. WOLNER Dean for Research and Professional Development Air Force Institute of Technology (AIC) Wright-Patterson AFB OH 45433</p> | | | |
| 20. DISTRIBUTION/AVAILABILITY OF ABSTRACT UNCLASSIFIED/UNLIMITED <input checked="" type="checkbox"/> SAME AS RPT. <input type="checkbox"/> DTIC USERS <input type="checkbox"/> | | 21. ABSTRACT SECURITY CLASSIFICATION Unclassified | |
| 22a. NAME OF RESPONSIBLE INDIVIDUAL E. J. Brunelle, Professor | | 22b. TELEPHONE NUMBER (Include Area Code) 513-255-2362 | 22c. OFFICE SYMBOL AFIT/ENY |

Using affine transformations and suitably recasting the buckling and vibration differential equations, the eigenvalue problem of antisymmetric cross-ply and antisymmetric angle-ply laminated rectangular plates has been reduced to a function of two strong material constants, the generalized rigidity ratio, whose range is in the closed interval from 0 to 1, and the ratio of principal lamina stiffnesses.

With the reduction in number of constants an exhaustive parameter study of buckling and vibration solution trends, is possible. The buckling coefficients decrease with decreasing value of generalized rigidity ratio for both antisymmetric cross-ply and antisymmetric angle-ply laminates. For a given aspect ratio, and ratio of principal lamina stiffnesses, the buckling and frequency coefficient for antisymmetric cross-ply laminates vary linearly with the value of the generalized rigidity ratio, so that one may accurately interpolate between the values of the generalized rigidity ratio.

The buckling and frequency coefficients increase with increasing F for antisymmetric cross-ply laminates. No such trend could be established for antisymmetric angle-ply laminates.

A simple and fairly accurate method has been established for estimating the buckling and vibration coefficients for antisymmetric cross-ply laminates. *→ see + required include:*

4-200-1473

END

FILMED

5-85

DTIC